
Electronic Theses and Dissertations, 2004-2019

2007

Mechanisms Promoting Phosphorylation Of The Nf2 Tumor Suppressor And Its Effects On Schwann Cell Development

Courtney Lynn Thaxton
University of Central Florida

 Part of the [Microbiology Commons](#), and the [Molecular Biology Commons](#)
Find similar works at: <https://stars.library.ucf.edu/etd>
University of Central Florida Libraries <http://library.ucf.edu>

This Doctoral Dissertation (Open Access) is brought to you for free and open access by STARS. It has been accepted for inclusion in Electronic Theses and Dissertations, 2004-2019 by an authorized administrator of STARS. For more information, please contact STARS@ucf.edu.

STARS Citation

Thaxton, Courtney Lynn, "Mechanisms Promoting Phosphorylation Of The Nf2 Tumor Suppressor And Its Effects On Schwann Cell Development" (2007). *Electronic Theses and Dissertations, 2004-2019*. 3382.
<https://stars.library.ucf.edu/etd/3382>

MECHANISMS PROMOTING PHOSPHORYLATION OF THE NF2 TUMOR
SUPPRESSOR AND ITS EFFECTS ON SCHWANN CELL DEVELOPMENT

by

COURTNEY THAXTON
B.S. University of Central Florida, 2002

A dissertation submitted in partial fulfillment of the requirements
for the degree of Doctor of Philosophy
in the Department of Biomedical Sciences
in the College of Medicine
at the University of Central Florida
Orlando, Florida

Fall Term
2007

Major Professor: Cristina Fernandez-Valle

© 2007 Courtney Thaxton

ABSTRACT

Neurofibromatosis type 2 is an autosomal dominant disease characterized by the formation of schwannomas and other peripheral neuropathies. The *nf2* gene encodes the protein Schwannomin, or merlin. Schwannomin (Sch) is a membrane-cytoskeletal linking protein that suppresses cell proliferation at high cell density and modulates cell shape. Sch's tumor suppressive activity is regulated by its localization, conformation, and phosphorylation at serine 518 (S518). Sch's localization is dependent on binding the scaffold protein, paxillin. Phosphorylation of Sch at S518 regulates its conformation and tumor suppressor function. In a negative feedback loop, unphosphorylated Sch restricts cell proliferation downstream of Rac and p21-activated kinase (Pak), whereas Pak-induced phosphorylation inactivates Sch's ability to inhibit Pak and cell proliferation. Little is known about the function of the phosphorylated form of Sch, or the molecular mechanisms leading to its phosphorylation. Here we demonstrate that Sch-S518 phosphorylation is dependent on paxillin-binding and plasma membrane localization in SCs. Phosphorylation of Sch at the plasma membrane is mediated by Cdc42-Pak and results in altered SC morphology and polarity. Moreover, we have identified two extracellular stimuli that trigger Sch-S518 phosphorylation; these are neuregulin (NRG) and laminin, two potent activators of SC proliferation and myelination. NRG promotes Sch-S518 phosphorylation downstream of ErbB2/ErbB3 through PKA, whereas laminin-1 stimulation of β 1 integrin promotes Pak- dependent phosphorylation of Sch-S518. Additionally, we find that Sch promotes process formation and elongation in primary and myelinating SCs, independent of Sch S518 phosphorylation. However, Sch phosphorylation was found to influence SC differentiation, as expression of an unphosphorylatable variant, Sch-S518A, facilitated SC myelination, whereas

expression of a phospho-mimicking variant, Sch-S518D, reduced the SC's ability to myelinate. Together, these findings have identified receptor-mediated and paxillin-dependent pathways that regulate phosphorylation and inactivation of Sch's tumor suppressor function. Additionally, these results have elucidated novel normal functions for Sch during peripheral nerve development and myelination, and identify novel therapeutic targets for treatment of NF2 and other peripheral neuropathies.

ACKNOWLEDGMENTS

I would like to thank Dr. Fernandez-Valle, Jorge Lopera, and Marga Bott for all your guidance, help and support. I would also like to thank my committee members for all of your insightful comments and suggestions. And last, but not least, I would like to thank my parents and family for always supporting me in every endeavor, and for allowing me to follow my dreams.

TABLE OF CONTENTS

LIST OF FIGURES	xii
CHAPTER 1 GENERAL INTRODUCTION	1
1.1 Neurofibromatosis Type 2	1
1.2 Schwannomin, A Novel Membrane-Cytoskeletal Protein Regulating Cell Proliferation. ...	3
1.2.1 Structure And Function Of Schwannomin.....	3
1.2.2 Conformational Regulation Of Schwannomin Activity	4
1.2.3 Phosphorylation Of Schwannomin S518 Is Mediated By p21-Activated Kinase And Protein Kinase A.....	5
1.2.4 Schwannomin's Regulation of Actin Polymerization Dynamics	7
1.2.5 Protein Interactions Regulating Schwannomin Function	9
1.3 Schwann Cells: The Myelinating Glia Of The Peripheral Nervous System.....	13
1.3.1 Signals Determining SC Differentiation And Myelination	14
1.3.2 Extracellular Matrix Mediated SC Development: Signaling from Laminins and β 1 integrin	16
1.3.3 Axonal Cues Regulating SC Development: The Roles Of Neuregulin And ErbB2 In SC Myelination	18
2.1 Introduction.....	21
2.2 Materials and Methods.....	24
2.2.1 Materials	24
2.2.2 Cell Culture.....	24
2.2.3 Transfections.....	25

2.2.4 Immunoprecipitation And Western Blotting	25
2.2.5 Immunostaining	25
2.2.6 Pak-CRIB Pull Down Assay	26
2.3 Results.....	28
2.3.1 Deletion Of Paxillin Binding Domain 1 Prevents Sch Phosphorylation	28
2.3.2 Deletion Of PBD2 Is Not Associated With Increased P-Pak Levels.....	29
2.3.3 Expression Of Active Forms Of Cdc42 And Rac Indiscriminately Increases P-Pak Levels In SCs	30
2.3.4 Expression Of Active Cdc42 And Rac Does Not Promote Unrestricted Phosphorylation Of Endogenous Sch But Does Increase Phosphorylation Of Sch-GFP.....	31
2.3.5 Inhibition Of Rac-GTP Does Not Reduce Phosphorylation Of Sch S518 Or Pak	32
2.3.6 PS518-Sch And Paxillin Co-Localize With Cdc42 And P-Pak In Membrane Protrusions	33
2.3.7 Sch Serine 518 Phosphorylation Modulates Morphology In SCs	33
2.4 Discussion.....	35
2.4.1 Interactions With Paxillin Regulate Sch S518 Phosphorylation.....	35
2.4.2 Evidence For Cdc42-Pak Dependent S518 Phosphorylation.....	36
2.4.3 Activation Of Cdc42-Pak Dependent Sch S518 Phosphorylation.....	37
2.4.4 Sch Regulates The Organization Of The Actin Cytoskeleton	38
2.4.5 Two Pools Of Sch With Distinct Functions.....	39

CHAPTER 3 NEUREGULIN AND LAMININ STIMULATE PHOSPHORYLATION OF THE NF2 TUMOR SUPPRESSOR IN SCHWANN CELLS BY DISTINCT PROTEIN KINASE A AND P21-ACTIVATED KINASE DEPENDENT PATHWAYS	60
3.1 Introduction.....	60
3.2 Materials and Methods.....	62
3.2.1 Materials	62
3.2.2 Cell Culture.....	62
3.2.3 Immunostaining	63
3.2.4 Western Blotting	63
3.2.5 Immunoprecipitation.....	64
3.2.6 Transfections.....	64
3.3 Results.....	65
3.3.1 NRG1 β and Laminin-1 Induce Phosphorylation of Sch at SC Distal Tips and Radial Membrane Protrusions	65
3.3.2 NRG1 β Promotes Sch Phosphorylation Through PKA.....	66
3.3.3 Laminin-1 Promotes Phosphorylation Of Sch-S518 By Pak.....	67
3.3.4 β 1 Integrin And ErbB2 Exist As A Functional Co-Receptor Complex On The SC Surface	68
3.3.5 Dual Stimulation With NRG1 β And Laminin-1 Does Not Synergistically Increase Sch Phosphorylation	70
3.4 Discussion.....	72
3.4.1 Two Distinct Receptor Mediated Pathways Promote Sch Phosphorylation.....	72

3.4.2 ErbB2 Modulates β 1 Integrin Signaling.....	74
3.4.3 Implications For Schwannoma Development.....	74
CHAPTER 4 EXPRESSION OF THE NF2 TUMOR SUPPRESSOR IN SCHWANN CELLS PROMOTES PROCESS EXTENSION AND MYELINATION.....	
4.1 Introduction.....	97
4.2 Materials and Methods.....	100
4.2.1 Materials	100
4.2.2 Cell Culture.....	100
4.2.3 Transfection Of Schwann Cell And Dorsal Root Ganglion Neuron Co-Cultures.....	101
4.2.4 Immunostaining	101
4.3 Results.....	102
4.3.1 Sch Expression Promotes Process Extension In SCs.....	102
4.3.2 Sch Expression Increases Myelin Internodal Length.....	103
4.3.3 Myelin Formation But Not Internodal Length Is Dependent On Sch-S518 Phosphorylation	104
4.3.4 Sch-S518 Phosphorylation Decreases With The Onset Of Myelination	105
4.3.5 GFP-Positive Myelin Segments Express CASPR and P-ERM at the Paranode and Node of Ranvier	106
4.4 Discussion.....	108
4.4.1 Control of Process Formation and Extension By Sch.....	109
4.4.2 SC Myelination is Regulated by Sch-S518 Phosphorylation	109
4.4.3 Implications for the Development of Myelin Abnormalities and Neuropathies.....	110

CHAPTER 5 GENRAL DISCUSSION.....	121
5.1 Schwannomin-S518 Phosphorylation Is Dependent On Paxillin Binding and Plasma Membrane Localization	121
5.2 Schwannomin-S518 Phosphorylation Is Stimulated By NRG And Laminin-1 Through Distinct PKA And Pak Mediated Pathways.....	122
5.3 Schwannomin Promotes Process Elongation In Primary And Myelinating SCs And Controls Myelination In A Phosphorylation Dependent Manner	124
5.4 Implications for Schwannomin Phosphorylation During SC Development: Control Of SC Process Formation and Extension, Migration, Proliferation, And Myelination	125
5.5 Implications for the Development of Schwannomas and Neurofibromatosis Type 2..	130
APPENDIX: EXPERIMENTAL PROCEDURES	133
A.1 Molecular Cloning Procedures.....	134
A.1.1 Bacterial Transformation of Plasmid DNA	134
A.1.2 Mini Prep of Plasmid DNA (Qiagen QIAprep Miniprep Protocol/Method)	136
A.2 Biochemical Procedures.....	137
A.2.1 Transfection of Primary Rat Schwann Cells (Lipofectamine 2000).....	137
A.2.2 Transfection of Dissociated Schwann Cell/ Dorsal Root Ganglion Neuron Co-cultures (Lipofectamine 2000).....	139
A.2.3 Extraction of Primary Rat Schwann Cells (transfected and non-transfected)	141
A.2.4 Lowry Method For The Determination Of Cell Lysate Protein Concentration.....	143
A.2.5 Immunoprecipitation using Total Schwann Cell Extract.....	144
A.2.6 Magnetic Bead Immunoprecipitation of $\beta 1$ integrin.....	146

A.2.7 Preparation Of SDS-PAGE Gel And Electrophoretic Separation Of Proteins	147
A.2.8 Electrophoretic Transfer Of SDS-PAGE To A PVDF Membrane.	149
A.2.9 Immunoblotting.....	150
A.2.10 Immunostaining of Primary Rat Schwann Cells.....	151
A.2.11 Immunostaining of Dissociated Schwann Cell/ Dorsal Root Ganglion Neuron Co- cultures.....	152
A.3 Cell Culture Procedures	154
A.3.1 Rat Sciatic Nerve Dissection.....	154
A.3.2 THY 1.1 Treatment.....	158
A.3.3 Rat Dorsal Root Ganglion Dissection.....	160
A.3.4 Laminin Coating	166
LIST OF REFERENCES.....	170

LIST OF FIGURES

Figure 2.1 PBD1 Is Required For Serine 518 Phosphorylation Of Sch.....	41
Figure 2.2 Sch-GFP Is Phosphorylated At Restricted Plasma Membrane Domains.	43
Figure 2.3 Deletion Of PBD2 Is Not Associated With Increased Pak Activity In SCs.....	45
Figure 2.4 Expression Of Active Cdc42 And Rac Increases Endogenous P-Pak Levels.	47
Figure 2.5 Expression Of Active Cdc42 and Rac Does Not Increase Phosphorylation of Endogenous Sch.....	49
Figure 2.6 Expression Of Active Cdc42 And Rac Increases S518 Phosphorylation Of Exogenous Sch-GFP.....	51
Figure 2.7 Inhibition of Rac GTPase Does Not Reduce Sch S518 and Pak Phosphorylation.....	53
Figure 2.8 Sch-PS518, Paxillin, Cdc42, P-Pak, But not Rac Colocalize In Membrane Protrusions.	56
Figure 2.9 Sch Phosphorylation Status Alters SC Morphology.	58
Figure 3.1 Phosphorylated Forms Of ErbB2, Sch, And Pak Co-localize With Paxillin And Cdc42 In Processes, Their Distal Tips And Radial Protrusions Following Acute Stimulation With NRG1 β	78
Figure 3.2 NRG1 β And Laminin-1 Induce Sch Phosphorylation In SC Processes.....	80
Figure 3.3 NRG1 β Stimulates Phosphorylation Of Sch By PKA	83
Figure 3.4 Laminin-1 Stimulates Phosphorylation Of Sch.....	85
Figure 3.5 Catalytically Inactive Pak Inhibits Sch Phosphorylation In SCs Adhering To Laminin- 1.....	87

Figure 3.6 β 1 integrin And ErbB2 Exist As A Complex On The Plasma Membrane.	89
Figure 3.7 AG825 Increases Sch Phosphorylation In Response To Laminin-1 And NRG1 β	93
Figure 3.8 Model Of ErbB And β 1 Integrin Induced Phosphorylation Of Sch And Inactivation Of Its Tumor Suppressor Function In Subconfluent SCs.....	95
Figure 4.1 Expression Of Sch Increases SC Process Length.....	113
Figure 4.2 Sch Increases The Myelin Internodal Length And The Frequency Of Myelination Is Dependent On S518 Phosphorylation.	115
Figure 4.3 Sch-S518 Phosphorylation Decreases In SC At The Onset Of Myelination.....	117
Figure 4.4 Expression Of Sch Phospho-variants Does Not Alter CASPR Or P-ERM Localization In Myelinating SC/DRGN Co-Cultures.....	119

CHAPTER 1

GENERAL INTRODUCTION

1.1 Neurofibromatosis Type 2

Neurofibromatosis type 2 (NF2) is an autosomal dominant inherited disease affecting approximately 1 in 25,000 individuals (reviewed in Ferner, 2007). NF2 is characterized by the formation of multiple benign nervous system tumors, including schwannomas, meningiomas, and ependymomas, as well as ocular abnormalities (Gutmann et al., 1997; Ferner 2007). The hallmark of NF2 is the formation of bilateral vestibular schwannomas on the 8th cranial nerve, resulting in loss of hearing and tinnitus, and loss of balance and dizziness (reviewed in Houshmandi and Gutmann, 2007). Individuals with NF2 can also develop cutaneous schwannomas, focal amyotrophy resulting in foot drop, facial mononeuropathy, cataracts, orbital meningiomas, and retinal hamartomas. Most of these symptoms present themselves in children with inherited NF2, as opposed to adults with non-inherited NF2 (reviewed in MacCollin and Mautner, 1998). Although NF2 has been found in children under the age of 15, and as young as 2, the average age of onset is between 18-24 years (Evans et al, 1992). The later onset of NF2 can be partially explained by the fact that 50% of individuals with NF2 have a non-inherited, sporadic form that arises after an individual acquires spontaneous mutations in the *NF2* gene, and therefore the appearance of symptoms can take years to manifest. Another factor contributing to the delayed onset of NF2 symptoms is the slow growth of the schwannomas. Moreover, the growth rate of the tumors appears to decrease with increasing age (Patronas et al., 2001). The major factor accounting for the highest rate of morbidity and mortality in NF2 is the formation of cranial meningiomas that occur in approximately 45% of NF2 patients (Evans et al.,

2005). Other factors contributing to the mortality of individuals with NF2 are the severity of the disease, the location and amount of tumors, the age at diagnosis, and the treatment regimen.

NF2 is caused by mutations within the *nf2* gene located on chromosome 22q12.2. *NF2* comprises 17 exons, and naturally occurring mutations can be found throughout all exons. These mutations include missense, non-sense, frameshift, splice site and somatic mosaicism (Baser et al., 2005). The severity of NF2 depends on the type of mutation, non-sense and frameshift being the most severe, and the exon in which the mutation occurs. Splice site mutations found in exons 1-5, and particularly those in exons 2-3, indicate a more severe phenotype than those arising from exons 11-15 (Baser et al., 2005). The criteria for diagnosis of NF2 has evolved, as initially family history was a prerequisite for disease development, but as mentioned above, non-inherited NF2 comprises 50% of all cases. The current clinical criteria for diagnosis include the appearance of tumors other than bilateral vestibular schwannomas that develop in both familial and non-familial cases (reviewed in Hanemann and Evans, 2006). Treatment for individuals with NF2 is limited, and consists of surgery to remove tumors, tumor-focused radiological surgery, and auditory brainstem implants, but all of these treatments involve high risks. Surgery to remove the tumors often results in facial nerve damage, corneal ulceration, disfigurement, and permanent hearing loss, and is only recommended in severe cases involving large tumor growth, and brainstem compression (Evans et al., 2005). Stereotactic radiosurgery, where radiation is applied directly to the tumor growth, can delay hearing loss, but it can also lead to the development of other brain malignancies (Rowe et al., 2002). The auditory brainstem implant has been shown to alleviate the loss of hearing and improve cochlear nerve function, but unless

NF2 is diagnosed early, this treatment might not benefit the patient (Lustig et al., 2006). Any advancement in the detection and treatment would not only benefit those individuals afflicted with NF2, but individuals with other neuropathies such as Schwannomatosis.

1.2 Schwannomin, A Novel Membrane-Cytoskeletal Protein Regulating Cell

Proliferation.

1.2.1 Structure And Function Of Schwannomin

The *nf2* gene encodes a 595 amino acid protein termed Schwannomin, or Merlin, that is approximately 68kD (Rouleau et al., 1993; Trofatter et al., 1993). Schwannomin is ubiquitously expressed, and found in all tissues, but the highest levels of expression are found in Schwann cells, peripheral neurons, meningeal cells and the lens (Claudio et al., 1997; den Bakker et al., 1999). Schwannomin was found to be mutated or absent in individuals with NF2, and was therefore classified as a tumor suppressor. Unlike classical tumor suppressors, such as p53 and Rb that inhibit proliferation by acting directly on the cell cycle, Schwannomin's growth suppression is indirect, and occurs through its association with plasma membrane components and the actin cytoskeleton.

Schwannomin is related to the ERM (ezrin, radixin, and moesin) family of membrane-cytoskeletal linking proteins (Troffater et al., 1993). Because the related ERMs lack the ability to suppress cell growth, Schwannomin is a unique family member (Rouleau et al., 1993; Troffater et al., 1993). Schwannomin and ERM share the highest homology within the N-

terminus, referred to as the FERM domain. The FERM domain is a globular structure comprised of three subdomains, F1-F3, that structurally resembles a cloverleaf (reviewed in Ramesh, 2004). This structure is responsible for the interaction and localization of ERMs and Schwannomin to the plasma membrane (reviewed in Tsukita and Yonemura, 1999; Brault et al., 2001). The C-terminus of ERM and Schwannomin are less homologous, and therefore suggests that Schwannomin's inhibitory function might be encoded within this domain. Unlike ERMs, Schwannomin's C-terminus does not contain an actin binding region. However, Schwannomin can bind actin through a region localized within the N-terminus (Xu et al., 1998; Brault et al., 2001; James et al., 2001).

1.2.2 Conformational Regulation Of Schwannomin Activity

Key to the activity of ERMs and Schwannomin is their ability to form intramolecular and intermolecular associations (Sherman et al., 1997; Hamada et al., 2000; Pearson et al., 2000). Additional functions important to the activity of Schwannomin and ERMs include the phosphorylation and localization of each within the cell. ERMs and Schwannomin can bind to one another, creating dimers and/ or oligomers. They can also self-associate in a “head-to-tail” fashion, where the N-terminal FERM domain binds and masks the charged C-terminus. For ERMs, self association renders the proteins inactive, as they can no longer associate with actin. However, for Schwannomin, the closed, self-associated conformation is considered to be the active tumor suppressor form (Surace et al., 2004; reviewed in Okada et al., 2006). Both intramolecular and intermolecular associations are relieved by interactions with phospholipids like phosphoinositol-4, 5-bisphosphate, and phosphorylation (Hamada et al., 2000).

Phosphorylation occurs at a conserved C-terminal threonine in ERMS, and at serine 518 in Schwannomin (Hirao et al., 1996; Matsui et al., 1998; Gonzalez-Agosti et al., 1999; Rong et al., 2004). In the open, phosphorylated conformation, ERMs can actively associate with membrane components and bind actin, allowing for extracellular stimulus induced restructuring of the actin cytoskeleton (reviewed in Tsukita and Yonemura, 1999). For Schwannomin, the role S518 phosphorylation plays on regulating its function remains elusive. Studies have shown that S518 phosphorylation negatively regulates Schwannomin's ability to suppress growth, but it does not concomitantly increase cell proliferation (Shaw et al., 2001; Surace et al., 2004). Furthermore, the morphological and physiological changes that phosphorylation of Schwannomin at S518 imparts on the cell are poorly understood.

1.2.3 Phosphorylation Of Schwannomin S518 Is Mediated By p21-Activated Kinase And Protein Kinase A

Until recently, the only characterized phosphorylation site on Schwannomin was the C-terminal serine 518 residue. Schwannomin S518 can be phosphorylated by two kinases, p21-activated kinase (Pak) and protein kinase A (PKA; Kissil et al., 2002; Xiao et al., 2002). Little is known about the upstream mechanisms leading to either Pak- or PKA-mediated phosphorylation of Schwannomin in any cell type. Moreover, only 2 papers out of 24 have examined Schwannomin phosphorylation in Schwann cells, the afflicted cell in NF2 (Rangwala et al., 2005; Muranen et al., 2007). What is known, is that phosphorylation of Schwannomin S518 by Pak is dependent on the activity of Rac and/or Cdc42, members of the Rho GTPase family of actin cytoskeleton regulators (Shaw et al., 2001; reviewed in Hall, 2005). Studies performed in schwannoma cells

indicated that Schwannomin and Pak might co-regulate the activities of one another, as these cells expressed high levels of active Pak and Rac in the absence of Schwannomin expression (Kaempchen et al., 2003). Indeed, Schwannomin and Pak participate in a negative feedback loop, whereby Pak phosphorylation of S518 inactivates Schwannomin's growth suppression. Conversely, Schwannomin in an unphosphorylated state can bind and inhibit Pak activity (Kissil et al., 2003; Hirokawa et al., 2004). There is, however, a debate pertaining to the residues within Schwannomin that bind and inhibit Pak activity. One study suggests that Schwannomin binds Pak at its CRIB domain (Cdc42/Rac interactive binding domain), through the C-terminal residues 447-524 (Hirokawa et al., 2004). The binding of Rac/Cdc42-GTP to Pak's CRIB domain results in a conformational change that releases the autoinhibitory domain of Pak from its kinase domain, allowing Pak to autophosphorylate (at T423; Thompson et al., 1998; Zenke et al., 1999). Another study suggests that Schwannomin binds Pak through an N-terminal region, and that this interaction prevents Pak from targeting to the plasma membrane and to focal adhesions (Kissil et al., 2002). Although these studies provide insight into Schwannomin's ability to inhibit growth, it is important to note that both studies were performed *in vitro*, and not in cells. Similarly, PKA was shown through *in vitro* binding and kinase assays, to associate with and phosphorylate Schwannomin, at S518, in a Pak independent manner. Aside from these results, little else is known about the mechanisms contributing to PKA-dependent phosphorylation of Schwannomin in any cell type (Alfthan et al., 2004). Interestingly, there is now evidence that Akt/protein kinase B can phosphorylate an alternative serine (S315), as well as a threonine (T280) within the N-terminus of Schwannomin, targeting Schwannomin for ubiquitin-mediated degradation (Tang et al., 2007).

Many factors regulate the overall phosphorylation state of Schwannomin at S518, such as cell density, cell attachment, and growth factors (Shaw et al., 1998; Morrison et al., 2001; Lallemand et al., 2003). With increasing cell density, Schwannomin phosphorylation is reduced, allowing contact-dependent inhibition of growth. The suppression of growth observed may be mediated by the interaction of Schwannomin with the plasma membrane receptors N-cadherin and CD44 (Morrison et al., 2001; Lallemand et al., 2003). Studies performed in NIH-3T3 cells demonstrated that loss of adhesion resulted in decreased Schwannomin phosphorylation. Accordingly, attachment of the cells to fibronectin, a component of the extracellular matrix, resulted in phosphorylation of Schwannomin (Shaw et al., 1998). Stimulation of a rat schwannoma cell line (RT4) expressing exogenous Schwannomin with hyaluronic acid resulted in the reduction of Schwannomin phosphorylation levels (Morrison et al., 2001).

1.2.4 Schwannomin's Regulation of Actin Polymerization Dynamics

Aside from tumor suppression, Schwannomin also has the ability to rearrange the cortical actin cytoskeleton and induce morphological changes in cell structure, but the mechanism(s) that allow Schwannomin to regulate morphology are unclear. Over-expression of Schwannomin results in the formation of processes and microspikes in cells of fibroblast origin and schwannoma cells (Gutmann et al., 1999; Stokowski and Cox, 1999; Kissil et al., 2002; Surace et al., 2004). In these cells, Schwannomin is localized at the plasma membrane, along microspikes and in membrane ruffles, similar to the localization of ERMs (Scherer and Gutmann, 1996; Shaw et al., 1998; Brault et al., 2001; Kissil et al., 2002). Schwannoma cells lacking functional

Schwannomin expression, assume a more rounded shape, with elaborated stress fibers (Pelton et al., 1998; Kaempchen et al., 2003; Nakai et al., 2006). Upon reintroduction of Schwannomin, the schwannoma cells begin to assume a spindle, bipolar morphology, reminiscent of normal Schwann cells. In similar studies using RT4 rat schwannoma cells, the reintroduction of exogenous wild-type Schwannomin caused the tumorigenic cells to assume a typical SC morphology (Surace et al., 2004).

One possible mechanism that might contribute to Schwannomin's ability to direct actin polymerization dynamics involves S518 phosphorylation. Studies utilizing RT4 schwannoma and LLC-PKI epithelial cells, examined the expression patterns and localizations of Schwannomin S518 phospho-variants (Surace 2004, Kissil 2002). A phospho-mimicking form of Schwannomin, where S518 was mutated to an aspartate (S518D), localized within vesicular structures in LLC-PKI cells, whereas both the wild type and an unphosphorylatable form of Schwannomin, where S518 was mutated to an alanine (S518A) localized in a typical fashion to the plasma membrane (Kissil et al., 2002). RT4 schwannoma cells expressing Schwannomin S518D formed elongated processes, while the wild-type and Schwannomin S518A assumed a normal plasma membrane distribution (Surace et al., 2004). These findings emphasize the fact that Schwannomin not only functions as a growth regulator but also as an active regulator of actin dynamics, a process that may be regulated by phosphorylation. Therefore any discoveries regarding the effect(s) of S518 phosphorylation on Schwannomin's function would lead to increased understanding of Schwannomin's role during the development of peripheral neuropathies, like NF2.

1.2.5 Protein Interactions Regulating Schwannomin Function

Schwannomin interacts with several proteins associated with focal adhesion formation, cell-cell adhesion, proliferation and survival. These proteins include paxillin, β 1 integrin, ErbB2, as well as, cadherins, CD44, Akt and HEI10 (Morrison et al., 2001; Fernandez-Valle et al., 2002; Lallemand et al., 2003; Rangwala et al., 2005; Gronholm et al., 2006; tang et al., 2007). An interaction of significant physiological relevance is Schwannomin's association with paxillin. Schwannomin contains two paxillin binding domains (PBD; Fernandez-Valle et al., 2002). PBD1, located between amino acids 50-70 in the N-terminus of Schwannomin, is responsible for Schwannomin's localization to the plasma membrane. PBD1 is encoded by exon 2 of Schwannomin, a region that when conditionally deleted in mice results in a characteristic NF2 phenotype consisting of Schwann cell hyperplasia, schwannoma formation, and dysmyelination (Giovannini et al., 2000; Fernandez-Valle et al., 2002). Patients with mutations within this exon present the more severe forms of NF2, indicating that paxillin-mediated plasma membrane localization is critical for Schwannomin's tumor suppressor function. PBD2, located between amino acids 425-450, has no known function and is encoded by exons 11 and 12 of the *NF2* gene. Mutations within this region have been identified, but are not usually linked to an increased severity of NF2.

Paxillin is an adaptor protein that serves as a molecular scaffold for several interacting proteins involved in focal adhesion formation, such as focal adhesion kinase (FAK), in receptor mediated signal transduction, such as β 1 integrin and ErbB2, and in actin rearrangement, such as talin and

vinculin (reviewed in Turner, 2000). Paxillin contains four double Zn²⁺ finger LIM domains and five leucine aspartate (LD) rich regions. LIM domains 2-3 are responsible for paxillin's membrane localization, whereas the LD domains are responsible for binding the majority of paxillin's numerous interacting signaling proteins. FAK binds paxillin at LD2, facilitating the indirect interaction of paxillin with receptor tyrosine kinases, like ErbB2, through the SH2/SH3 binding domains of FAK (Brown et al., 1996). Another LD-mediated association that could have great significance to NF2 is the indirect interaction of Pak with paxillin. The association of Pak with paxillin is mediated through its interaction with the Pak-interacting exchange factor (Pix) and the paxillin kinase linker (PKL; Turner et al., 1999). PKL binds paxillin at LD4, and is an ARF-associated guanine nucleotide activating protein (GAP). GAPs regulate the activity of small G-proteins, like ARF and the Rho GTPases by inactivating them through the hydrolysis of GTP to GDP. Pix binds both Pak and PKL, and is a guanine nucleotide exchange factor (GEF) that activates the Rho GTPases by exchanging GDP for GTP. Pix facilitates the activation of Pak due its ability to activate both Rac and/or Cdc42. Interestingly, Schwannomin can bind paxillin at both LD2 and LD3 (unpublished observations, CFV and SEG). Whereas LD2 has other binding partners like FAK and vinculin, no other protein is known to associate with the LD3 domain of paxillin. Although Schwannomin and Pak, if bound to paxillin, would be in a close molecular proximity that could allow for the phosphorylation of Sch-S518, it is not known whether paxillin binding is required for this event. Due to the significance of paxillin binding to Schwannomin function, the molecular consequence of this interaction would be critical in determining both Schwannomin's and paxillin's role during the development of NF2.

Integrins are a group of transmembrane cell adhesion molecules that are heterodimeric in nature and are composed of an α and a β subunit. These receptors are activated in response to binding extracellular matrix (ECM) components such as fibronectin, laminin, vitronectin, and collagen (reviewed in Lee and Juliano, 2004). Through interactions of their cytoplasmic tails with focal adhesion molecules, integrins associate with the actin cytoskeleton, linking the extracellular environment with the inner cytoarchitecture of cells. Aside from adhesion, integrins are also important regulators of proliferation, differentiation, survival, apoptosis, migration and cell morphology in many cell types (reviewed in Hynes, 2002). Integrins can engage in bi-directional signaling whereby extracellular signals can trigger intracellular events (outside-in signaling), or intracellular events can induce integrins to adhere to the ECM (inside-out signaling). The intracellular transduction of signals induced by integrins can also occur in two ways: either (1) directly downstream of the integrin subunits alone (in-cis), or (2) through the co-activation of other membrane receptors such as growth factor stimulated receptor tyrosine kinases (in-trans). Downstream signaling molecules activated in response to integrin adherence to the ECM include, FAK, MAP kinases (MAPKs), extracellular signal regulated kinase (Erk), c-Jun kinase (JNK) and the Rho GTPases, Rac, Cdc42, and Rho, and Pak; all important regulators of cell proliferation, cell spreading and cell morphology (reviewed in Lee and Juliano, 2004). Another important molecule found to interact with integrins is paxillin, which was shown to directly associate with peptides mimicking the common region of the intracellular domain of β 1 integrin, and to directly bind the intracellular tail of α 4 integrin (Schaller et al., 1995; Tanaka et al., 1996; Han et al., 2001). Interestingly, Schwannomin can also associate with β 1 integrin, and more specifically it can bind to the intracellular cytoplasmic domain of β 1 integrin directly

(Obremski et al., 1998; unpublished observation, CFV). Although Schwannomin can interact with integrins, the physiological consequences of this interaction are unknown. Because $\beta 1$ integrin can associate with paxillin and lead to the activation of Rac, Cdc42, and Pak, it is possible that stimulation of $\beta 1$ integrin through adherence to the ECM could regulate Schwannomin function.

The ErbB receptors are members of the EGF superfamily of receptor tyrosine kinases that are stimulated in response to growth factors. There are four family members, ErbB1 (EGFR), ErbB2, ErbB3, and ErbB4. Upon binding to growth factors, ErbB1, ErbB3, and ErbB4 initiate the formation of hetero- and homo-dimeric signaling complexes (reviewed in Citri et al., 2003). Schwann cells express significant amounts of ErbB2 and ErbB3, and very low levels of ErbB4. The ErbB2/ErbB3 heterodimer is the most prevalent and widely studied signaling complex activated in Schwann cells (reviewed in Nave and Salzer, 2006). Interestingly, ErbB3 can bind ligand but it is deficient in kinase activity, whereas ErbB2 cannot bind ligand but has an active catalytic domain; therefore the signaling from either ErbB2 or ErbB3 can only be achieved when the receptors dimerize (Guy et al., 1994; Klapper et al., 1999). The growth factor family present within the nervous system that activates ErbB2/ErbB3 is known as the neuregulins (NRG), and they are needed for every stage of Schwann cell development. Upon binding NRG, ErbB3 and ErbB2 dimerize, allowing the activation of downstream signaling pathways leading to proliferation, such as Ras-MEK (from ErbB2), and survival, such PI3K and Akt (from ErbB3). ErbB2 is considered a potent oncogene and its overexpression or constitutive activation is found in multiple cancer types, such as breast, lung, prostate, and ovarian cancers (reviewed in Hsieh

and Moasser, 2007). Schwannoma cells deficient in Schwannomin expression have also been shown to have upregulated ErbB2 signaling (Hansen and Linthicum, 2004). Additionally, the RT4 schwannoma cell line contains a point mutation within the catalytic domain of ErbB2 that causes constitutive activation of ErbB2, and hyperproliferation of these cells (Nikitin et al., 1991). This evidence suggests that Schwannomin signaling might regulate ErbB2 function. Indeed, Schwannomin was shown to participate in receptor internalization dynamics of EGFR and regulate its activity in mouse embryonic fibroblasts (Curto et al., 2007). Moreover, Schwannomin was shown to indirectly associate with ErbB2 through paxillin (Fernandez-Valle et al., 2002). Although Schwannomin and ErbB2 interact in a cooperative signaling pathway, the consequences of this association on Schwannomin function have not been explored. ErbB2 has been shown to stimulate the activities of Pak and the Rho GTPases, Rac and Cdc42 (reviewed in Lee and Juliano, 2004). It therefore is possible that activation of ErbB2 may alter Schwannomin's ability to suppress growth by promoting its Pak-dependent phosphorylation.

1.3 Schwann Cells: The Myelinating Glia Of The Peripheral Nervous System

Schwann cells (SC) are specialized glia of the peripheral nervous system that are responsible for myelinating axons to allow for the proper and fast conduction of the action potential. SCs arise from neural crest cells (NCC), and through stages of regulated development these cells can mature into SC precursors, then immature SCs, and finally either non-myelinating or myelinating SCs. Unlike oligodendroglia in the central nervous system, SC myelination and development is reversible, that is, upon axonal injury myelinating SCs can de-differentiate and revert back to an immature SC stage. As the axon re-innervates the muscle, the SCs will re-contact and

remyelinate axons (reviewed in Jessen and Mirsky, 2005). Each stage of SC development is intimately coordinated and dependent on axonal cues and the extracellular environment, most notably the axonal mitogen NRG1 type 3, and laminin, a component of a specialized form of ECM formed by SCs. Both NRG1 type 3 and laminin are required for all stages of SC development including maturation, proliferation, migration, and differentiation. Whereas NRG1 type 3 is expressed by NCCs and in all stages of axonal and SC development, the basal lamina is present only after NCCs mature into SCs. Aside from NRG and laminin, several additional proteins have been identified as specific markers for the different stages of SC development, such as activator protein 2 α (AP2 α) that is present in NCCs and SC precursors, Cadherin 19 that is expressed in SC precursors only, and glial fibrillary acidic protein (GFAP), S100 calcium binding protein (S100), Oct6, and O4 that are only expressed in immature and mature SCs. Although several proteins are known to be present at certain stages of development, the molecular mechanisms controlling SC differentiation and myelination have been only partially elucidated.

1.3.1 Signals Determining SC Differentiation And Myelination

Myelination is a process that requires the formation of a one-to-one relationship of a SC with a large diameter axon. Ensheathment involves the extension of multiple processes from one SC around multiple small diameter axons. Several morphological steps are involved in the initiation of myelination. First, in a process termed radial sorting, axon bundles are separated by the extension of multiple SC processes around and through axons. This process is coordinated with proliferation, as the segregation of axons enables SCs to sense the numbers and diameters of

axons that will need to be myelinated. After radial sorting and the identification of large diameter axons, the SCs destined to myelinate must retract some processes and instead extend processes bi-directionally along the axon to form the internode, the region between two Nodes of Ranvier. Once the internode is established, a SC will then extend an expansive membrane laterally and envelop and wrap an axon, creating a multi-lamellar layer. Like the other stages of SC development, myelinating SCs can be identified by the expression of proteins like myelin basic protein (MBP), P0, and β 4 integrin (reviewed in Jessen and Mirsky 2005). MBP and P0 are proteins involved in the compaction of the myelin layer, while β 4 integrin is thought to be responsible for anchoring the external SC membrane to the basal lamina. β 4 integrin is able to stabilize the SC cytostructure more effectively because it has a longer cytoplasmic domain that interacts directly with intermediate filaments rather than actin filaments. Other proteins regulated during SC myelination are the transcription factors Krox-20 and octamer-binding transcription factor 6 (Oct-6). These transcription factors are inversely regulated upon SC differentiation. Oct-6 expression is downregulated in myelinating SCs, whereas Krox-20 expression and function is upregulated, as its expression is known to precede and be required for transcription of the myelin genes, P0 and MBP. Peripheral neuropathies such as Charcot-Marie-Tooth (CMT) disease and congenital hypomyelinating neuropathy (CGN) are caused by mutations in Krox-20, resulting in demyelination and myelin abnormalities (Yoshihara et al., 2000; Decker et al., 2006). While it is known that proteins like MBP, P0 and β 4 integrin are upregulated, and the expression of transcription factors like Krox20 and Oct-6 are controlled during myelination, the mechanisms inducing differentiation of an immature SC into a myelinating SC are still elusive.

1.3.2 Extracellular Matrix Mediated SC Development: Signaling from Laminins and β 1 integrin

Basement membrane(s), or basal lamina, is a specialized form of extracellular matrix (ECM) that surrounds individual cells and is mostly comprised of laminin (reviewed in Colognato and Yurchenco, 2000). Laminins are a family of glycoproteins that form heterotrimers containing an α , β , and γ subunit. Laminins can self-associate, as well as interact with other ECM components such as collagen and fibronectin. Laminins are responsible for providing the structural integrity of the basal lamina, and are key regulators of cellular events in Schwann cell development, like proliferation, migration, and differentiation. The deposition of basal lamina by SCs is important to their maturation into a myelinating phenotype. Several peripheral neuropathies, such as CMT, and muscular dystrophies, such as merosin-deficient muscular dystrophy, are caused by mutations in laminin isoforms (reviewed in Feltri and Wrabetz, 2005). Seven laminin genes are present in the mammalian neuromuscular system including, α 1, α 2, α 4, α 5, β 1, β 2 and γ 1 (reviewed in Patton, 2000). From the seven laminin genes expressed the neuromuscular system, seven laminin isoforms are produced, laminins 1, 2, 4, 8, 9, 10, and 11. Present in all the laminin isoforms is the laminin γ 1 subunit (reviewed in Patton, 2000). Conditional ablation of laminin γ 1 in mouse Schwann cells leads to dysmyelination, as SCs are unable to radial sort and initiate myelination. Furthermore, depending on the stage of development when the laminin genes are knocked out, it can also lead to reduced SC proliferation and apoptosis (Chen and Strickland, 2003; Yu et al., 2005).

The receptors on SCs responsible for binding laminins are the integrins, $\beta 1$ and $\beta 4$, and dystroglycan. Similar to the conditional deletion of the laminin $\gamma 1$ gene, conditional knockout of $\beta 1$ integrin in mice results in the failure of SCs to radially sort axons within bundles, leading to impaired myelination. A recent attempt to characterize the downstream signaling events deregulated in $\beta 1$ integrin null mice showed that conditional deletion of Rac, a member of the Rho GTPase family of cytoskeletal regulators, in SCs results in failed radial sorting and myelination, similar to the phenotype of $\beta 1$ integrin null SCs (Benninger et al., 2007; Nodari et al., 2007). These results support the findings that Rac activation occurs in response to $\beta 1$ integrin stimulation, and that the morphological changes occurring in response to integrin activation are mediated through Rac (Del Pozo et al., 2004). The Rac null SCs, like the $\beta 1$ integrin null, failed to produce radial membrane protrusions required for the extension of multiple processes and the separation of axons. Although advancements are being made in understanding the extracellular signals required for SC myelination, the mechanisms induced downstream of these molecules controlling SC morphology still remain unclear. Interestingly, as mentioned earlier, Schwannomin not only interacts with $\beta 1$ integrin but it is also phosphorylated downstream of Rac activation, and this event alters actin dynamics. Additionally, the conditional disruption of Schwannomin in mice results in dysmyelination, suggesting that Schwannomin may function downstream of laminin, $\beta 1$ integrin, and Rac to allow for the restructuring of the actin cytoskeleton, and process formation.

1.3.3 Axonal Cues Regulating SC Development: The Roles Of Neuregulin And ErbB2 In SC Myelination

As mentioned earlier, SC development is intimately coordinated by and dependent on axonal cues. One of the most significant axonal proteins involved in every stage of SC maturation is the Neuregulin-1 (NRG1) family of epidermal-like growth factors, or mitogens. Axonal NRG1 can either be membrane-associated or secreted into the extracellular environment. There are more than 15 isoforms of NRG1 present throughout the body, but the most abundant forms found in the nervous system are NRG1 types 1-3 (reviewed in Nave and Salzer, 2006). NRG1 types 1-3 are expressed by motor neurons, dorsal root ganglia neurons, and by glia (reviewed in Falls, 2003). Not only are NRGs implicated in nervous system development and neuropathies like schizophrenia, but they are also essential for heart development and breast function, as perturbed neuregulin signaling results in heart disease and breast cancer. The most relevant of all the NRG1s to SC development and myelination is NRG1 type 3. The expression of NRG1 type 3 was found to be required for the maturation of NCCs to SC precursor and to myelination, as conditional disruption of NRG1 type 3 in mice lead to hypomyelination, slowed conduction velocities, as well as aberrant proliferation, migration and maturation of SCs (Michailov et al., 2004; Lai, 2005; Taveggia et al., 2006). When examined, it was found that SCs in NRG1 type 3 null mice were localized near dorsal root ganglia, resulting from the inability of these SCs to contact, migrate, and defasciculate axons (reviewed in Garratt et al., 2000b). Re-expression of NRG1 type 3 in the null mice rescued the aberrant defects in proliferation, migration, and myelination, while exogenous expression in normal neurons, both large and small diameter, resulted in hypermyelination and increased myelin thickness (reviewed in Lai, 2005).

The principal receptor(s) on SCs that bind axonal NRG1 is the heterodimer, ErbB2/ErbB3 (Vartanian et al., 1997). Consistent with NRG1 type 3 null mice, disruption of either ErbB2 or ErbB3 in SCs results in reduced proliferation, migration and differentiation (Garratt et al., 200a; Michailov et al., 2004; Lyons et al., 2005). The disruption of ErbB2 and ErbB3 in mice is conditional from SCs, as a complete knockout of ErbB2 and ErbB3 results in embryonic lethality, as these mice have impaired cardiac development, as do NRG1 knockout mice (reviewed in Citri et al., 2003). Recently, it was suggested that Cdc42 functions downstream of NRG1 during SC myelination, as mice with a conditional deletion of Cdc42 in SCs resulted in reduced SC proliferation and amyelination similar to the phenotype of NRG1 null SCs (Benninger et al., 2007). Further analysis showed that stimulation of SCs with NRG1 increased the activity of Cdc42 significantly. These results provided a partial mechanism for NRG signaling in SCs, but how this stimulation results in the inability of SCs to migrate and myelinate is unknown. Like β 1 integrin and Rac, Schwannomin was shown to participate in downstream signaling from both ErbB2 and Cdc42. Cdc42 is known to regulate the activity of Schwannomin, while the functional consequences of the interaction of Schwannomin with ErbB2 are unclear.

In assessing Schwannomin function during SC development and NF2, we find that its activity as a tumor suppressor and in actin dynamics is regulated by its phosphorylation, localization and

conformation. Phosphorylation occurs through Rac-or Cdc42-dependent activation of Pak, or through PKA, and allows for the stabilization of an open conformation and the inactivation of Schwannomin's growth suppression, but the underlying mechanisms promoting its phosphorylation remain unclear (Kissil et al., 2002; Xiao et al., 2002; Alfthan et al., 2004). Localization of Schwannomin to the plasma membrane, and its interaction with the membrane receptors, β 1 integrin, and ErbB2, is mediated through paxillin binding, but the physiological relevance of β 1 integrin, and ErbB2 interaction on Schwannomin function is unknown (Fernandez-Valle et al., 2002). Schwannomin also appears to have a role in SC development and differentiation, as conditional deletion of Schwannomin exon 2, encoding paxillin binding domain 1, in mouse SCs results in dysmyelination and the formation of schwannomas (Giovannini et al., 2000; Fernandez-Valle et al., 2002). Although the conditional mice reveal that paxillin binding is physiologically relevant to not only the development of NF2 but to Schwannomin function in myelination, our understanding of Schwannomin's role during myelination is unknown. Three molecules recurring as key regulators of Schwannomin activity, NF2 and peripheral neuropathy development, and SC myelination are paxillin, β 1 integrin, and ErbB2. In order to understand how these molecules regulate Schwannomin activity, and how Schwannomin functions in both NF2 and SC development, three questions will be addressed in this dissertation: (1) Is paxillin binding and membrane localization required for Schwannomin S518 phosphorylation? (2) What are the mechanisms promoting Schwannomin S518 phosphorylation downstream of NRG and laminin? (3) What are the effects of Schwannomin S518 phosphorylation on SC morphology and myelination?

CHAPTER 2

PHOSPHORYLATION OF THE NF2 TUMOR SUPPRESSOR IN SCHWANN CELLS IS MEDIATED BY CDC42-PAK AND REQUIRES PAXILLIN BINDING

2.1 Introduction

Neurofibromatosis type 2 (NF2) is an inherited disorder characterized by formation of bilateral vestibular schwannomas. NF2 is associated with mutations in the *nf2* gene that leads to loss of expression of Schwannomin (Sch), also called merlin (Rouleau et al., 1993; Trofatter et al., 1993). Sch is a member of the Band 4.1 superfamily of membrane-cytoskeleton linking proteins that includes ezrin, radixin and moesin (ERM). These proteins bind F-actin either directly or indirectly and modify actin polymerization dynamics (Takeuchi et al., 1994; Gary and Bretscher, 1995; Bretscher et al., 1997; Sainio et al., 1997; Scoles et al., 1998; James et al., 2001). Loss of Sch function in schwannoma cells is associated with F-actin instability, formation of excessive ruffling membranes, and persistent but slow proliferation (Pelton et al., 1998; Gutmann et al., 1999a; Sherman and Gutmann, 2001, Bashour et al., 2002). Reintroduction of Sch into schwannoma cells reverses some of the cytoskeletal defects including the reduction of ruffling membranes and surface area (Gutmann et al., 1999a; Bashour et al., 2002; Schulze et al., 2002; Surace et al., 2004).

Sch and ERMs exists in an open and a closed conformation mediated by intramolecular association of the N- and C-termini (Gary and Bretscher, 1995; Huang et al., 1998; Gonzalez-Agosti et al., 1999; Gutmann et al., 1999b). Phosphorylation of Sch's C-terminus appears to stabilize the open conformation that localizes to the plasma membrane (Shaw et al., 1998;

Gonzalez-Agosti et al., 1999; Bretscher et al., 2000; Rong et al., 2004). Conformation and phosphorylation regulate Sch's tumor suppressor activity (Gutmann et al., 1999b; Surace et al., 2004). The closed, unphosphorylated conformation of Sch is associated with an anti-proliferative function, whereas the open, phosphorylated conformation is associated with a growth permissive function (Sherman et al., 1997; Gutmann et al., 1999b; Morrison et al., 2001; Surace et al., 2004).

Sch contains multiple phosphorylated residues, but the only characterized phosphorylation site is serine 518 in the C-terminus, by p21 activated kinase (Pak) and protein kinase A (Shaw et al., 1998, 2001; Kissil et al., 2002; Xiao et al., 2002; Alfthan et al., 2004). Of note, Sch and Pak both associate with paxillin, a 70kDa adaptor protein (Turner et al., 1999; Fernandez-Valle et al., 2002). Sch binds paxillin directly through two paxillin binding domains (PBD1 and PBD2; Fernandez-Valle et al., 2002). PBD1, amino acids 50-70, is encoded by exon 2 and PBD2, amino acids 425-450, overlaps with a putative Pak inhibitory domain (Hirokawa et al., 2004). Pak binds paxillin indirectly through association with paxillin kinase linker (PKL/GIT1), an Arf-GTPase activating protein, and PIX, a Cdc42/RacGTPase Exchange Factor (GEF; Manser et al., 1998; Turner et al., 1999, 2000; West et al., 2001). The binding of Sch and Pak to paxillin allows for the stable association of each protein with the plasma membrane (Turner et al., 1999; Fernandez-Valle et al., 2002). Paxillin mediates formation of integrin dependent focal adhesions and allows transduction of signals from integrins, receptor tyrosine kinases, and G-protein coupled receptors (Hildebrand et al., 1995; Schaller et al., 1995; Tachibana et al., 1995; reviewed in Turner et al., 2000; Chen et al., 2000, Fernandez-Valle et al., 2002). Sch and Pak have not

been studied together in any cell type and the upstream events leading to Sch phosphorylation are not well understood.

Here, we report that Sch binding to paxillin through PBD1, but not PBD2, is essential for Sch phosphorylation. Only a subset of Sch molecules is phosphorylated at specific membrane domains where they colocalize with paxillin, P-Pak, Cdc42, but not Rac. SchS518A/D-GFP variants both localize to the plasma membrane where they promote distinct morphologies. Together our findings suggest that plasma membrane associated Sch locally alters cytoskeletal organization of SCs in a Cdc42-Pak dependent manner.

2.2 Materials and Methods

2.2.1 Materials

Sch-EGFP-N1, Sch Δ PBD1 (residues 50-70 deleted)-EGFP-C1, Sch Δ PBD2 (residues 425-450 deleted)-EGFP-C1, Sch $\Delta\Delta$ PBD1&2 (residues 50-70 and 425-450 deleted)-EGFP-C1, Sch-pcDNA3.1 HisC (N-terminal Xpress tag), Sch Δ PBD1-pcDNA3.1 HisC, Sch Δ PBD2-pcDNA3.1 HisC, and Sch $\Delta\Delta$ PBD1&2-pcDNA3.1 HisC were described previously or were constructed in the laboratory using standard techniques (Fernandez-Valle et al., 2002). Antibodies were purchased from the following sources: Rac antibodies from Santa Cruz Biotechnology and BD Biosciences, paxillin antibody from BD Biosciences, phospho-Pak antibody from Rockland Immunologicals, Inc, phospho-serine518-Sch antibody from Abcam, Myc antibody from Cell Signaling Technologies and Xpress antibody from Invitrogen.

2.2.2 Cell Culture

Primary rat SC cultures were prepared from neonatal pups using the Brockes method as previously described (Brockes et al., 1979, Chen et al., 2000). SCs were expanded on poly-L-lysine coated (200 μ g/ml in borate buffer, pH 8.6, Sigma) tissue culture dishes in Dubelcco's Modified Eagle Medium (Gibco/BRL) with 10% heat inactivated FBS (Hyclone), 2 μ M forskolin (Sigma) and 20 μ g/ml bovine pituitary extract (D10M; Biomedical Technologies, Inc.). Cultures were expanded no more than six times before use.

2.2.3 Transfections

SCs were transfected using Lipofectamine 2000 (Invitrogen) following manufacturer's protocol. Briefly, SCs were incubated in Opti-MEM (Invitrogen) and Lipofectamine with either 2 μ g of Xpress-tagged plasmid DNA or 250ng of EGFP-tagged plasmid DNA. After four hours, the transfection medium was removed and was replaced with standard growth medium. The cells were analyzed 36 hours later and were either extracted for use in immunoprecipitations or were immunostained for visualization of cell morphology.

2.2.4 Immunoprecipitation And Western Blotting

SCs were lysed in TAN buffer (10mM Tris-acetate, 1% IGEPAL, 100mM NaCl) with a cocktail of inhibitors as previously described (Chen et al., 2000). Approximately 100 μ g of total protein was used for immunoprecipitation with anti-Xpress antibody after pre-clearing using normal mouse IgG as previously described (Chen et al., 2000). The samples were loaded onto a 10% SDS-PAGE gel and proteins were separated at 200V for 50 minutes and were transferred onto PVDF membranes. The membranes were blocked using 5% bovine serum albumin (BSA) in TBS-T for 1 hour at room temperature. The primary antibodies were incubated for either 1 hour at room temperature, or overnight at 4°C, in 5% BSA/TBS-T. Horseradish peroxidase conjugated secondary antibody was applied for 30 minutes and was detected using Super Signal West Pico Chemiluminescent Substrate (Pierce).

2.2.5 Immunostaining

Primary rat SCs were grown on German glass coverslips coated with poly-L-lysine (200 μ g/ml in borate buffer, pH 8.6), and laminin (25 μ g/ml in carbonate buffer, Invitrogen) until 80%

confluent. SCs were transfected with EGFP-plasmid DNA as described above. SCs were washed in phosphate buffer (pH 7.6), were fixed in 4% paraformaldehyde for 10 minutes at room temperature and were permeabilized with 4% paraformaldehyde + 0.2% Triton X-100 for 10 minutes. SCs were incubated with 10% normal goat serum for 30 minutes followed by incubation with primary antibodies for 1 hour. Alexa Fluor (Molecular Probes) conjugated secondary antibodies were added for 30 minutes and SCs were post-fixed for 5 minutes in 4% paraformaldehyde and were mounted in Gel-Mount (Biomed). For each experiment, 2-4 coverslips were transfected with each construct and 3-4 repetitions were carried out. All coverslips were imaged and representative cells were selected. Images were obtained on a Zeiss LSM510 confocal microscope and were processed identically.

2.2.6 Pak-CRIB Pull Down Assay

Assays were performed using an EZ-Detect GTPase Activation kit according to the manufacturer's protocol (Pierce). Briefly, SCs were incubated in D10M with or without 100 μ M NSC23766 (Calbiochem) overnight, at 37°C. SCs were extracted in 1x Lysis/Binding/Wash buffer (Pierce). Approximately 500 μ g of total lysate was incubated with a Swell Gel Immobilized Glutathione Disc (Pierce), along with 20 μ g of GST-Pak CRIB. For controls, 500 μ g of SC lysate were incubated with either GTP γ S, for a positive control and with GDP, for a negative control. Samples were incubated with GST-Pak CRIB for 1hr at 4°C while rocking. The samples were centrifuged, washed, and eluted. After elution, the equivalent of 250 μ g of sample was run on a 10% SDS-PAGE gels and was transferred as described above. The membranes were probed first for Rac, then GST, and were then stripped and re-probed for

Cdc42. Rac- and Cdc42-GTP expression levels were normalized to GST- Pak CRIB levels.

Total SC lysates were analyzed for PS518, Rac, Cdc42, P-Pak and GAPDH. Expression levels of total Rac, Cdc42, PS518, and P-Pak were normalized to GAPDH.

2.3 Results

2.3.1 Deletion Of Paxillin Binding Domain 1 Prevents Sch Phosphorylation

To determine if binding to paxillin influences Sch phosphorylation, plasmids encoding Xpress-tagged PBD deletion variants of Sch were transiently transfected into primary rat SCs. The fusion proteins were immunoprecipitated with anti-Xpress antibody and were immunoblotted with a Sch PS518 antibody (PS518; Figure 2.1). Full-length Sch containing both PBDs and Sch Δ PBD2 lacking the C-terminal binding domain, were phosphorylated on S518. In contrast, Sch Δ PBD1 lacking the N-terminal binding domain, and Sch $\Delta\Delta$ PBD1/2, lacking both PBDs were not phosphorylated (Figure 2.1 and data not shown). The membranes were then re-probed for paxillin. Paxillin co-immunoprecipitated with both full length Sch and Sch Δ PBD2, but not with Sch Δ PBD1. This suggests that Sch-S518 phosphorylation requires paxillin binding at PBD1 and localization to the plasma membrane.

To confirm these results using a cellular assay, SCs were transiently transfected with plasmids directing expression of GFP-tagged PBD deletion variants of Sch. After 36 hours, SCs were immunostained with PS518 antibody (Figure 2.2). SCs expressing full length Sch-GFP become very elongated and thin, and GFP fluorescence was observed throughout cellular processes, radial protrusions, and at the plasma membrane surrounding the cell body. However, a high level of PS518 fluorescence was found only at the tips of atypical radial membrane protrusions that formed along major processes, and colocalized with Sch-GFP fluorescence. Sch-GFP present along the plasma membrane, in areas lacking cellular protrusions as well as within the

cell, was not phosphorylated. This suggests that Sch was phosphorylated by endogenously expressed kinases active at specific membrane domains. SCs expressing Sch Δ PBD1-GFP displayed spread morphology. There was diffuse intracellular GFP and PS518 fluorescence but membrane-associated fluorescence was not present. This is consistent with the requirement of PBD1 for directed translocation of Sch to the plasma membrane (Fernandez-Valle et al., 2002). SCs expressing Sch $\Delta\Delta$ PBD1/2-GFP behaved as those expressing Sch Δ PBD1-GFP (data not shown). SCs expressing Sch Δ PBD2-GFP were also atypically elongated and resembled SCs expressing Sch-GFP. There was a marked increase in total PS518 fluorescence in SCs expressing Sch Δ PBD2-GFP compared to SCs expressing Sch-GFP. The majority of Sch Δ PBD2-GFP molecules appeared to be phosphorylated regardless of their localization. These results suggest that each PBD in Sch has a unique function that impacts phosphorylation at serine 518.

2.3.2 Deletion Of PBD2 Is Not Associated With Increased P-Pak Levels

PBD2 (amino acids 425-450) overlaps with a putative domain (amino acids 447-524) reported to inhibit Pak activity by interfering with binding of Cdc42/Rac-GTP to Pak's CRIB domain (Hirokawa et al., 2004). This has been proposed as a regulatory loop between Sch and Pak. To determine if the increase in PS518 fluorescence observed when Sch Δ PBD2-GFP was expressed in SCs could be due to increased Pak activity, we immunostained SCs expressing Sch PBD deletion variants with phosphothreonine 423-Pak (P-Pak) antibody (Figure 2.3). SCs expressing Sch-GFP had a dramatic increase in P-Pak expression, but it was restricted to radial membrane protrusions that formed along SC processes, similar to those in Figure 2.2, which displayed

increased PS518 fluorescence. P-Pak and Sch-GFP colocalized in these domains and were also observed within filopodia extending periodically along the cell length. In SCs expressing Sch Δ PBD1-GFP, P-Pak expression was detectable only at high magnification within radially extending filopodia that did not contain Sch Δ PBD1-GFP. In SCs expressing Sch Δ PBD2-GFP, P-Pak expression was found at the tips of radial filopodia and at the peripheral-most aspects of membrane protrusions where it colocalized with Sch Δ PBD2-GFP. P-Pak was not observed within membrane protrusions or in SC processes that contained high levels of Sch Δ PBD2-GFP fluorescence. It is unlikely that the increase in PS518 fluorescence observed for Sch Δ PBD2-GFP in Figure 2.2 is due to the disruption of Sch's Pak inhibitory domain.

2.3.3 Expression Of Active Forms Of Cdc42 And Rac Indiscriminately Increases

P-Pak Levels In SCs

To determine whether Pak could phosphorylate Sch at the plasma membrane, we first tested the ability of active forms of Cdc42 and Rac to increase Pak activity, as assessed by Pak autophosphorylation at threonine 423. SCs were transiently transfected with Myc-Q61LCdc42 and Myc-Q61LRac plasmids and were immunostained with P-Pak and Myc antibodies (Figure 2.4). SCs expressing Myc-Q61LCdc42 had an overall increase in P-Pak expression compared to surrounding untransfected cells. A focal increase in P-Pak fluorescence was found at the distal tips of process extensions where it co-localized with a focal increase in Myc-Q61LCdc42 fluorescence (Figure 2.4, arrows). SCs transfected with Myc-Q61LRac also displayed a uniform increase in P-Pak expression compared to surrounding untransfected cells. The P-Pak and Myc-

Q61LRac fluorescence co-localized throughout the cell. This demonstrates that both active forms of Cdc42 and Rac can increase overall Pak activity in SCs.

2.3.4 Expression Of Active Cdc42 And Rac Does Not Promote Unrestricted Phosphorylation Of Endogenous Sch But Does Increase Phosphorylation Of Sch-GFP

To assess whether Cdc42 and Rac function equivalently to promote Pak-dependent phosphorylation of endogenously expressed Sch, SCs were transiently co-transfected with Myc-Q61LCdc42 and Myc-Q61LRac and GFP and were immunostained with PS518 and Myc antibodies (Figure 2.5). Dominant negative forms of Cdc42 and Rac (T17N) were also transfected into SCs but repeatedly resulted in cell death precluding analysis of their effects. Expression of GFP alone did not alter the level or distribution of PS518 fluorescence with respect to adjacent untransfected cells. Endogenous PS518 fluorescence was diffusely present in the perinuclear cytosol and in cellular processes. Surprisingly, expression of Myc-Q61LCdc42 and Myc-Q61LRac did not lead to an increase in PS518 fluorescence throughout the cell as was observed for P-Pak. SCs expressing both GFP and Myc-tagged Cdc42 and Rac had similar levels of PS518 as untransfected SCs. A slight increase in PS518 fluorescence that co-localized with Myc-Q61LCdc42 was observed at the cell periphery and in cellular processes (Figure 2.5, arrows). This suggests that the majority of endogenous Sch is not readily accessible for Cdc42 and Rac dependent phosphorylation.

To assess whether Cdc42 and Rac function equivalently to promote phosphorylation of exogenously expressed Sch, Myc-Q61LCdc42 and Myc-Q61LRac plasmids were transiently co-transfected with Sch-GFP into SCs (Figure 2.6). In SCs expressing Sch-GFP alone, there was a

high level of Sch-GFP fluorescence along cellular processes, membrane protrusions, and at the plasma membrane surrounding the cell body. PS518 fluorescence did not concomitantly increase in all GFP-labeled domains. It was expressed in some membrane protrusions and along major processes, but was absent from the plasma membrane surrounding the cell body that had multiple filopodia containing Sch-GFP (Figure 2.6, arrowheads). Co-expression of Sch-GFP and Myc-Q61LCdc42 and Myc-Q61LRac increased PS518 fluorescence throughout the SC. There was a near complete overlap of Sch-GFP, PS518 and Myc fluorescence. These results suggest that both active Cdc42 and Rac can equally promote unrestricted Pak-dependent phosphorylation of Sch-GFP when expressed in SCs.

2.3.5 Inhibition Of Rac-GTP Does Not Reduce Phosphorylation Of Sch S518 Or Pak

To further discriminate between Cdc42 and Rac dependent phosphorylation of endogenous Sch, SCs were incubated with and without NSC23766, an inhibitor of Rac-GTP (Gao et al., 2004).

Pak-CRIB pull down assays were performed and the amount of Cdc42-GTP and Rac-GTP were assessed, as were the levels of endogenous Sch S518 and Pak phosphorylation (Figure 2.7).

Normalization of Rac-GTP to the amount of GST-CRIB in each lane revealed a 72% reduction in Rac-GTP levels in NSC23766 treated, compared to untreated SCs (Figure 2.7A, C).

Normalization to GST-CRIB revealed only a 21% reduction in Cdc42-GTP compared to untreated SCs (Figure 2.7B, D). Total lysates of treated and untreated SCs were immunoblotted for Rac, Cdc42, PS518, and P-Pak (Figure 2.7E, G). No reduction in total Rac and Cdc42 levels were observed in SCs treated with and without NSC23766. Normalization of PS518 to the GAPDH loading control also revealed no difference in the amount of PS518 in NSC23766-treated and untreated SCs (Figure 2.7F). P-Pak levels were also unchanged in response to

NSC23766 treatment (Figure 2.7G). These results suggest that endogenous Sch is effectively phosphorylated on S518 by Cdc42-Pak in SCs.

2.3.6 PS518-Sch And Paxillin Co-Localize With Cdc42 And P-Pak In Membrane

Protrusions

We sought to identify proteins localized in membrane protrusions that form at the ends of and along cellular processes in normal SCs (Figure 2.8). These resemble the atypical radial membrane protrusions that form along the cellular processes when Sch-GFP is expressed. Phosphorylated Sch and Cdc42 colocalized in cellular processes, radial membrane protrusions and often at the distal tips of SCs. Paxillin and PS518 also colocalized along processes and at the distal ends. Paxillin was found within the perinuclear cytosol and periodically along processes, in membrane protrusions and in distal tips of processes, but did not colocalize with Rac. Rac immunofluorescence was much weaker than observed for Cdc42 and was largely restricted to the perinuclear cytosol, and was only weakly expressed at the distal tips. P-Pak colocalized with Cdc42 in membrane protrusions and cellular processes. This result suggests that a paxillin-Cdc42-Pak dependent phosphorylation of Sch can occur at the plasma membrane and within radial membrane protrusions.

2.3.7 Sch Serine 518 Phosphorylation Modulates Morphology In SCs

We sought to determine the effect of Sch phosphorylation at S518 on SC morphology by transiently transfecting SCs with GFP-tagged SchS518 variants (Figure 2.9A). All GFP positive SCs were categorized into six groups based on morphology (Figure 2.9B). In SCs expressing GFP alone and Sch-GFP, the majority displayed the bipolar shape typical of confluent SCs. At

least 40% of the total number of GFP and Sch-GFP positive SCs were bipolar. GFP localized to the nucleus, whereas Sch-GFP localized to the plasma membrane and to microspikes. SCs expressing SchS518A-GFP, representing an unphosphorylatable form, often extended a sole elongated process from the SC body. The frequency of occurrence of this unipolar morphology in SCs expressing SchS518A-GFP was 35% compared to approximately 18% and 20% of SCs expressing GFP and Sch-GFP, respectively. SchS518A-GFP localized to the plasma membrane as was observed for Sch-GFP, however it was not found in the plasma membrane of lamellipodia. SCs expressing SchS518D-GFP, that mimics the phosphorylated form, assumed both multipolar and bipolar morphologies. The multipolar phenotype was defined as a SC with more than four processes extending from the SC body. At least 25% of the SchS518D-GFP positive SCs were multipolar compared to approximately 13% and 19% of SCs expressing GFP and Sch-GFP, respectively. SchS518D-GFP localized to the plasma membrane along the multiple processes. The appearance of extensive lamellipodia was low in SchS518D-GFP expressing SCs compared to those expressing SchS518A-GFP.

2.4 Discussion

Previously we demonstrated that localization of Sch at the plasma membrane requires interaction of its N-terminal PBD1 with paxillin (Fernandez-Valle et al., 2002). We now report that PBD1 is required for phosphorylation of Sch at S518. In addition, Sch S518 phosphorylation occurs in restricted plasma membrane domains, where active Pak, Cdc42 and paxillin are found. The results presented here suggest that paxillin binding and translocation to the plasma membrane precede S518 phosphorylation that occurs predominantly by Cdc42-Pak in specific membrane domains of subconfluent SCs.

2.4.1 Interactions With Paxillin Regulate Sch S518 Phosphorylation

Recent work has raised the question of whether phosphorylation is required for Sch localization to the plasma membrane (Kissil et al., 2002; Surace et al; 2004). Using both biochemical and cellular assays, we find that phosphorylation of Sch on serine 518 requires paxillin binding to PBD1, but is independent of paxillin binding to PBD2. The inability of Sch Δ PBD1 to become phosphorylated results from its inability to associate with the plasma membrane, as both Sch-GFP and Sch Δ PBD2-GFP localize to the plasma membrane and undergo S518 phosphorylation. This result is independent of the tag, Xpress or GFP, fused onto either the N or C-terminus. In SCs expressing Sch-GFP, the vast majority of the molecules are at the plasma membrane but only a small subset become PS518 positive. Phosphorylated Sch-GFP is confined to the most peripheral aspects of lamellipodia, microspikes, and radial membrane protrusions (Figure 2.2). P-Pak is enriched at these subdomains consistent with Pak as the effector kinase (Figure 2.3). In contrast, nearly all Sch Δ PBD2-GFP molecules are PS518 positive regardless of their cellular

localization. The possibility that deletion of PBD2 impairs negative regulation of Pak by Sch is unlikely, because increased levels of phospho-threonine 423 Pak, that is required for Pak activity, was not observed in SCs expressing Sch Δ PBD2-GFP (Zenke et al., 1999). The focal increase in P-Pak fluorescence in radial membrane protrusions observed in SCs expressing full-length Sch-GFP was not observed in SCs expressing the PBD2 deletion variant. A possible explanation for the deregulation of S518 phosphorylation is that conformation of the C-terminus in the PBD2 deletion variant is perturbed, impairing intra- and inter-molecular interactions that usually restrict access to S518. Alternatively, this variant is not effectively dephosphorylated. Furthermore, neither Sch Δ PBD1-S518A nor Sch Δ PBD1-S518D localize to the plasma membrane (unpublished observations). Both GFP-tagged SchS518A/D variants localize effectively to the plasma membrane (Figure 2.8A). This suggests that Sch phosphorylation occurs following translocation to the plasma membrane, into areas containing active surface receptors that promote Pak activity.

2.4.2 Evidence For Cdc42-Pak Dependent S518 Phosphorylation

Both Pak and protein kinase A have been reported to phosphorylate S518 (Kissil et al., 2002; Xiao et al., 2002; Alftan et al., 2004). We used constitutively active forms of Cdc42 and Rac to discriminate between Pak and PKA mediated SchS518 phosphorylation. Introduction of both constructs into SCs effectively increases P-Pak levels but does not promote indiscriminate phosphorylation of endogenous SchS518. GST-Pak CRIB pull down assays from SCs treated with and without NSC23766, reveal that SchS518 and Pak phosphorylation are not reduced concomitantly with the reduction in Rac-GTP levels. This observation, together with the localization of Cdc42 but not Rac at the plasma membrane, strongly suggests that in

subconfluent SCs, the majority of Sch phosphorylation is due to Cdc42-dependent activation of Pak. It has also been shown that Cdc42-GTP binds with a higher affinity to Pak than Rac-GTP, and that only very low amounts of active Rac are present at the plasma membrane in human Schwann cells (Thompson et al., 1998; Nakai et al., 2006). The limited phosphorylation of membrane-associated Sch-GFP at domains containing elevated P-Pak is consistent with tight spatial and temporal regulation of Cdc42-Pak activity at the plasma membrane.

2.4.3 Activation Of Cdc42-Pak Dependent Sch S518 Phosphorylation

The Rho family of GTPases are activated in response to ligand-receptor interactions at the plasma membrane (reviewed in Kjoller and Hall et al., 1999). Our earlier work demonstrated that Sch and paxillin localize at the plasma membrane and associate with $\beta 1$ integrin and ErbB2 in SCs (Fernandez-Valle et al., 2002). These receptors play fundamental and essential roles in regulating all aspects of SC function, including survival, proliferation, migration, differentiation and myelination (Fernandez-Valle et al. 1994; Garrett et al., 2000; Feltri et al., 2002; Michailov 2004, Lyons et al., 2005; Taveggia et al., 2005). Activation of each receptor is coupled to immediate changes in the actin cytoskeleton through activation of Rho-family GTPases (Otey and Burridge, 1990; Akiyama, 1996; Adam et al., 1998; Feldner and Brandt; 2002; Juliano et al., 2004). Work by others has shown that Pak and paxillin are recruited to integrin and ErbB2 receptors (Adams et al., 1998; Turner et al., 1999; del Pozo et al., 2000; reviewed in Turner, 2000; Juliano et al., 2004; Hildebrand et al., 1995, Tachibana et al., 1995, Fernandez-Valle et al., 2002). Our previous work suggests that $\beta 1$ integrin and ErbB2 receptors are likely candidates for Cdc42 and Pak activation at the plasma membrane.

2.4.4 Sch Regulates The Organization Of The Actin Cytoskeleton

Loss of Sch expression, in human schwannomas alters the characteristic spindle shape of SCs. Schwannomas display severe cytoskeletal defects including excessive membrane ruffling, loss of stress fiber formation, and increased surface area (Pelton et al. 1998; Rosenbaum et al., 1998; Bahsour et al., 2002). We find that introduction of Sch-GFP into SCs reinforces their innate spindle shape. Sch-GFP localizes to the plasma membrane and promotes extensive cell elongation. Overall, SCs remain bipolar but become longer and thinner than those expressing GFP alone. This is consistent with the introduction of a negative regulator of Rac, which further limits cell spreading. The expression of SchS518-GFP variants in SCs similarly promotes cell elongation. The S518 variants additionally influence the finer organization of the actin cytoskeleton and SC polarity. SchS518D-GFP promotes branching of bipolar cellular processes, often promoting extension of multiple processes from the cell body. Both are atypical phenotypes for SCs and are reminiscent of oligodendrocyte morphology. SchS518A-GFP promotes extension of a single process from the cell body and elaboration of a large lamellipodia from the opposite pole. This morphology resembles that reported for SCs migrating along axons *in vitro* (Gatto et al., 2003). Deletion of PBD1 from these constructs abrogates their morphological effects, as neither localize to the plasma membrane (unpublished observation, CFV). Therefore, a function of membrane-associated Sch appears to be promotion of cellular elongation. Its S518 phosphorylation state influences cell polarity and the final branching pattern of processes. The SchS518D variant has also been reported to promote extension of multiple processes in RT4 schwannoma cell lines (Surace et al., 2004). Establishment and

maintenance of a bipolar phenotype and dynamic regulation of actin polymerization are critical for SC function (Billings-Gagliardi et al., 1974; Fernandez-Valle et al., 1997).

2.4.5 Two Pools Of Sch With Distinct Functions

Recently it was shown in endothelial cells, that expression of Sch S518A sequesters Rac in the cytosol, preventing its localization to the plasma membrane (Okada et al., 2005). The morphological and proliferative abnormalities in schwannomas have been attributed to increased levels of Rac activity at the plasma membrane (Shaw et al., 2001; Hirokawa et al., 2003; Kaempchen et al., 2003; Kissil et al., 2003; Nakai et al., 2005). Here, we show in primary SCs that very little endogenous Rac is found at the plasma membrane or in cellular processes. The majority is present within the perinuclear cytosol. In contrast, we show here and in previous work that, Cdc42 and RhoA and B are abundantly expressed at the plasma membrane, along processes, and within their distal endings (Taylor et al., 2003). Sch likely exists in two distinct pools within subconfluent SCs. A membrane-associated pool consisting of open, S518 phosphorylated and unphosphorylated molecules, that participate in cytoskeletal reorganization; and a cytosolic pool, consisting of closed, S518 unphosphorylated molecules that negatively regulate Rac and/or Pak activity by preventing localization of Rac to the plasma membrane.

In summary, we demonstrate that phosphorylation of Sch requires paxillin binding and plasma membrane localization, where a subset can be phosphorylated on S518 by Cdc42-Pak.

Membrane-associated Sch is poised to coordinate cytoskeletal reorganization in response to receptor activity. This dynamic regulation of the actin cytoskeleton is fundamental for effective interactions of SC processes with axons during development and regeneration of peripheral nerves.

Figure 2.1 PBD1 Is Required For Serine 518 Phosphorylation Of Sch.

Primary rat SCs were transiently transfected with plasmids encoding Xpress-tagged Sch PBD deletion variants and β -galactosidase (LacZ) as a control. SCs were extracted 36 hours after transfection and Xpress-tagged proteins were immunoprecipitated using Xpress antibody and were immunoblotted with Sch PS518 and paxillin antibodies. Full-length Sch (Sch) and the PBD2 deletion variant (Sch Δ 2) were positive for PS518 and co-immunoprecipitated with paxillin. Sch variants lacking PBD1 (Sch Δ 1 and Sch $\Delta\Delta$ 1/2; data not shown) and Xpress- β -galactosidase (LacZ) were not positive for PS518 and did not co-immunoprecipitate with paxillin. This experiment was performed four times with identical results. This suggests that Sch-PBD1 binding to paxillin and association with the membrane is required for Sch phosphorylation.

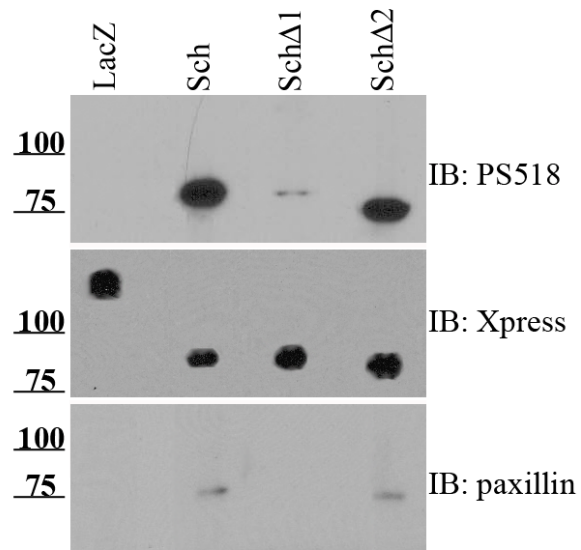


Figure 2.1 PBD1 Is Required For Serine 518 Phosphorylation Of Sch.

Figure 2.2 Sch-GFP Is Phosphorylated At Restricted Plasma Membrane Domains.

SCs expressing of Sch-GFP often formed radial membrane protrusions along the SC process.

These radial protrusions were not observed in SCs expressing Sch variants lacking PBD1. The protrusions contained enhanced Sch-GFP and PS518 fluorescence; colocalization was observed in the distal most aspects of the specialization (insets). Sch-GFP found within processes and along the plasma membrane lacking specializations was associated with only weak PS518 fluorescence. SCs expressing Sch Δ PBD1-GFP did not have increased PS518 fluorescence as observed in SCs expressing Sch-GFP or in untransfected SCs. Sch Δ PBD1-GFP was present in the perinuclear cytosol and within processes but did not colocalize with PS518 fluorescence. In SCs expressing Sch Δ PBD2-GFP, a significant increase in PS518 fluorescence as was observed compared to SCs expressing Sch-GFP. Sch Δ PBD2-GFP and PS518 fluorescence colocalized irrespective of cellular localization and membrane morphology. This indicates that the presence of each PBD influences the phosphorylation dynamics at serine 518 in Sch. This result was observed consistently in four individual experiments.

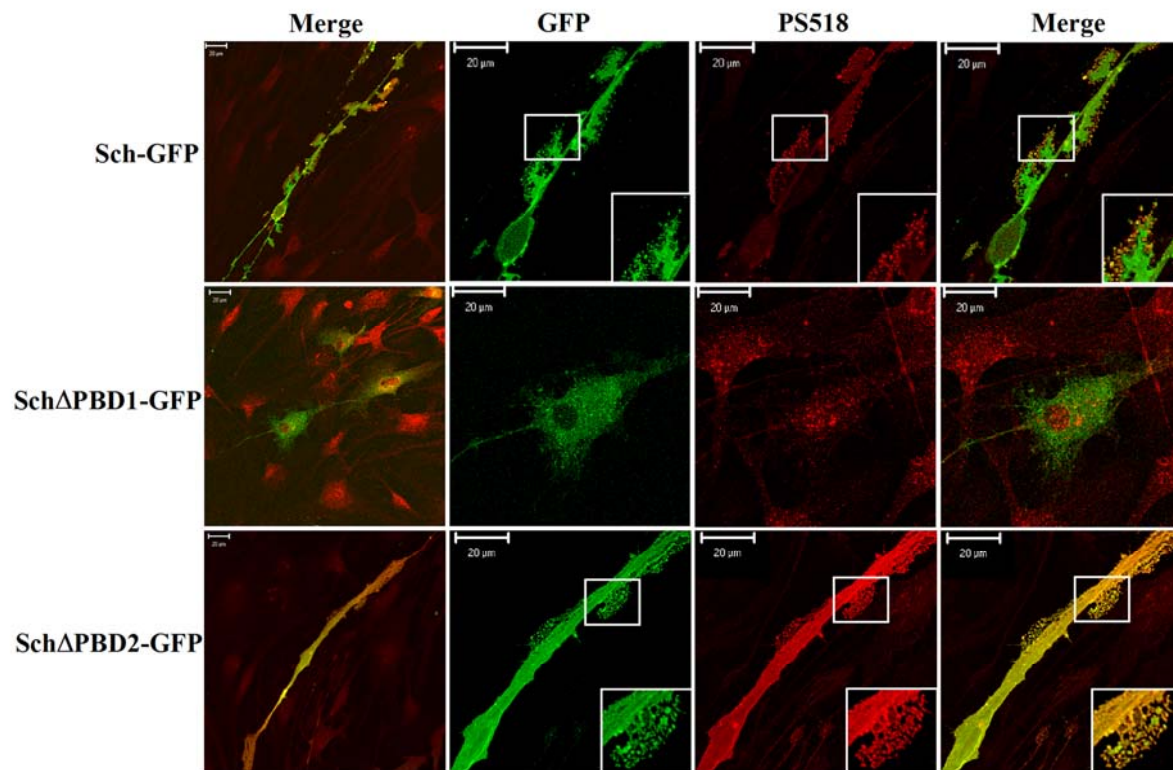


Figure 2.2 Sch-GFP Is Phosphorylated At Restricted Plasma Membrane Domains.

Figure 2.3 Deletion Of PBD2 Is Not Associated With Increased Pak Activity In SCs.

SCs were transiently transfected with plasmids encoding GFP-tagged Sch PBD deletion variants. SCs were immunostained with Pak phosphothreonine 423 (P-Pak) antibody. Expression of Sch-GFP was associated with increased P-Pak fluorescence in radial membrane protrusions (inset) and in filopodia. Intracellular Sch-GFP found within processes did not colocalize with P-Pak fluorescence. Expression of Sch Δ PBD1-GFP was not associated with changes in P-Pak fluorescence intensity or distribution as compared to untransfected and Sch-GFP expressing SCs. Expression of Sch Δ PBD2-GFP did not promote an overall increase in P-Pak fluorescence as was observed for PS518 fluorescence. P-Pak fluorescence was largely restricted to distal tips of radial filopodia (inset) and to the peripheral-most aspects of a large membrane protrusion where it colocalized with Sch Δ PBD2-GFP.

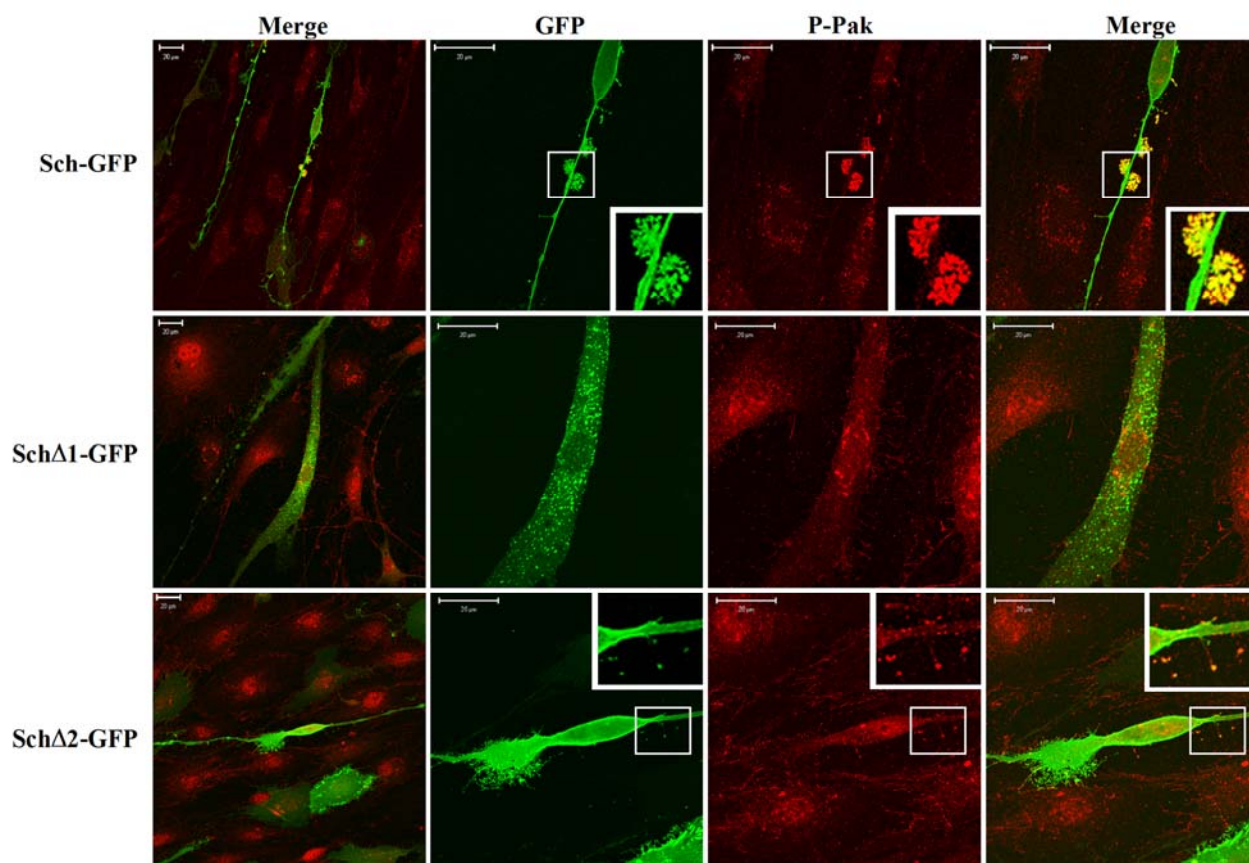


Figure 2.3 Deletion Of PBD2 Is Not Associated With Increased Pak Activity In SCs.

Figure 2.4 Expression Of Active Cdc42 And Rac Increases Endogenous P-Pak Levels.

SCs were transiently transfected with plasmids encoding active Myc-tagged Q61LCdc42 and Q61LRac. SCs were immunostained with phospho-threonine 423-Pak and Myc antibodies. SCs expressing Myc-Q61LCdc42 and Myc-Q61LRac had increased P-Pak fluorescence throughout the cell compared to adjacent untransfected SCs. There was a focal increase in P-Pak and Myc staining in distal tips of processes when active Cdc42 was expressed (arrows).

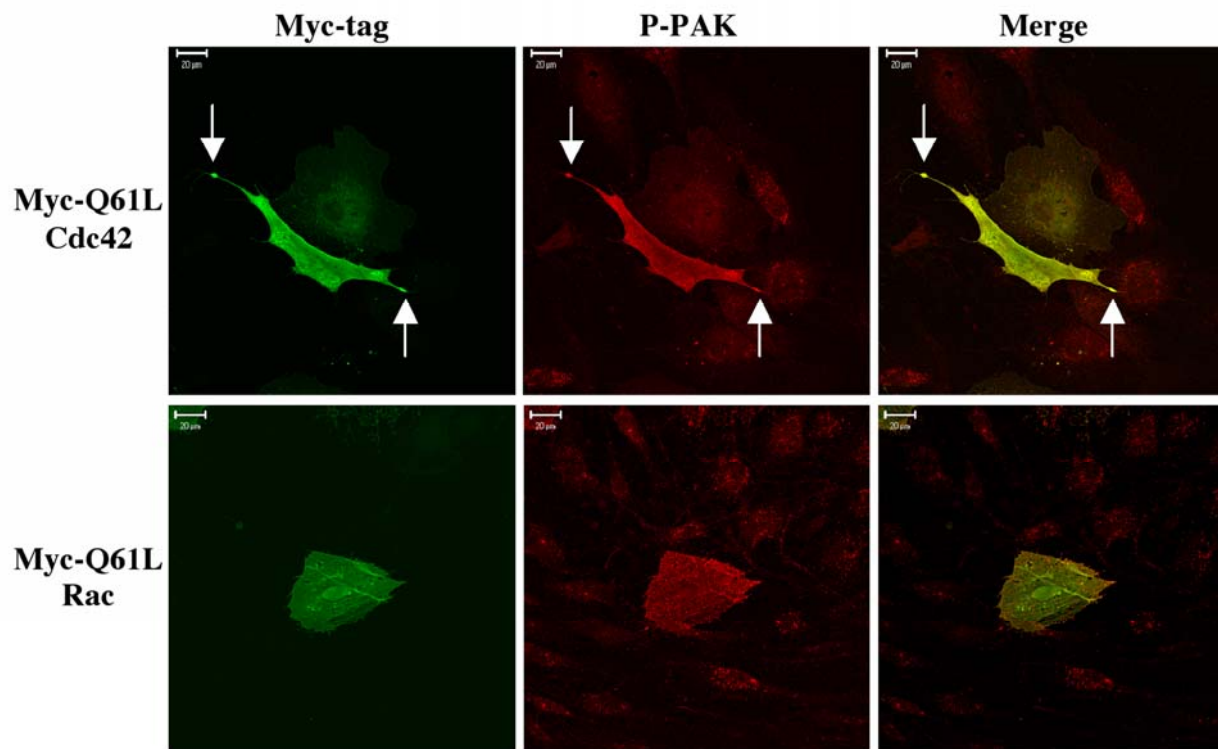


Figure 2.4 Expression Of Active Cdc42 And Rac Increases Endogenous P-Pak Levels.

Figure 2.5 Expression Of Active Cdc42 and Rac Does Not Increase Phosphorylation of Endogenous Sch.

SCs were transiently co-transfected with GFP and Myc-tagged Q61LCdc42 and Q61LRac. SCs were immunostained with PS518 and Myc antibodies. Co-expression of GFP with Myc-Q61L-Cdc42 and Rac did not lead to an overall increase in endogenous PS518 fluorescence as was observed for endogenous Pak. In Myc-Q61LCdc42 transfected SCs, there were areas of increased PS518 fluorescence that colocalized with Myc staining. These were along short cytoplasmic processes (arrows). Similar areas in Myc-Q61LRac transfected SCs did not show elevated PS518 expression (arrowheads). Each experiment was repeated three times with identical results.

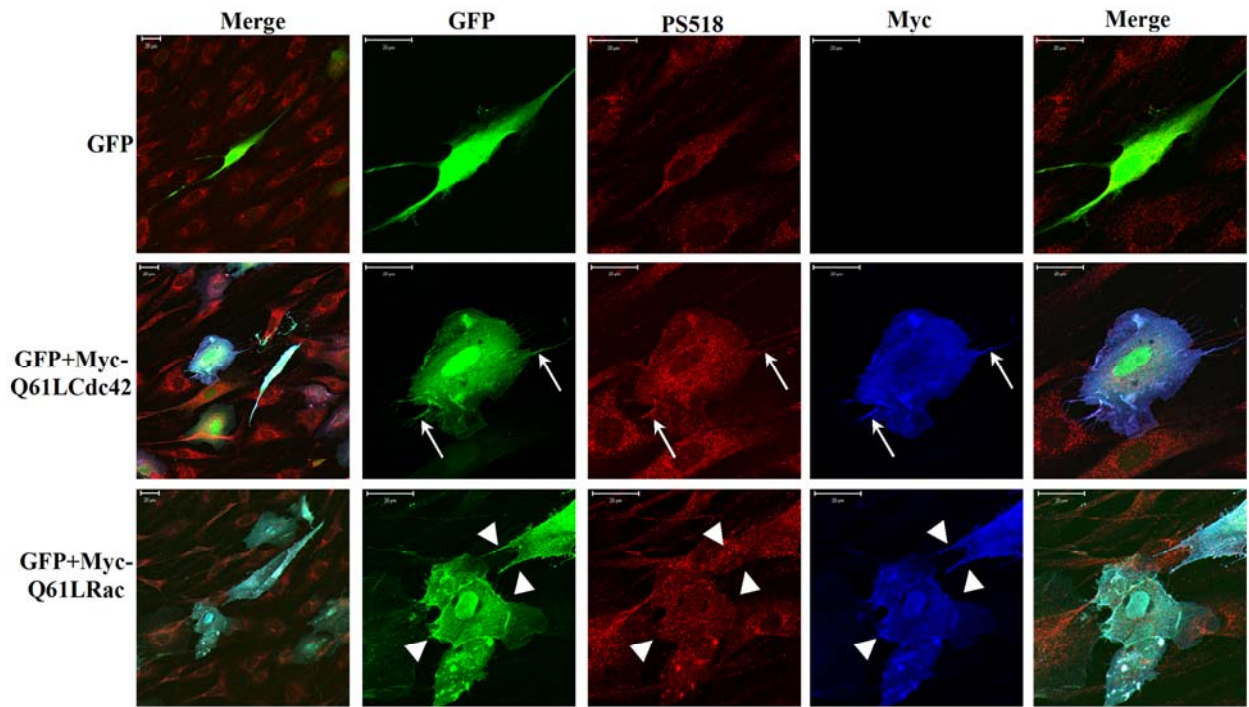


Figure 2.5 Expression Of Active Cdc42 and Rac Does Not Increase Phosphorylation of Endogenous Sch.

Figure 2.6 Expression Of Active Cdc42 And Rac Increases S518 Phosphorylation Of Exogenous Sch-GFP.

SCs were transiently transfected with expression plasmids for Sch-GFP, alone and with Myc-tagged Q61LCdc42 and Q61LRac. SCs were immunostained with PS518 and Myc antibodies. In SCs expressing only Sch-GFP, fluorescence was observed at the plasma membrane and within cellular processes. Co-localization of Sch-GFP with PS518 fluorescence revealed that only a subset of Sch-GFP molecules was phosphorylated. The PS518-positive molecules were found at distal aspects of membrane protrusions, but not along the plasma membrane surrounding the cell body from which many filopodia protruded (arrowhead). Co-expression of Sch-GFP with either Myc-Q61LCdc42 or Myc-Q61LRac led to similar increases in Sch PS518 fluorescence throughout the cell as compared to untransfected and Sch-GFP transfected SCs. All membrane domains containing Sch-GFP were positive for PS518 when activated Cdc42 and Rac were co-expressed. Identical results were obtained in three experiments with 2-4 coverslips per transfection group.

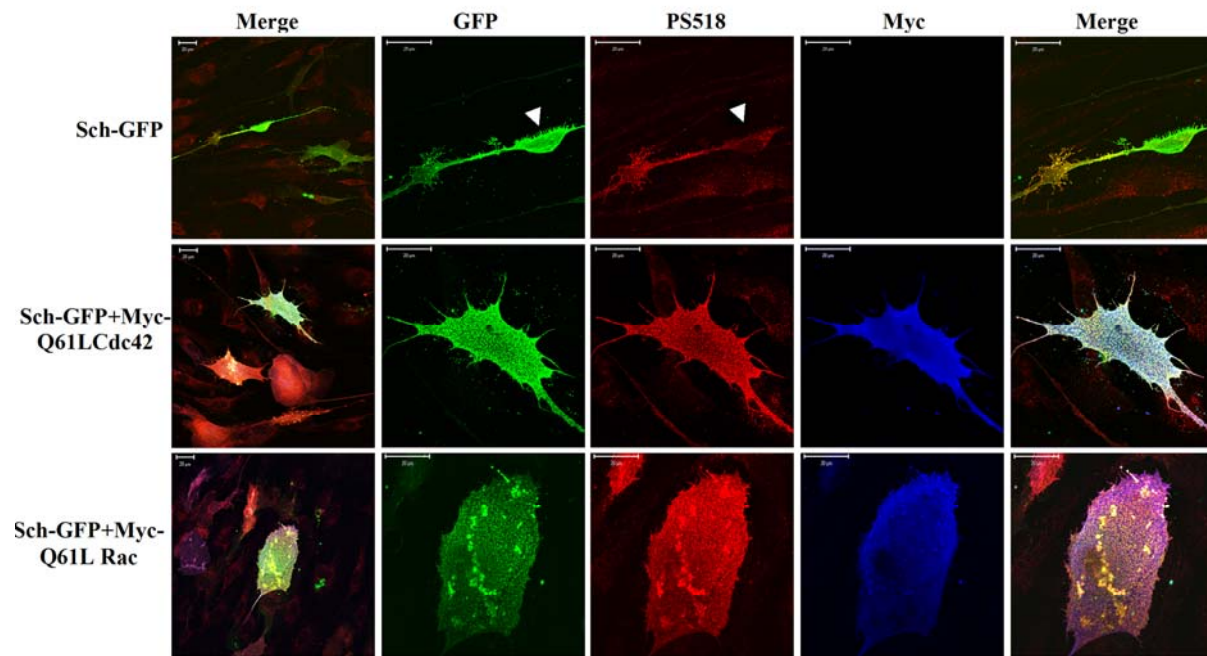


Figure 2.6 Expression Of Active Cdc42 And Rac Increases S518 Phosphorylation Of Exogenous Sch-GFP.

Figure 2.7 Inhibition of Rac GTPase Does Not Reduce Sch S518 and Pak Phosphorylation.

A, B) GST- Pak CRIB pull down assays were conducted using lysates from SCs incubated overnight with (+) and without (-) NSC23766, an inhibitor of Rac GTPase activity. The membrane was blotted for Rac, then for GST and was stripped and was re-blotted for Cdc42. Positive (+GTP) and negative (+GDP) controls were also performed. C, D) Normalization of the amount of Rac-GTP and Cdc42-GTP to GST demonstrated that NSC23766 reduced Rac-GTP by 72% of the untreated control level, whereas it reduced Cdc42-GTP by only 21% of untreated controls. E) Lysates of SCs incubated with and without NSC23766 were immunoblotted for total Rac, Cdc42, and PS518. NSC23766 did not reduce the levels of total Rac and Cdc42 or PS518. F) Sch phosphorylation levels were normalized to GAPDH and no reduction in Sch-PS518 was observed in response to NSC23766 treatment. G) Lysates of SCs incubated with and without NSC23766 were immunoblotted for P-Pak. No reduction of P-Pak levels was observed in treated compared to untreated SCs. This experiment was performed twice with identical results and is consistent with Cdc42-Pak dependent phosphorylation of Sch-S518.

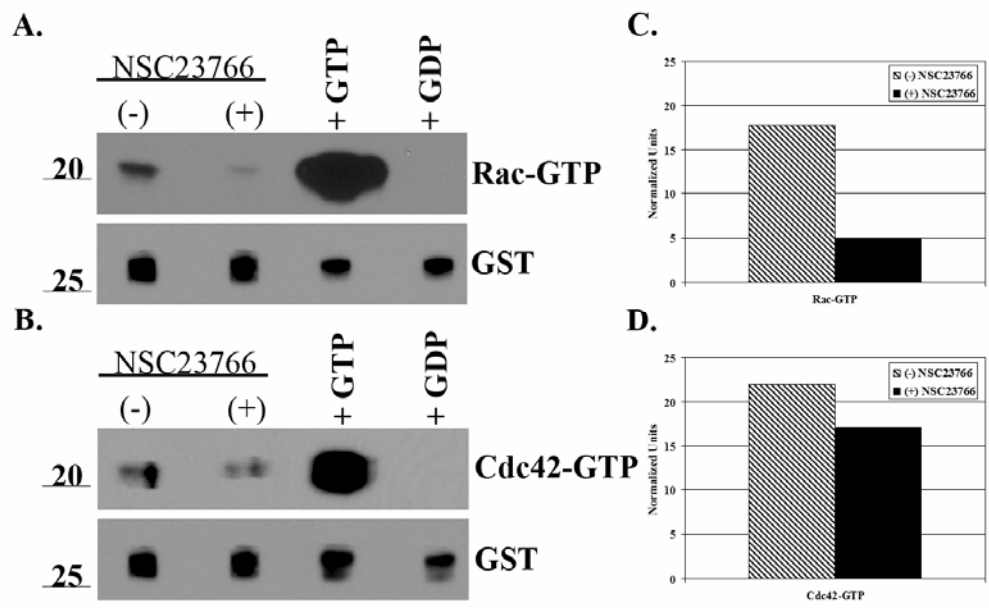
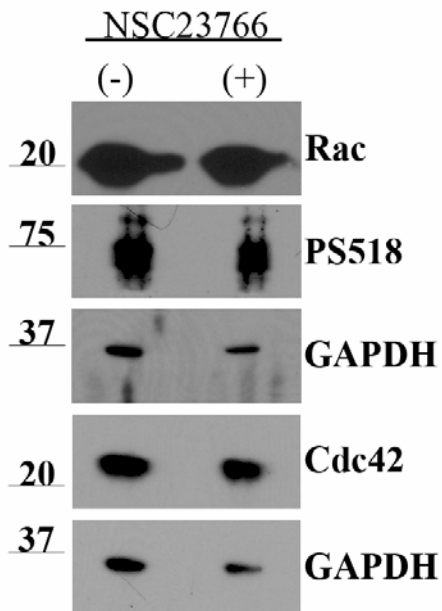
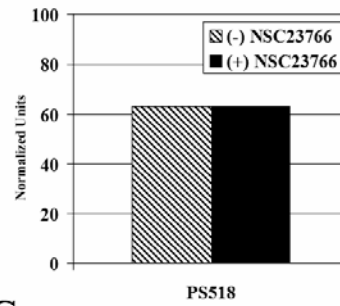


Figure 2.7 Inhibition of Rac GTPase Does Not Reduce Sch S518 and Pak Phosphorylation.

E.



F.



G.

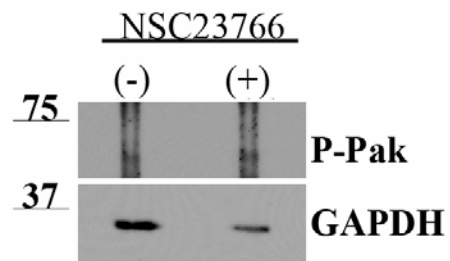


Figure 2.7 Inhibition of Rac GTPase Does Not Reduce Sch S518 and Pak Phosphorylation.

Figure 2.8 Sch-PS518, Paxillin, Cdc42, P-Pak, But not Rac Colocalize In Membrane

Protrusions.

Subconfluent SCs grown under standard conditions were immunostained with antibodies for PS518, paxillin, Cdc42, Rac and P-Pak to ascertain if the proteins colocalized at the cell periphery. Cdc42 and PS518, as well as paxillin and PS518 colocalize along cellular processes, membrane protrusions and at their distal tips. In contrast, paxillin and Rac were not colocalized. Only weak fluorescence was observed for Rac within the cytosol and at the plasma membrane. P-Pak colocalized with Cdc42 in cellular processes and radial membrane protrusions. All images were obtained using identical settings and were processed identically.

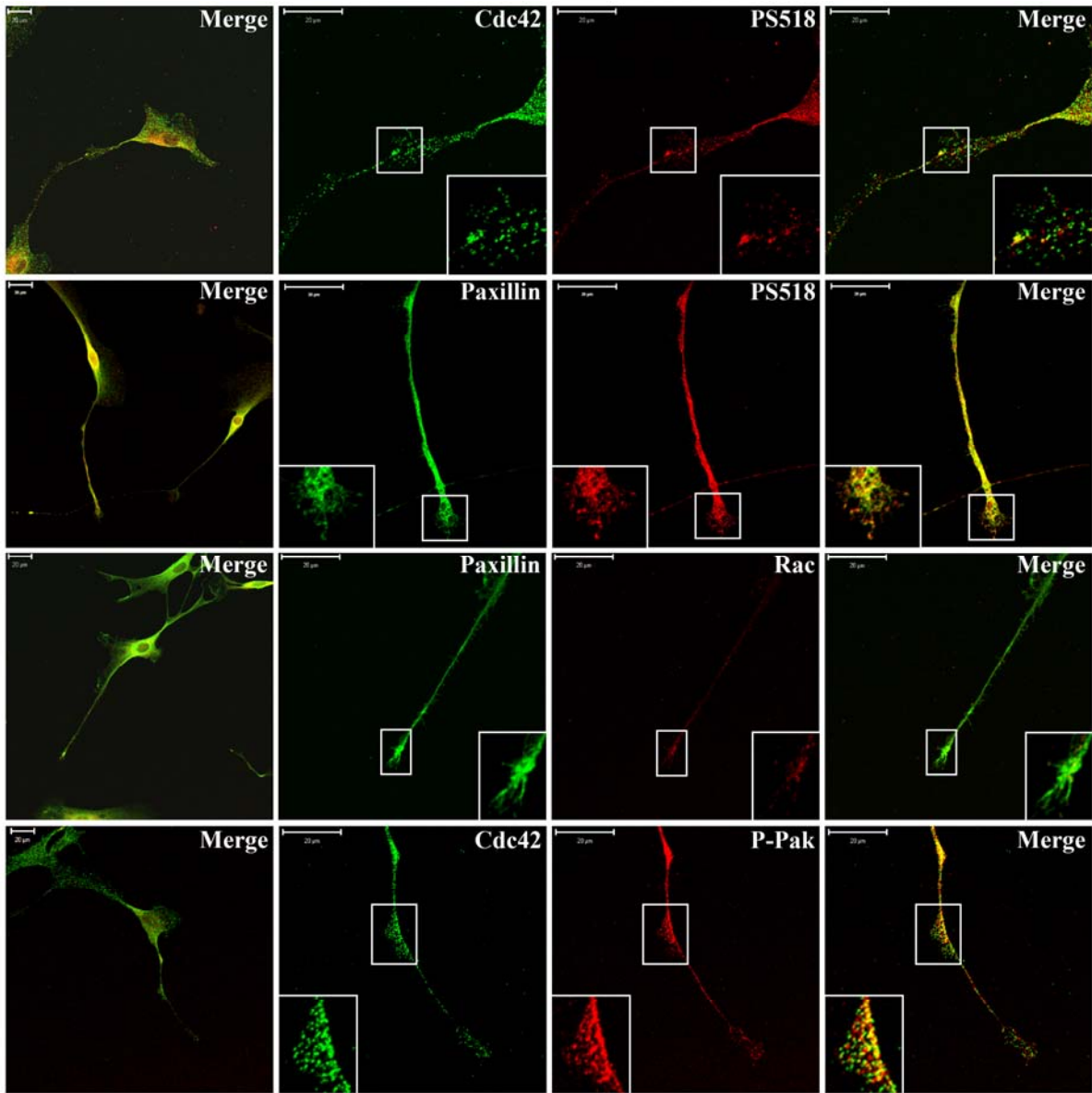


Figure 2.8 Sch-PS518, Paxillin, Cdc42, P-Pak, But Not Rac Colocalize In Membrane Protrusions.

Figure 2.9 Sch Phosphorylation Status Alters SC Morphology.

A) Confluent SCs were transfected with Sch S518 variants and were stained with phalloidin to visualize F-actin 36 hours after transfection. SCs expressing GFP alone and Sch-GFP were typically bipolar. SCs expressing Sch-S518A-GFP were most frequently unipolar with a single elongated process, whereas SCs expressing Sch-S518D-GFP were typically multipolar or bipolar with heavily branched processes. B) Morphological changes were assessed by counting all GFP-positive SCs in each group and categorizing their shape. The counts were obtained from three independent experiments in which a total of 1500-3000 SCs per group were assessed.

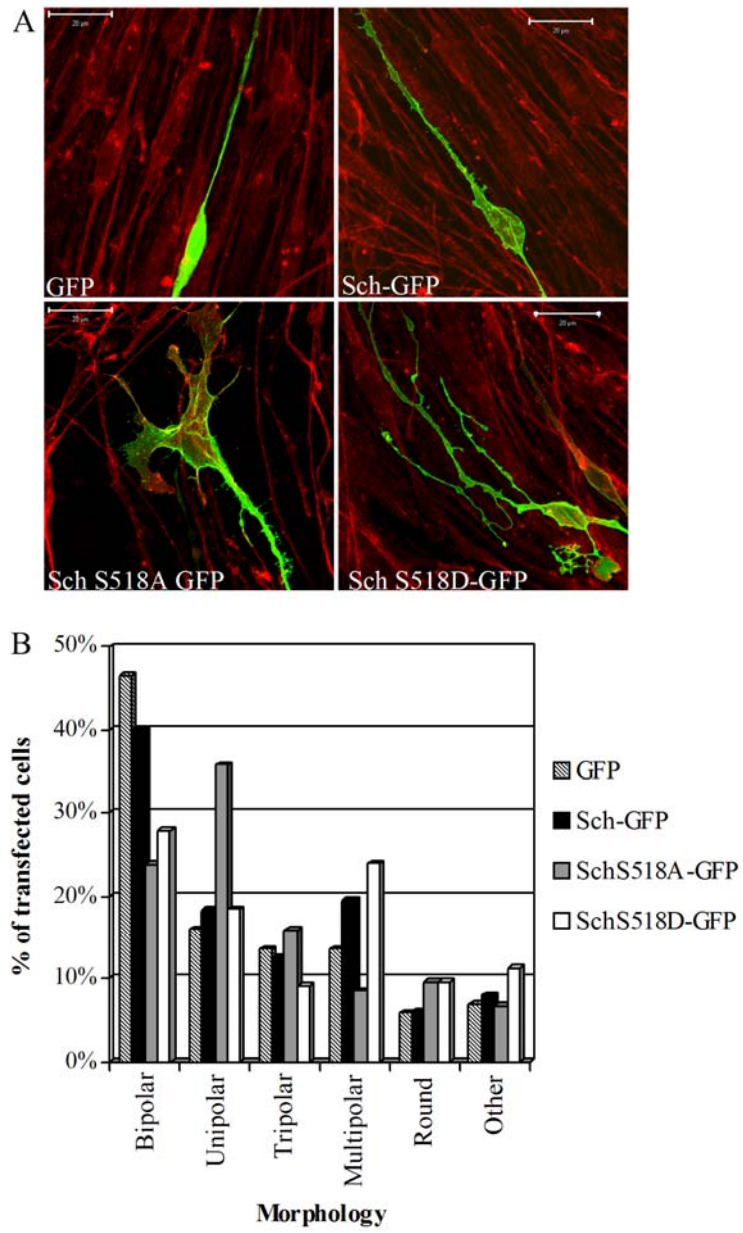


Figure 2.9 Sch Phosphorylation Status Alters SC Morphology.

CHAPTER 3

NEUREGULIN AND LAMININ STIMULATE PHOSPHORYLATION OF THE NF2 TUMOR SUPPRESSOR IN SCHWANN CELLS BY DISTINCT PROTEIN KINASE A AND P21-ACTIVATED KINASE DEPENDENT PATHWAYS

3.1 Introduction

The Neurofibromatosis type 2 (NF2) tumor suppressor Schwannomin (Sch), also known as merlin, is a membrane-cytoskeleton linking protein (Rouleau et al., 1993; Trofatter et al., 1993). Mutations in the NF2 gene predispose individuals to benign, slow-growing schwannomas. Sch's conformation, localization, and phosphorylation are important determinants of its ability to regulate proliferation and actin organization (reviewed in McClatchey and Giovannini, 2005). The tumor suppressor function of Sch is associated with its closed, intracellular form lacking phosphorylation on serine 518 (S518; Rong et al., 2004; Shaw et al., 2001). In this conformation, Sch inhibits Rac-mediated signaling cascades and progression through the G1 phase of the cell cycle (reviewed in Okada et al., 2007). Phosphorylation of Sch-S518 is believed to stabilize Sch in the open conformation, inhibiting its tumor suppressor function while unmasking binding sites for trans-membrane receptors and actin-associated proteins (James et al., 2001; Rong et al., 2004). P21-activated kinase (Pak) and protein kinase A (PKA) phosphorylate Sch on S518, but the receptor mechanisms leading to Sch phosphorylation are unknown (Kissil et al., 2002; Xiao et al., 2002; Alfthan et al., 2004).

Previously, we demonstrated that Sch localization to the plasma membrane, and its phosphorylation on S518 requires direct binding of residues 50-70 within Sch's N-terminus to

the scaffold protein, paxillin (Fernandez-Valle et al., 2002, Thaxton et al., 2007). We also demonstrated that Sch is present at the plasma membrane of subconfluent Schwann cells (SCs), where Sch and paxillin interact with $\beta 1$ integrin and ErbB2; receptors critical for SC adhesion, motility, proliferation and myelination (Fernandez-Valle et al., 2002; reviewed in Garratt et al., 2000; reviewed in Chernousov and Carey, 2000). Paxillin also recruits Pak to the plasma membrane, and serves as a scaffold for Sch-Pak interactions by binding multiple regulators of Rac and Cdc42, members of the Rho family of GTPases, as well as actin binding proteins and components of focal complexes and adhesions (reviewed in Turner, 2000).

Here, we demonstrate that NRG1 β and laminin-1, ligands for ErbB and $\beta 1$ integrin receptors, respectively, induce Sch phosphorylation in SCs through two independent pathways, NRG1 β by PKA, and laminin-1 by Pak. NRG1 β and laminin-1 do not synergize to increase Sch phosphorylation, but rather NRG1 β partially antagonizes laminin-induced Sch phosphorylation. These findings show that Sch is a convergence point for transduction of signals from ErbB and $\beta 1$ integrin receptors that regulate proliferation, differentiation and cytoskeletal dynamics in SCs during peripheral nerve development.

3.2 Materials and Methods

3.2.1 Materials

The following materials were used: Natural mouse laminin-1 and Lipofectamine 2000 (Invitrogen; Carlsbad, CA, USA), AG825 and PKI₁₄₋₂₂ amide (EMD Biosciences; San Diego, CA, USA). Sch-GFP constructs were described previously (Thaxton *et al.*, 2007). Recombinant human NRG-1 beta/type II (NRG1 β) was a generous gift from Mark Marchionni. Myc-Pak K299A and Myc-Pak L107F, T423E (Myc-Pak T423E) constructs were generous gifts from Gary Bokoch (The Scripps Research Inst., La Jolla, CA, USA). Antibodies were purchased from the following sources: ErbB2 and Sch (C18) from Santa Cruz Biotechnology (Santa Cruz, CA, USA); β 1 integrin from BD Transduction Labs (San Jose, CA, USA); Pak, Myc, and P-CREB from Cell Signaling (Boston, MA, USA); PS518-Sch and P-ErbB2 (Y1248) from Abcam (Cambridge, MA, USA); P-Pak (T423) from Rockland Immunologicals, Inc. (Gilbertsville, PA, USA); Xpress from Invitrogen; ErbB2 from EMD Biosciences; and Alexa Fluor conjugated secondary antibodies from Invitrogen.

3.2.2 Cell Culture

Primary rat SC cultures were prepared from neo-natal day 1 rat pups as described previously (Chen *et al.*, 2000). Subconfluent SC cultures were grown on glass coverslips coated with poly-L-lysine (PLL; 200 μ g/ml) alone or sequentially with laminin-1 (25 μ g/ml). Cultures were starved overnight in Dulbecco's Modified Eagle Medium with 0.5 % fetal bovine serum (D0.5) before use. The SCs were either left unstimulated, or were stimulated with NRG1 β (10ng/ml)

for 30 minutes. For laminin-1 stimulation, primary rat SCs were grown on PLL coated glass coverslips and were starved overnight in D0.5. The SCs were then stimulated with soluble laminin-1 (10 μ g/ml) or were left unstimulated.

3.2.3 Immunostaining

The SCs were immunostained as described previously (Fernandez-Valle *et al.*, 2002). Cells were analyzed with a Zeiss laser scanning microscope and LSM 510 software. Images shown in each figure are single planes that were collected with identical settings and were processed identically.

3.2.4 Western Blotting

Primary rat SCs were grown to approximately 60% confluency on PLL coated dishes. The cultures were serum starved overnight in D0.5 and were either left in D0.5 or were pre-incubated with AG825 (1 μ M) or PKI₁₄₋₂₂ (50nM) for 1 hour. Next, the SCs were either left unstimulated or were stimulated with NRG1 β (10ng/ml) and/or laminin-1 (10 μ g/ml) in the presence and absence of AG825 (1 μ M) or PKI₁₄₋₂₂ (50nM) for 30 minutes. The SCs were extracted as described previously (Fernandez-Valle *et al.*, 2002) in either TAN buffer (10mM Tris-acetate pH8.0, 100mM NaCl, and 1% IGEPAL) or HEPES buffer (50mM HEPES, 1mM DTT, 150mM NaCl, 1% IGEPAL) containing protease inhibitors. Following extraction, the SC lysate was measured for protein concentration, and 10 μ g of total SC lysate was separated by SDS-PAGE and was transferred to PVDF membranes. The indicated primary antibodies were used, followed by corresponding HRP-conjugated secondary antibody and chemiluminescence detection. Densitometric analysis was conducted on all Western blots. Bands intensities were quantified

and normalized to GAPDH, and to their respective total proteins for phosphorylated forms.

Statistical analysis was acquired using the Student t-test by paired analysis.

3.2.5 Immunoprecipitation

Subconfluent SC cultures grown in medium containing 10% FBS, forskolin (2 μ M) and pituitary extract (20 μ g/ml) were extracted in TAN buffer and 500 μ g of lysate were immunoprecipitated with β 1 integrin antibody, as described previously (Chen *et al.*, 2000). Immunoprecipitation with β 1 integrin antibody covalently linked to magnetic beads was performed as described previously (Taylor *et al.*, 2003).

3.2.6 Transfections

Primary rat SC cultures were transfected using Lipofectamine 2000 as described previously (Thaxton *et al.*, 2007). Thirty-six hours after transfection, the SCs were immunostained.

3.3 Results

3.3.1 NRG1 β and Laminin-1 Induce Phosphorylation of Sch at SC Distal Tips and Radial Membrane Protrusions

NRG and laminin activate Cdc42/Rac GTPases and Pak in other cell types (Adam *et al.*, 1998; Del Pozo *et al.*, 2000). Work from this laboratory has demonstrated that Sch can interact with both ErbB2 and β 1 integrin, and that paxillin-dependent localization to the plasma membrane is required for phosphorylation of Sch by Cdc42-Pak (Fernandez-Valle *et al.*, 2002; Thaxton *et al.* 2007). Here, we sought to identify receptor(s) that trigger Pak activity and Sch phosphorylation. We stimulated subconfluent and serum-starved primary rat SCs grown on laminin-1 with NRG1 β for 30 minutes and assessed the phosphorylation states and localization of ErbB2, Sch and Pak. ErbB2, ErbB3, and Sch were found along SC processes and were concentrated at the distal tips. NRG1 β stimulation induced a focal enrichment of P-ErbB2 and PS518-Sch at the distal tips of SC processes and within membrane protrusions (Figure 3.1). These molecules co-localized with Cdc42 and paxillin. Phosphorylated Pak was also enriched in membrane protrusions and at the distal tips where it co-localized with ErbB2.

We quantified the changes in phosphorylation of ErbB2, Sch, and Pak in serum starved and NRG1 β stimulated SC processes (Figure 3.2 A, B). We found marked increases in fluorescence intensity along SC processes for P-ErbB2, PS518-Sch, and P-Pak, particularly at process tips of stimulated versus starved SCs (Figure 3.2 A). P-ErbB2 levels increased by 1.6-fold, PS518-Sch by 1.5-fold, and P-Pak by 1.9-fold in the processes of NRG1 β stimulated versus starved SCs

(Figure 3.2 B). These results demonstrate that acute stimulation of SCs with NRG1 β induces phosphorylation of Sch downstream of ErbB2/ErbB3, possibly by Pak.

As the SCs were grown on laminin-1, a ligand for β 1 integrin that mediates SC adhesion (Fernandez-Valle et al., 1994), we tested whether a 30-minute exposure to soluble laminin-1 stimulated Sch phosphorylation in subconfluent and serum-starved SCs grown on PLL. Laminin-1 promoted a strong increase in the fluorescence intensity of phosphorylated Sch and Pak compared to starved SCs (Figure 3.2 C). Quantification of fluorescence intensity along the processes revealed a 1.4-fold increase in PS518-Sch and a 1.7-fold increase in P-Pak levels compared to untreated SCs (Figure 3.2 D). These results demonstrate that adhesion to laminin-1 induces Sch phosphorylation at the plasma membrane, possibly by Pak.

3.3.2 NRG1 β Promotes Sch Phosphorylation Through PKA

To determine the relative contributions of ErbB2/ErbB3 and β 1 integrin activation on Sch phosphorylation, we repeated the experiments using SCs plated on PLL rather than laminin-1 and employed the use of AG825 to specifically inhibit ErbB2 kinase activity (Oshero *et al.*, 1993). Subconfluent SCs were starved and then were stimulated with NRG1 β in the presence and absence of AG825 (Figure 3.3). Western Blot analysis revealed that NRG1 β promoted a 4.9-fold increase in P-ErbB2 and a 2.7-fold increase in PS518-Sch levels compared to starved SCs. AG825 significantly reduced NRG1 β stimulated phosphorylation of ErbB2, as well as, Sch-S518 phosphorylation (Figure 3.3 A, B). Surprisingly, Pak phosphorylation was not

observed in NRG1 β stimulated SCs. When total protein levels were assessed, we found that NRG1 β stimulation reduced the amount of ErbB2 by 54% (Figure 3.3 C, D). This is consistent with rapid, ligand-induced degradation of ErbB2 receptors (Lotti et al., 1992; Iacovelli et al., 2007). AG825 partially attenuated the reduction in ErbB2 levels. These results suggest that NRG1 β triggers Sch phosphorylation independently of Pak in SCs.

PKA has been reported to phosphorylate Sch at S518 in vitro (Alfthan et al., 2004).

Additionally, NRG1 β stimulation has been suggested to induce PKA activity in SCs (Kim et al., 1997). Therefore, we tested whether PKA phosphorylated Sch in response to NRG1 β activation of ErbB2/ErbB3 receptors on SCs. Subconfluent SCs were serum starved and were stimulated with NRG1 β in the presence and absence of PKI₁₄₋₂₂ amide, a specific inhibitor of PKA activity (Figure 3.3 E, F). NRG1 β alone stimulated a 2.1-fold increase in phosphorylated Sch compared to starved SCs, and induced phosphorylation of the cyclic-AMP response element binding protein (P-CREB), a known substrate for PKA. PKI₁₄₋₂₂ reduced the levels of Sch and CREB phosphorylation in response to NRG1 β stimulation by 70%. Additionally, stimulation of starved SCs for 30 minutes with forskolin, an activator of adenylyl cyclase that increases intracellular cyclic-AMP and activates PKA, also induced phosphorylation of Sch and CREB. These results indicate that PKA phosphorylates Sch following NRG1 β binding to ErbB2/ErbB3 in SCs.

3.3.3 Laminin-1 Promotes Phosphorylation Of Sch-S518 By Pak

To determine if laminin-1 induced phosphorylation of Sch by Pak, we stimulated SCs grown on PLL with soluble laminin-1 for 30 minutes and conducted western blot analyses (Figure 3.4).

Laminin-1 promoted a substantial 3.5-fold increase in Sch-S518 phosphorylation and a 1.5-fold increase in Pak phosphorylation compared to starved SCs (Figure 3.4 A, B). The levels of total Sch and $\beta 1$ integrin did not significantly change in response to laminin-1, while the levels of total Pak fell by 27% (Figure 3.4 C, D). We additionally tested whether laminin-1 activated ErbB2 and PKA. Stimulation of SCs with laminin-1 did not induce the phosphorylation of ErbB2 or CREB. These findings are consistent with Pak mediated phosphorylation of Sch-S518 following laminin-1 binding to $\beta 1$ integrins expressed on the surface of subconfluent SCs.

To obtain additional evidence that Pak phosphorylates Sch in response to stimulation with laminin-1, we transiently co-transfected SCs plated on PLL and laminin-1 with GFP-tagged Sch and Myc-tagged Pak kinase mutant constructs (Figure 3.5). As previously shown, expression of wild-type Sch (Sch-GFP) resulted in increased S518 phosphorylation at the plasma membrane within discrete membrane protrusions that contain P-Pak (Thaxton et al., 2007). Co-expression of Sch-GFP with catalytically inactive Pak (Myc-Pak K299A) resulted in a loss of PS518-Sch fluorescence in these domains and throughout the SC, whereas co-expression with constitutively active Pak (Myc Pak T423E) resulted in unrestricted Sch-S518 phosphorylation. These results support Pak-mediated phosphorylation of Sch induced by $\beta 1$ integrin adhesion to laminin-1.

3.3.4 $\beta 1$ Integrin And ErbB2 Exist As A Functional Co-Receptor Complex On The SC Surface

To investigate the possibility that ErbB2 and $\beta 1$ integrin act as co-receptors to regulate Sch phosphorylation, we tested their ability to co-localize and co-immunoprecipitate. We found that

β 1 integrin and ErbB2 co-localized with PS518-Sch and P-ErbB2 at the distal tips of SC processes acutely stimulated with NRG1 β (Figure 3.6 A). β 1 integrin immunoprecipitations prepared from lysates of subconfluent SC cultures contained β 1 integrin and ErbB2, as well as, PS518-Sch and paxillin (Figure 3.6 B). To ascertain whether the receptors associated on the cell surface, β 1 integrins were clustered on suspended intact SCs using a β 1 integrin antibody immobilized on magnetic beads, and were subsequently lysed and the clustered receptor complexes were isolated (Figure 3.6 C). A subset of ErbB2 receptors and PS518-Sch were present in the β 1 integrin immunoprecipitate. RhoA, used as a control, was not present in the immunoprecipitate.

Trans-activation between integrins and receptor tyrosine kinases occurs and can lead to changes in receptor protein expression (reviewed in Lee and Juliano, 2004). To determine if trans-activation takes place in SCs, β 1 integrin and ErbB2 protein levels were measured following stimulation with NRG1 β or laminin-1 for 30 minutes. Stimulation with NRG1 β significantly increased β 1 integrin levels 2.0-fold, but decreased ErbB2 levels by half as compared to starved SCs (Figure 3.6 D, E). Stimulation of SCs with NRG1 β and AG825 suppressed NRG1 β 's effect on both β 1 integrin and ErbB2 protein levels. Stimulation of SCs with laminin-1 did not alter β 1 integrin protein levels, but did increase ErbB2 protein levels by a statistically significant 1.5-fold compared to untreated SCs (Figure 3.6 F, G). Surprisingly, stimulation with laminin-1 and AG825 decreased β 1 integrin levels by 58%, while ErbB2 levels slightly increased with respect to laminin-stimulated SCs. This is consistent with a basal level of autocrine activation of

ErbB2/ErbB3 in SCs. SCs have been shown to synthesize and secrete NRGs in response to serum deprivation, thereby transducing survival signals (Rosenbaum et al., 1997).

3.3.5 Dual Stimulation With NRG1 β And Laminin-1 Does Not Synergistically Increase Sch Phosphorylation

To determine if simultaneous activation of ErbB2/ErbB3 and β 1 integrin in SCs synergize to increase phosphorylation of Sch, we stimulated serum-starved SCs grown on PLL for 30 minutes with NRG1 β and soluble laminin-1, in the presence and absence of AG825 (Figure 3.7). Dual stimulation resulted in a significant 1.7-fold increase in PS518-Sch and a 2.1-fold increase in P-Pak compared to unstimulated SCs. This level of Sch phosphorylation was not higher than levels observed in SCs stimulated with either NRG1 β or laminin-1 alone, which were 2.7-fold and 3.5-fold higher than starved SCs, respectively (Figure 3.7 A, B compared to Figure 3.3 B and Figure 3.4B). Surprisingly, stimulation with NRG1 β and laminin-1 in the presence of AG825 promoted greater phosphorylation of Sch-S518 (a 4.6-fold increase) and Pak (a 3.1-fold increase) compared to starved SCs, suggesting that ErbB2 kinase activity partially inhibits Pak and its phosphorylation of Sch. PKA has been shown to directly phosphorylate and inhibit Pak (Howe and Juliano, 2000). We found that AG825 inhibited phosphorylation of CREB in response to NRG1 β in dually stimulated SCs, suggesting that ErbB activation of PKA might function to inhibit Pak in SCs following NRG1 β and laminin-1 stimulation (Figure 3.7 G). Sch, Pak and β 1 integrin protein levels were not significantly changed in SCs stimulated with NRG1 β and laminin-1 in the presence and absence of AG825 (Figure 3.7 C, D). Stimulation with NRG1 β and laminin-1 resulted in a 20% decrease in ErbB2 compared to starved SCs. These results

suggest that ErbB2 kinase activity inhibits or competes with Pak-dependent phosphorylation of Sch in response to laminin-1, possibly through PKA. A model consistent with our results is shown (Figure 3.8).

3.4 Discussion

Phosphorylation of S518 is a critical switch that controls Sch's tumor suppressor activity. Pak and PKA have been shown to phosphorylate Sch on S518 when overexpressed with Sch in cell lines and in in vitro kinase assays, but neither kinase has been linked to receptor activation and phosphorylation of endogenously expressed Sch in any cell type (Kissil et al., 2002; Xiao et al., 2002; Alfthan et al., 2004). Here, we identify two receptors that lead to rapid phosphorylation of Sch-S518 in SCs. Laminin-1 binding to $\beta 1$ integrin activates Pak, whereas NRG1 β binding to ErbB receptors activates PKA. Each kinase phosphorylates Sch-S518 within 30 minutes of stimulation. Both receptors regulate all stages of Schwann cell development including proliferation, and both play central roles in the tumorigenic and metastatic capacities of many additional cell types.

3.4.1 Two Distinct Receptor Mediated Pathways Promote Sch Phosphorylation

Our data provide strong evidence that NRG1 β binding to ErbB2/ErbB3 induces PKA-dependent phosphorylation of endogenous Sch. This conclusion is supported by the following results. First, serum-starved SCs have basal levels of phosphorylated Pak and Sch. NRG1 β inhibits basal Pak activity while increasing the amount of phosphorylated Sch, 2.7-fold. Second, inhibition of ErbB2 kinase activity by AG825 reduces Sch-S518 phosphorylation in response to NRG1 β by 120%. Third, the PKA inhibitor, PKI₁₄₋₂₂ similarly reduces Sch-S518 phosphorylation in response to NRG1 β by 70%. Lastly, although not as effective as NRG1 β , forskolin increases Sch phosphorylation. We also show that NRG1 β promotes phosphorylation of CREB, and that both AG825 and PKI₁₄₋₂₂ inhibit this phosphorylation, consistent with NRG1 β

stimulation of PKA activity. In support, others have also found evidence of PKA activation by NRG in SCs (Kim et al., 1997). Overall, our results indicate that NRG1 β binds to ErbB2/ErbB3 receptors and stimulates rapid phosphorylation of Sch on S518 by PKA.

Cell adhesion to extracellular matrix through integrins activates Pak (Del Pozo et al., 2000). Laminin-1 is present in the endoneurium of nerves in perinatal mice, and promotes strong in vitro adhesion, migration and proliferation of SCs (Milner et al., 1997; Dubovy et al., 2000). Previously we demonstrated that $\alpha 6\beta 1$ integrin is the predominant laminin-1 binding integrin present in SCs at this stage of development (Fernandez-Valle et al., 1994). Our new findings indicate that laminin-1 binding to $\alpha 6\beta 1$ integrin promotes Sch-S518 phosphorylation by Pak. Our evidence is as follows: First, stimulation of SCs with soluble laminin-1 increases both P-Pak (1.5-fold) and PS518-Sch (3.5-fold) over basal levels. Similarly, P-Pak and PS518-Sch are increased within SC processes as assessed by quantification of immunofluorescence. Second, Sch-GFP expressed in SCs adhering to laminin-1 is phosphorylated by an endogenous kinase, predominantly when localized at the plasma membrane of cellular processes and particularly in radial membrane protrusions. Previously, we reported that Cdc42-Pak rather than Rac-Pak was associated with phosphorylation of Sch in these domains (Thaxton et al., 2007). Consistently, we find that expression of catalytically inactive Pak inhibits phosphorylation of Sch-GFP in SCs adhering to laminin-1. Lastly, laminin-1 does not activate PKA or trans-activate ErbB2, as P-ErbB2 and P-CREB were not found, ruling out PKA dependent phosphorylation of Sch in response to laminin-1. It has been established that Pak is recruited to focal complexes through an indirect interaction with paxillin, stimulated by Cdc42 and Rac activity (Brown et al., 2002).

Together, our results indicate that aggregation of $\alpha 6\beta 1$ integrins by laminin-1 triggers translocation of a Pak-paxillin-Sch complex to nascent membrane protrusions where Sch-S518 is phosphorylated by Cdc42-Pak.

3.4.2 ErbB2 Modulates $\beta 1$ Integrin Signaling

Our data demonstrate that ErbB2/ErbB3 and $\beta 1$ integrin physically interact and function as co-receptors that regulate both the turnover rate of each receptor and their downstream signals.

ErbB2/ErbB3 and $\beta 1$ integrin co-immunoprecipitate and co-localize on the SC surface, and are enriched at the distal tips of SC processes stimulated with NRG1 β . Simultaneous activation of ErbB2/ErbB3 and $\beta 1$ integrin receptors does not synergistically increase Sch phosphorylation, but rather ErbB2 activity appears to antagonize Pak-dependent phosphorylation of Sch. In SCs stimulated with NRG1 β , laminin-1 and AG825, PS518-Sch and P-Pak levels are increased with respect to the levels in dually stimulated SCs, while CREB phosphorylation is eliminated.

AG825, in the absence of NRG1 β also increases basal levels of phosphorylated Pak and Sch (data not shown), consistent with autocrine stimulation of ErbB2 and PKA activity (Rosenbaum *et al.*, 1997). PKA has been shown to directly phosphorylate and inhibit Pak in NIH3T3 cells (Howe and Juliano, 2000). Together, these findings indicate that ErbB2, possibly through PKA, antagonizes Pak dependent phosphorylation of Sch downstream of $\beta 1$ integrin.

3.4.3 Implications For Schwannoma Development

$\beta 1$ integrin and ErbB receptors regulate SC proliferation during development. Conditional inactivation of genes encoding their respective ligands, the laminin $\gamma 1$ gene and the neuregulin

gene, in mice are associated with low proliferative capacity of SCs during development, demonstrating that both receptors are essential for SC proliferation (reviewed in Garratt et al., 2000; Chen and Strickland, 2003; Yang et al., 2005). Cooperation between receptor tyrosine kinase and integrin signaling is required for activation of the Ras-Raf-Mek-Erk pathway, which is active in both human and rodent SCs (reviewed in Lee and Juliano, 2004; Monje et al., 2006; Iacovelli et al., 2007). Activation of mitogenic receptor tyrosine kinases, in the absence of integrin-dependent adhesion, is coupled only to Ras and Raf and does not lead to Mek and Erk activity. Adhesion of integrins to extracellular matrix activates the Rho family of GTPases and Pak, allowing Pak phosphorylation of c-Raf and Mek. Mek then associates with, and phosphorylates Erk (Del Pozo et al., 2000; Coles and Shaw 2002). One mechanism by which Sch restricts proliferation is by inhibiting Rac-Pak activity in confluent cells (reviewed in Okada et al., 2007). Phosphorylation of Sch downstream of both ErbB and $\beta 1$ integrin receptors would inactivate this ability, and would allow Rac-Pak signaling to couple to Ras-Erk pathways and stimulate proliferation of subconfluent cells.

Consistent with the rapid turnover of focal contacts in subconfluent, motile cells, we find that $\beta 1$ integrin and ErbB2 protein levels are rapidly modulated by receptor activity. Whereas laminin-1 stimulates a 50% increase in ErbB2 protein expression over starved SCs, NRG1 β promotes a 55% decrease in ErbB2 receptors while increasing $\beta 1$ integrin levels 2.0 fold over the levels observed in starved SCs. AG825 attenuates the loss of ErbB2 protein in response to NRG1 β , and inhibits the increase in $\beta 1$ integrin, confirming that ErbB2 kinase activity modulates the fate of each receptor. In laminin-1 stimulated SCs, AG825 decreases $\beta 1$ integrin levels and increases

ErbB2 levels, consistent with autocrine stimulation of ErbB2 in SCs. These effects are likely mediated through changes in protein stability and/or degradation, as they occur within 30 minutes of stimulation. Moreover, our results show that each receptor has a different fate after activation, β 1 integrins are stabilized following NRG1 β stimulation, whereas ErbB2 is degraded. This also implies that ErbB2 dependent inhibition of Pak is transient, and that β 1 integrin and Pak dependent phosphorylation of Sch occurs during the time ErbB2 receptor expression on the plasma membrane is low.

Sch is at a critical convergence point for transduction of signals from these receptors, and reveals why loss of this protein in SCs predisposes them to tumor formation. There is evidence that Sch controls endocytosis of ErbB family members, possibly through its interaction with HRS (Scoles *et al.*, 2005; Maitra *et al.*, 2006). Additionally, other paxillin binding proteins regulate vesicle trafficking and receptor degradation (reviewed in Turner, 2000). Of note, human schwannoma cells have increased expression of β 1 integrin and activated ErbB2, Rac and Pak (Hansen and Linthicum, 2004; Kaempchen *et al.* 2003; Utermark *et al.*, 2003). Loss of Sch expression in SCs could allow unrestricted autocrine stimulation of ErbB2/ErbB3, resulting in increased β 1 integrin levels and prolonged activation of PKA, Rac-Pak, Ras-Erk and PI3K/AKT pathways. Activation of these signaling cascades would stimulate a slow, but continuous proliferation of SCs, characteristic of schwannoma growth in individuals with NF2.

In summary, we show that activation of ErbB2/ErbB3 and β 1 integrin receptors promotes phosphorylation of Sch through distinct PKA- and Pak-dependent pathways. *In vivo*, these

signaling cascades would cooperate to promote SC proliferation in response to axonal NRG and basal lamina adhesion. In its phosphorylated state, Sch would also permit Rac-Pak dependent changes in the actin cytoskeleton associated with extension of processes along axons, a critical function for myelination. Our findings shed light on Sch's function during development and pathogenesis in the peripheral nervous system.

Figure 3.1 Phosphorylated Forms Of ErbB2, Sch, And Pak Co-localize With Paxillin And Cdc42 In Processes, Their Distal Tips And Radial Protrusions Following Acute Stimulation With NRG1 β .

Subconfluent SCs plated on PLL/laminin-1 coated coverslips were serum-starved overnight and were then stimulated with NRG1 β for 30 minutes. Immunostaining was conducted for the indicated proteins to assess their phosphorylation states and localizations. SCs are shown at low magnification (left), and the boxed area is shown at higher magnifications to the right and within insets. All proteins were present in the cytosol, along SC processes and were focally enriched at radial membrane protrusions and distal tips. Scale bars represent 20 μ m.

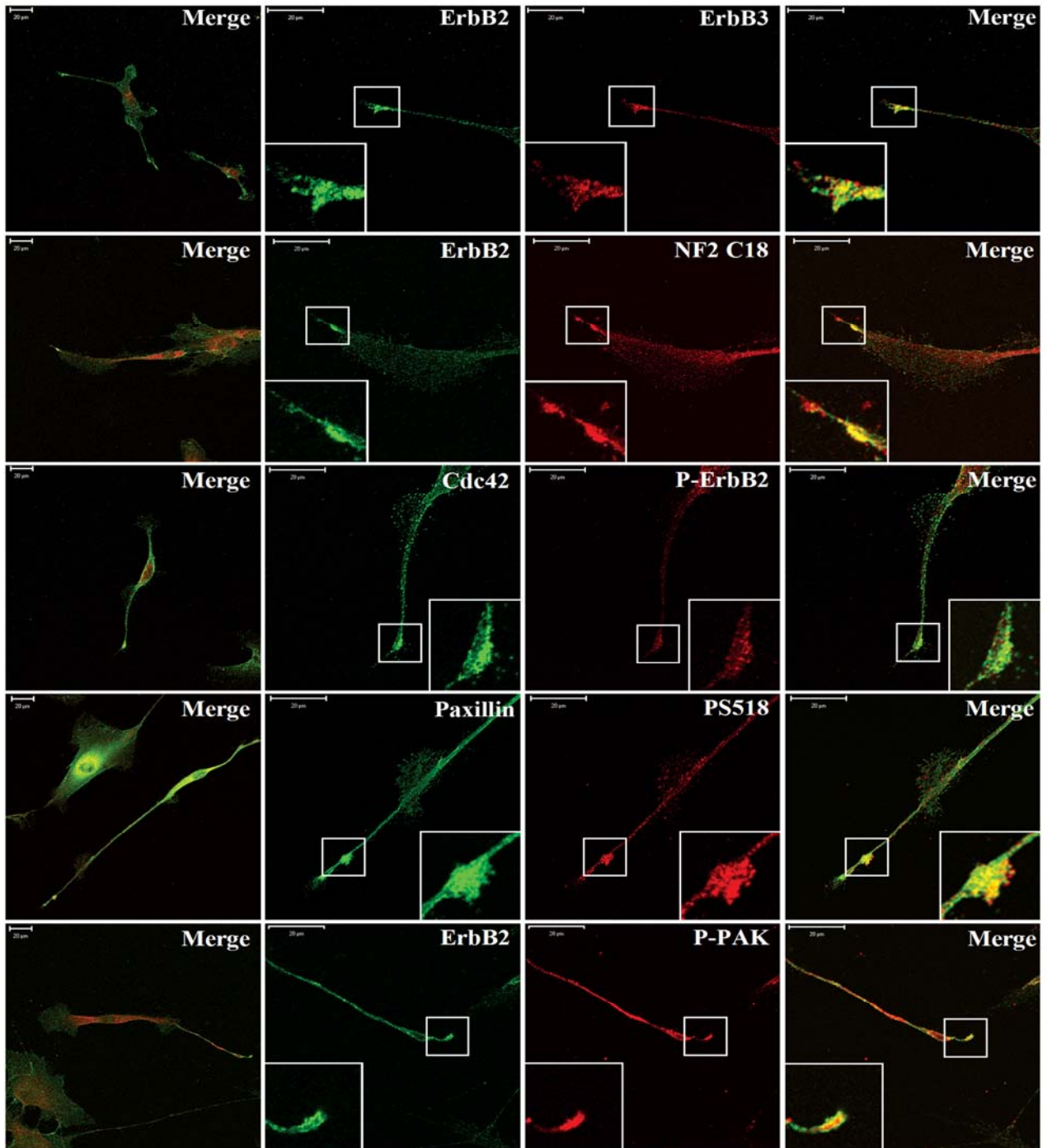


Figure 3.1 Phosphorylated Forms Of ErbB2, Sch, And Pak Co-Localize With Paxillin And Cdc42 In Processes, Their Distal Tips And Radial Protrusions Following Acute Stimulation With NRG1 β .

Figure 3.2 NRG1 β And Laminin-1 Induce Sch Phosphorylation In SC Processes.

Subconfluent SCs grown on PLL/laminin-1 were starved overnight (D0.5) and were left untreated, or were stimulated for 30 minutes with **A)** NRG1 β (N;10ng/ml) or **C)** laminin-1 (L;10 μ g/ml). Phosphorylation of ErbB2 (P-ErbB2), Sch (PS518-Sch), and Pak (P-Pak) was assessed by immunostaining with phospho-specific antibodies. **B, D)** Quantification of mean fluorescence intensity in 15-20 isolated SC processes per condition is shown. The graphs represent the average fold increase in three or more experiments. Error bars represent the SEM. p-values are ≤ 0.05 (*). Scale bars represent 20 μ m.

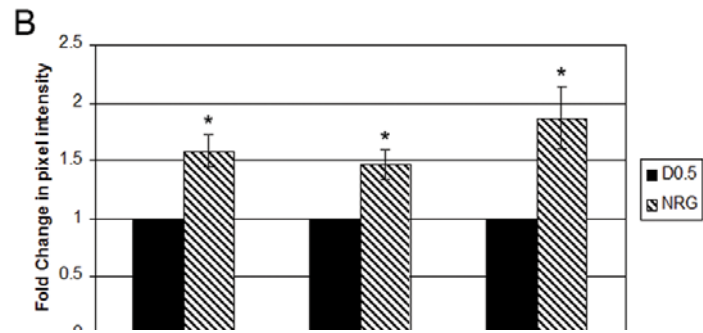
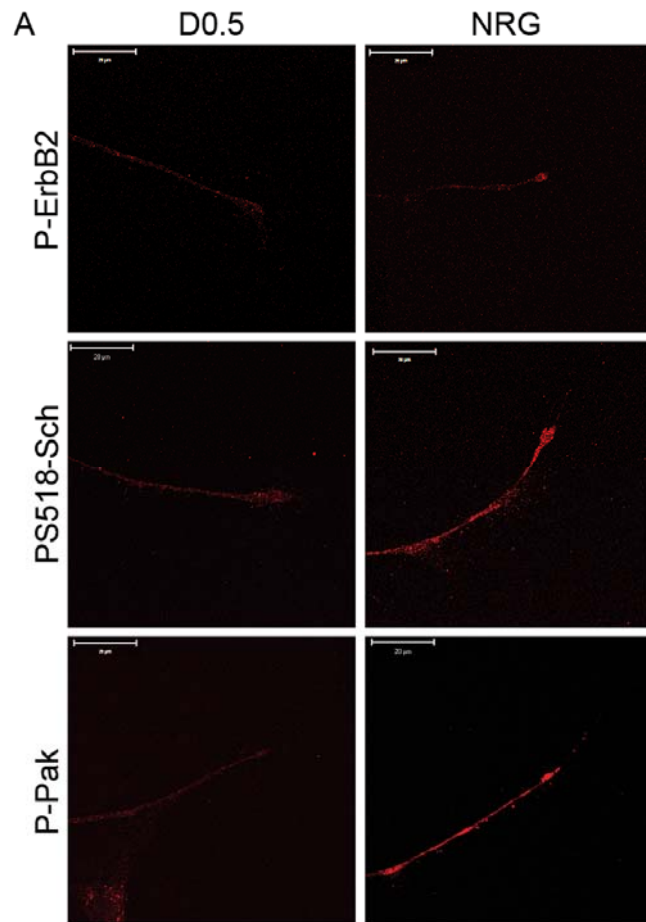


Figure 3.2 A,B) NRG1 β And Laminin-1 Induce Sch Phosphorylation In SC Processes

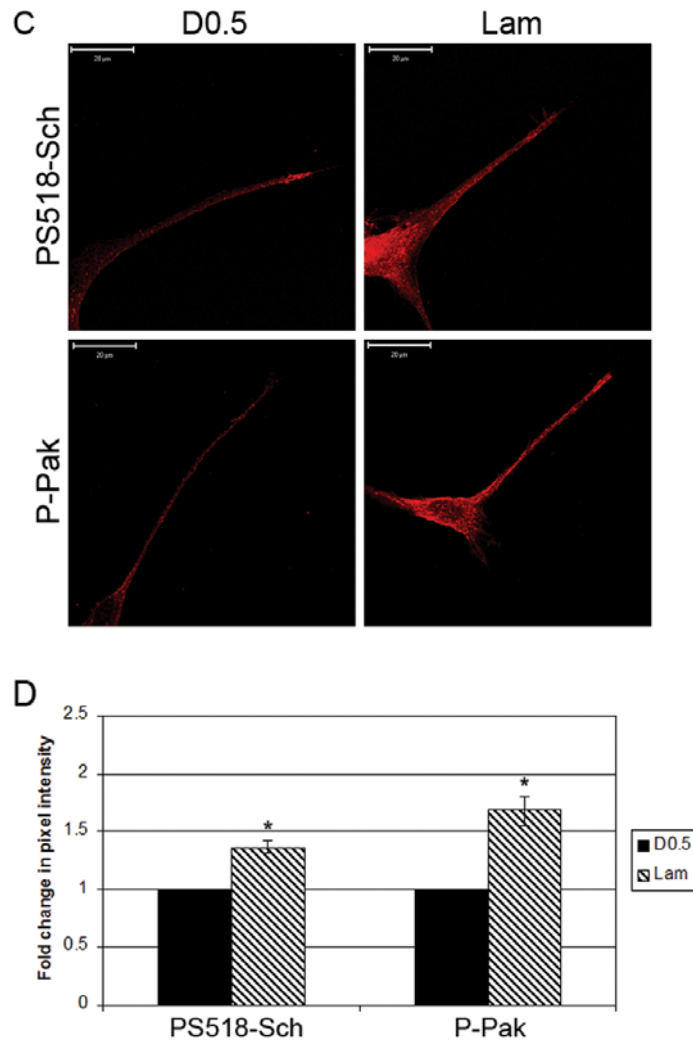


Figure 3.2 C,D) NRG1 β And Laminin-1 Induce Sch Phosphorylation In SC Processes

Figure 3.3 NRG1 β Stimulates Phosphorylation Of Sch By PKA

A, C) Subconfluent SC cultures grown on PLL were serum-starved overnight and were stimulated for 30 minutes with NRG1 β (10ng/ml) in the absence and presence of AG825 (1 μ M). Western blot analysis was used to determine the levels of phosphorylated and total ErbB2, Sch, and Pak. **B, D)** Quantification of the blots are shown for starved (D0.5), NRG1 β stimulated (N) and NRG1 β plus AG825 (N+A) stimulated cultures. **E)** Subconfluent SCs grown as above were stimulated for 30 minutes with NRG1 β in the presence and absence of PKI 14-22 (50nM), and with forskolin (FSK; 2 μ M) alone. Western blot analysis was used to determine the level of phosphorylated Sch (PS518-Sch) and CREB (P-CREB). **F)** Quantification of PS518-Sch in starved (D0.5) and NRG1 β (N), NRG1 β plus PKI 14-22 (N+P), and forskolin (FSK) stimulated cultures. GAPDH was used as a loading control. The graphs represent the average fold increase in three or more experiments. Error bars represent the SEM for each condition. p-values are \leq 0.05(*) and $<0.01(**)$ with respect to starved SCs or as indicated.

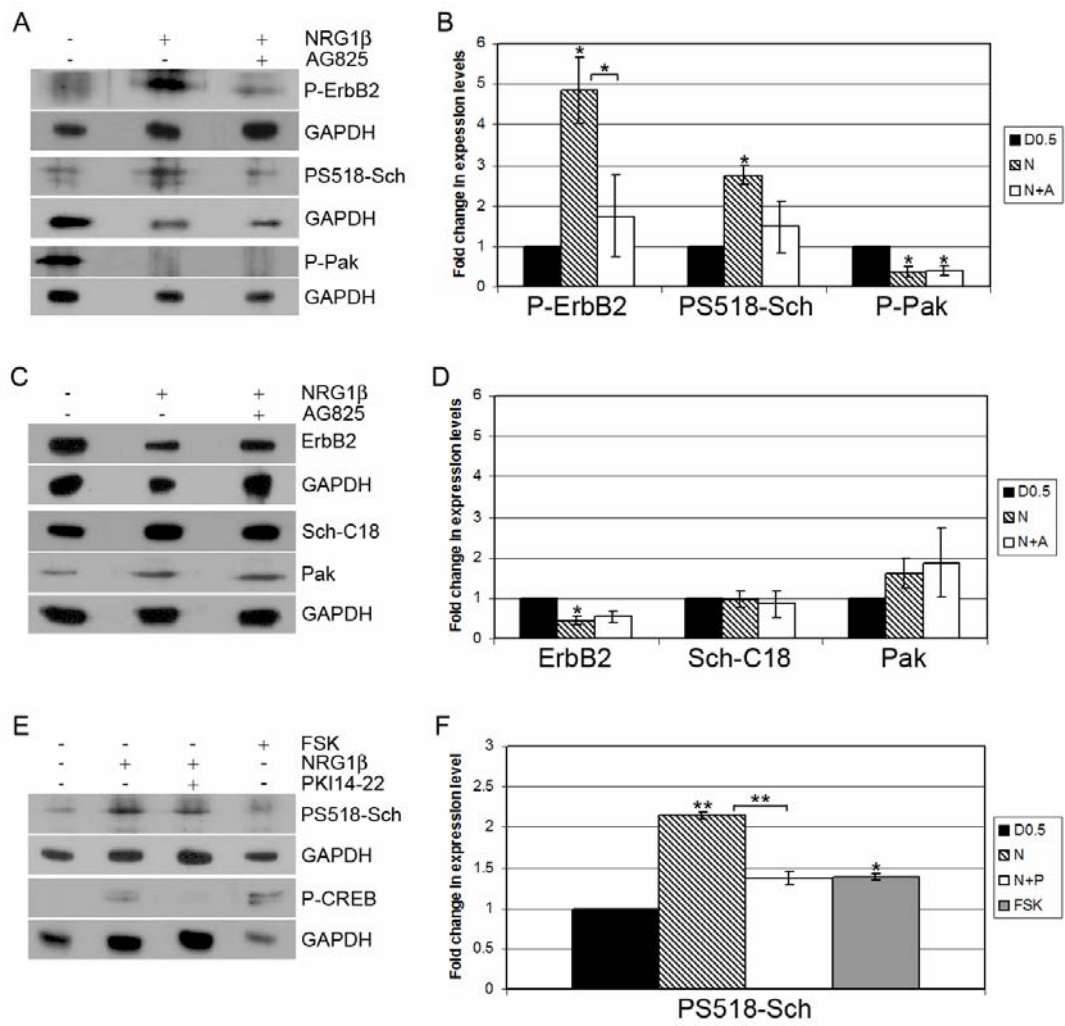


Figure 3.3 NRG1 Stimulates Phosphorylation Of Sch By PKA.

Figure 3.4 Laminin-1 Stimulates Phosphorylation Of Sch.

A, C) Subconfluent SC cultures grown on PLL were stimulated with laminin-1 (Lam; 10 μ g/ml) for 30 minutes after overnight serum starvation. Western blot analysis using phospho-specific for Sch (PS518-Sch), Pak (P-Pak), ErbB2 (P-ErbB2), and CREB (P-CREB), and antibodies against total Sch (Sch-C18), Pak, and β 1 integrin are shown. **B, D)** Quantification of Western blots for starved (D0.5) and laminin-1 stimulated (L) cultures is shown. The graphs represent the average fold increase observed in three or more experiments. GAPDH was used as a loading control for all blots. Error bars represent the SEM. p-values are ≤ 0.05 (*) and <0.01 (**).

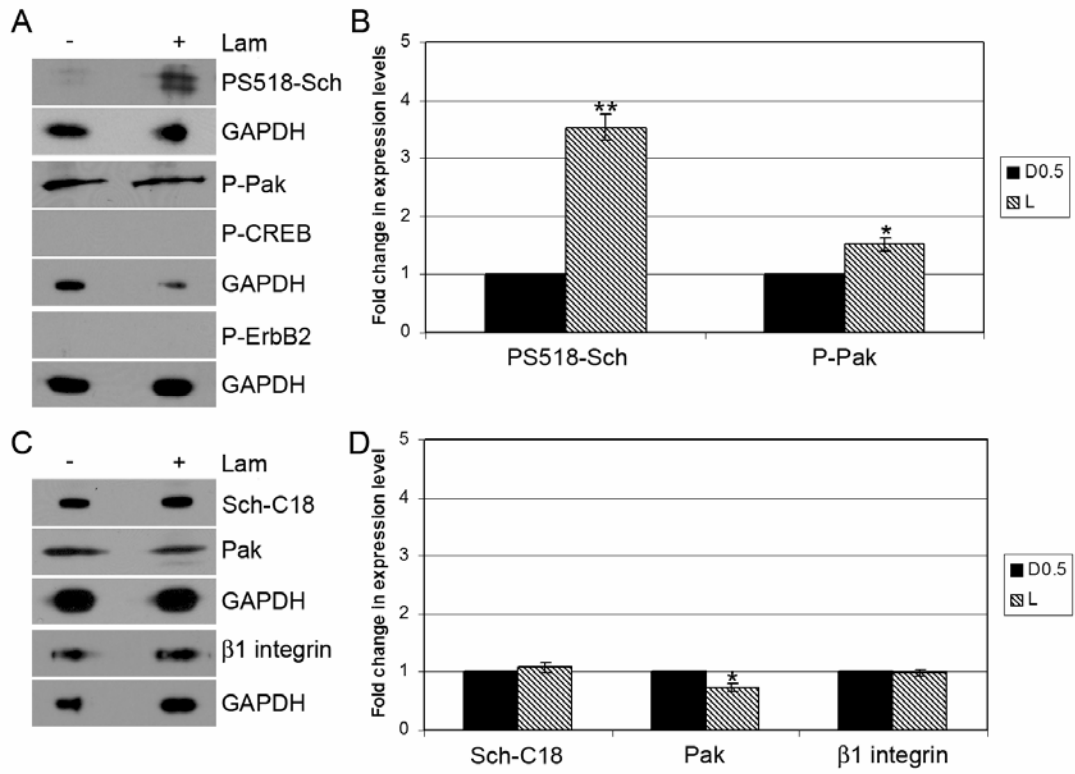


Figure 3.4 Laminin-1 Stimulates Phosphorylation Of Sch.

Figure 3.5 Catalytically Inactive Pak Inhibits Sch Phosphorylation In SCs Adhering To Laminin-1.

SCs plated on PLL and laminin-1 were transiently transfected with GFP-tagged full length Sch (Sch-GFP) alone or with Myc-tagged catalytically inactive Pak (Myc-Pak K299A) or Myc-tagged constitutively active Pak (Myc-Pak T423E), and were immunostained to assess Sch-S518 phosphorylation (PS518-Sch) and Myc-Pak expression (Myc). Scale bars represent 20 μ m.

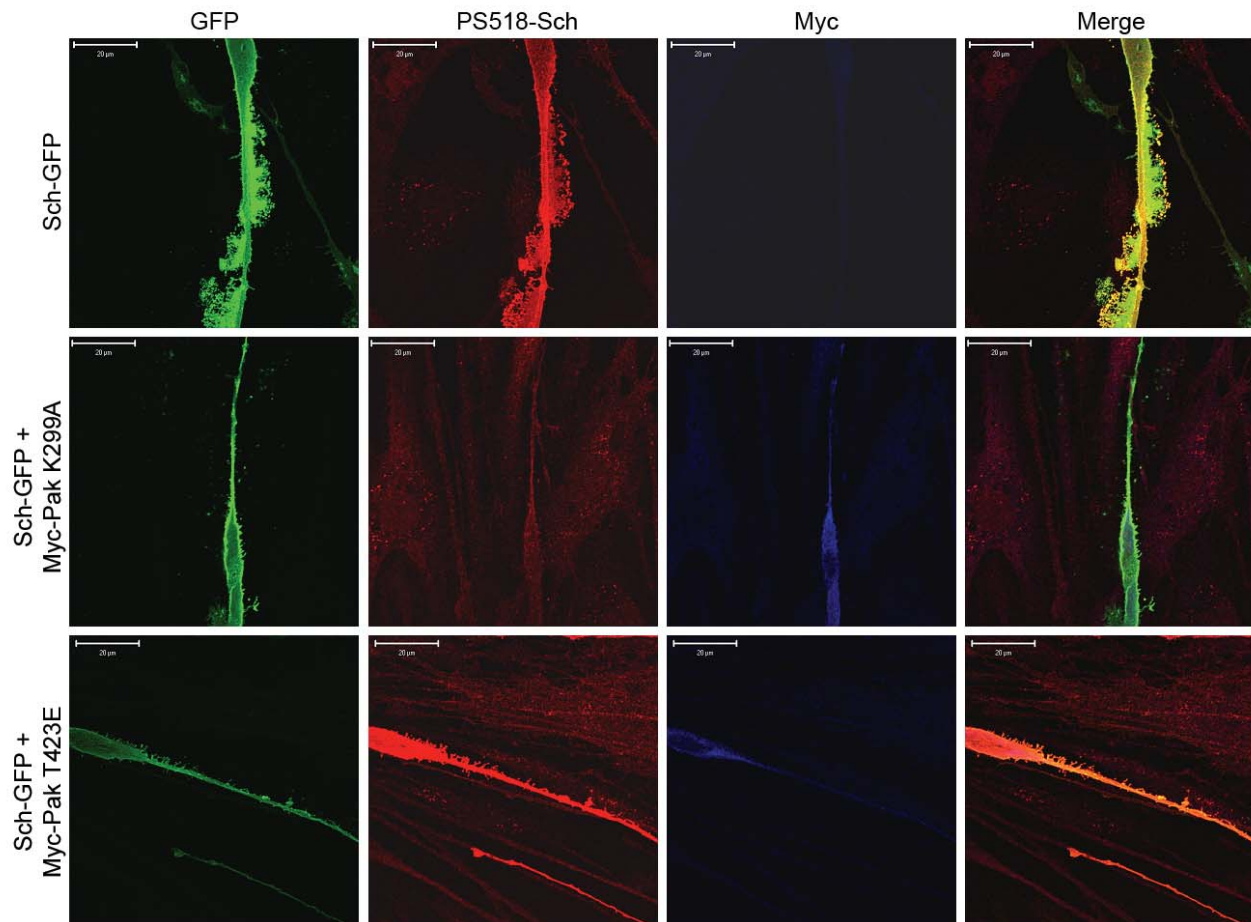


Figure 3.5 Catalytically Inactive Pak Inhibits Sch Phosphorylation In SCs Adhering To Laminin-1.

Figure 3.6 β 1 integrin And ErbB2 Exist As A Complex On The Plasma Membrane.

A) Subconfluent SC cultures grown on PLL and laminin-1 were starved overnight and were stimulated with NRG1 β (10ng/ml) for 30 minutes. SCs were triple-labeled with the indicated antibodies to assess protein co-localization. **B)** Subconfluent SC cultures were extracted and lysates (TE) were pre-cleared (PC) with normal IgG and were immunoprecipitated with β 1 integrin antibody (β 1 IP). Western blots analysis was conducted on the immunoprecipitate, pre-cleared, and total extracts (TE) with the indicated antibodies. **C)** Intact SCs in suspension were incubated with β 1 integrin antibody immobilized on magnetic beads to induce clustering. SCs were lysed, and the immunoprecipitate (β 1IP) and total cell extract (TE) were immunoblotted with the indicated antibodies. **D)** Subconfluent and serum-starved SCs grown on PLL were stimulated for 30 minutes with NRG1 β (10ng/ml) in the presence and absence of AG825 (1 μ M). Western blot analysis was conducted with the indicated antibodies. **E)** Quantification of total β 1 integrin and ErbB2 expression was assessed by densitometry in starved (D0.5), NRG1 β stimulated (N) and NRG with AG825 (N+A) stimulated cultures. **F)** Subconfluent SCs were starved overnight in D0.5 and then were stimulated for 30 minutes with laminin-1 (Lam; 10 μ g/ml) in the presence and absence of AG825 (1 μ M). Western blot analyses were conducted to examine changes in receptor expression levels. **G)** Quantification of total β 1 integrin and ErbB2 expression in starved (D0.5), laminin-1 (L) stimulated and laminin-1 + AG825 (L+A) stimulated cultures is shown. GAPDH was used as a loading control for all blots. The graphs represent the average fold increase in three or more experiments. Error bars represent the SEM.

p-values are ≤ 0.05 (*), <0.01 (**), and ≤ 0.005 (***) with respect to starved SCs or as indicated.

Scale bars represent $20\mu\text{m}$.

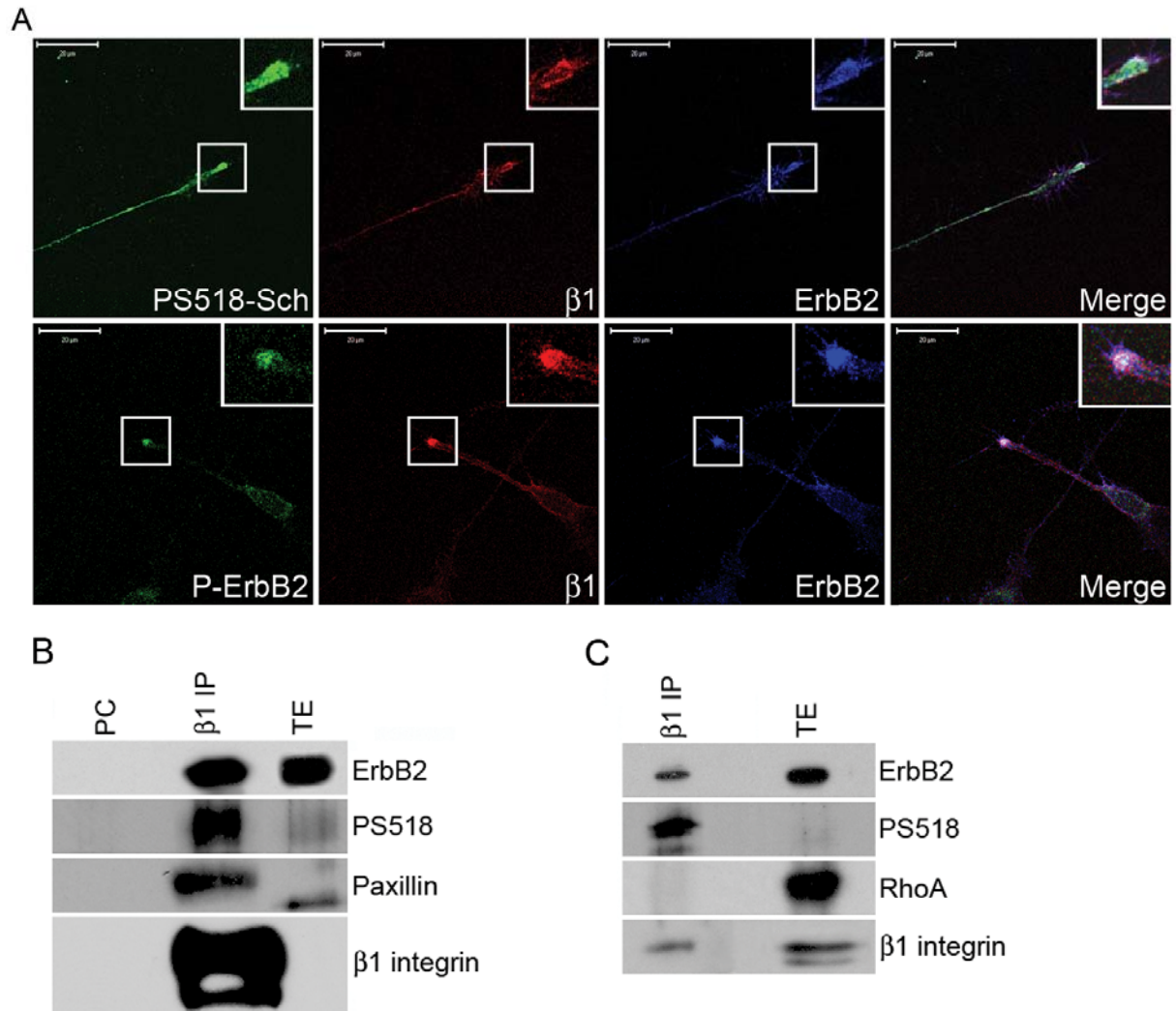


Figure 3.6 β 1 Integrin And ErbB2 Exist As A Complex On The Plasma Membrane.

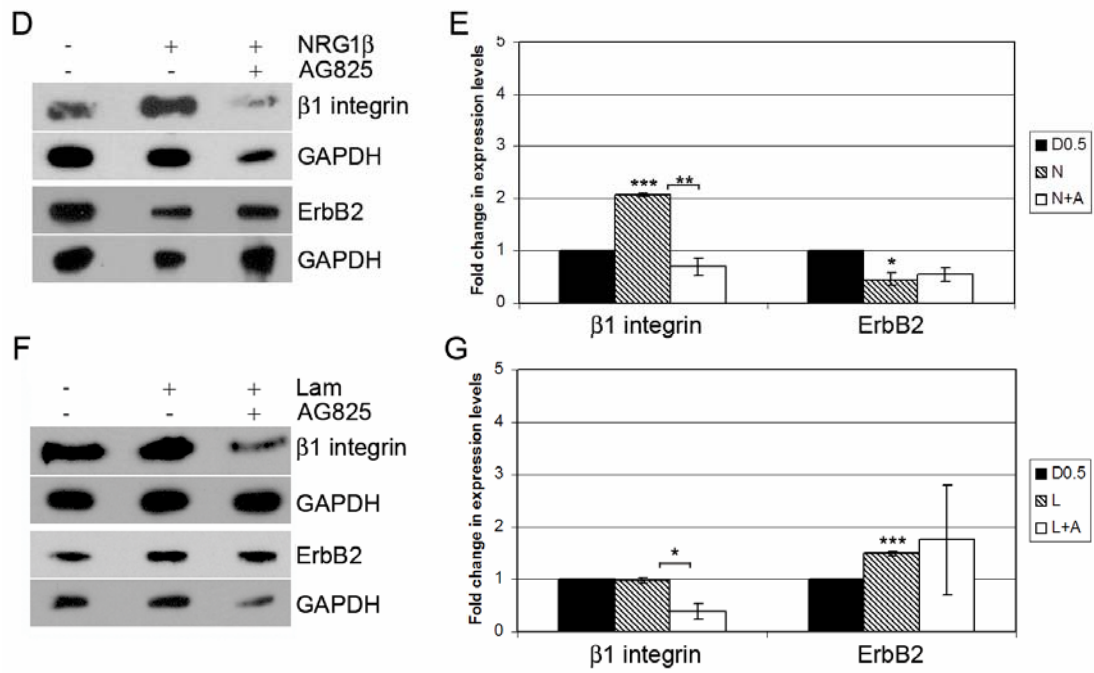


Figure 3.6 β 1 Integrin And ErbB2 Exist As A Complex On The Plasma Membrane.

Figure 3.7 AG825 Increases Sch Phosphorylation In Response To Laminin-1 And NRG1 β .

Subconfluent SC cultures grown on PLL were serum-starved overnight and were stimulated for 30 minutes with NRG1 β (10ng/ml) and laminin-1 (Lam; 10 μ g/ml) together, in the absence and presence of AG825 (1 μ M). **A, C, E, G)** Western blot analysis was conducted using phospho-specific antibodies for Sch (PS518-Sch), Pak (P-Pak), and CREB (P-CREB). Total protein expression was analyzed using antibodies against Sch (Sch-C18), Pak, β 1 integrin, and ErbB2. **B, D, F)** Quantification of the expression levels of phosphorylated forms of Sch (PS518-Sch) and Pak (P-Pak) were assessed in starved (D0.5), NRG1 β and laminin-1 stimulated (N+L), and NRG1 plus laminin-1 and AG825 (N+L+A) stimulated cultures. The amount of total Sch (Sch-C18), Pak, β 1 integrin, and ErbB2 proteins were measured by densitometry. GAPDH was used as a loading control. The graphs represent the average fold increase in three or more experiments. Error bars represent the SEM. p-values are ≤ 0.05 (*) with respect to starved SCs, or as indicated.

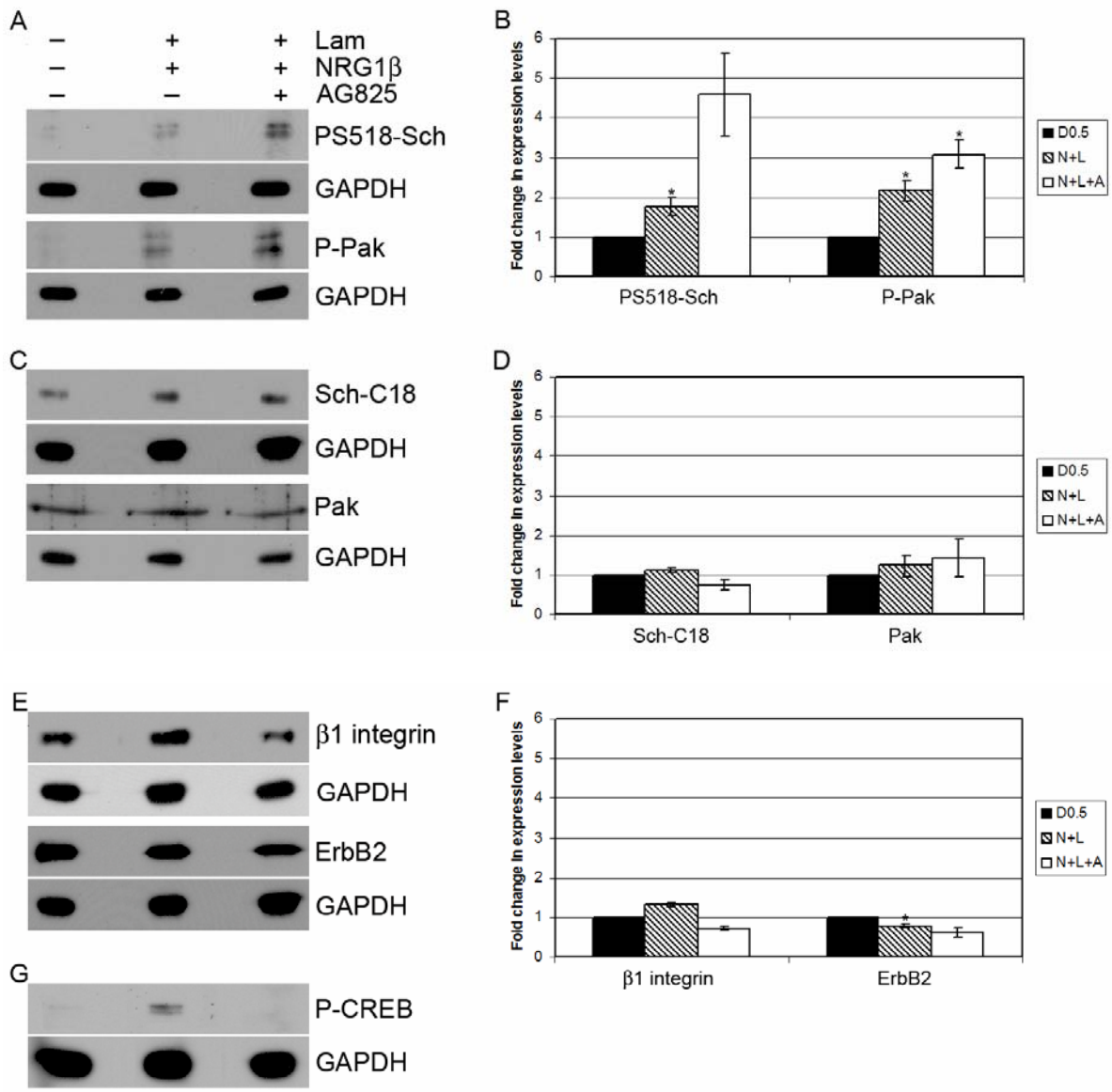


Figure 3.7 AG825 Increases Sch Phosphorylation In Response To Laminin-1 And NRG1 β .

Figure 3.8 Model Of ErbB And β 1 Integrin Induced Phosphorylation Of Sch And Inactivation Of Its Tumor Suppressor Function In Subconfluent SCs.

Unphosphorylated Sch restricts proliferation by inhibiting activation of the Rac-Pak pathway in confluent cells. In a regulatory loop, Pak phosphorylates Sch, inactivating its tumor suppressor ability. In subconfluent SCs, Sch is phosphorylated in response to activation of ErbB2/ErbB3 and α 6 β 1 integrin receptors by NRG1 β and laminin-1, respectively, through two distinct pathways involving PKA and Pak. Simultaneous co-activation of both receptors does not synergistically increase Sch phosphorylation, but rather ErbB2 antagonizes Pak phosphorylation of Sch, possibly through its activation of PKA (dashed line). Phosphorylated Sch is unable to inhibit Rac-Pak and allows transduction of ErbB and α 6 β 1 integrin signals that promote G1 progression. Additionally, the presence of this complex at the motile distal tip of SC processes coordinates motility along axons and other cytoskeletal changes in response to NRG and laminin, present in basal lamina, which is necessary for myelination of peripheral nerves during development.

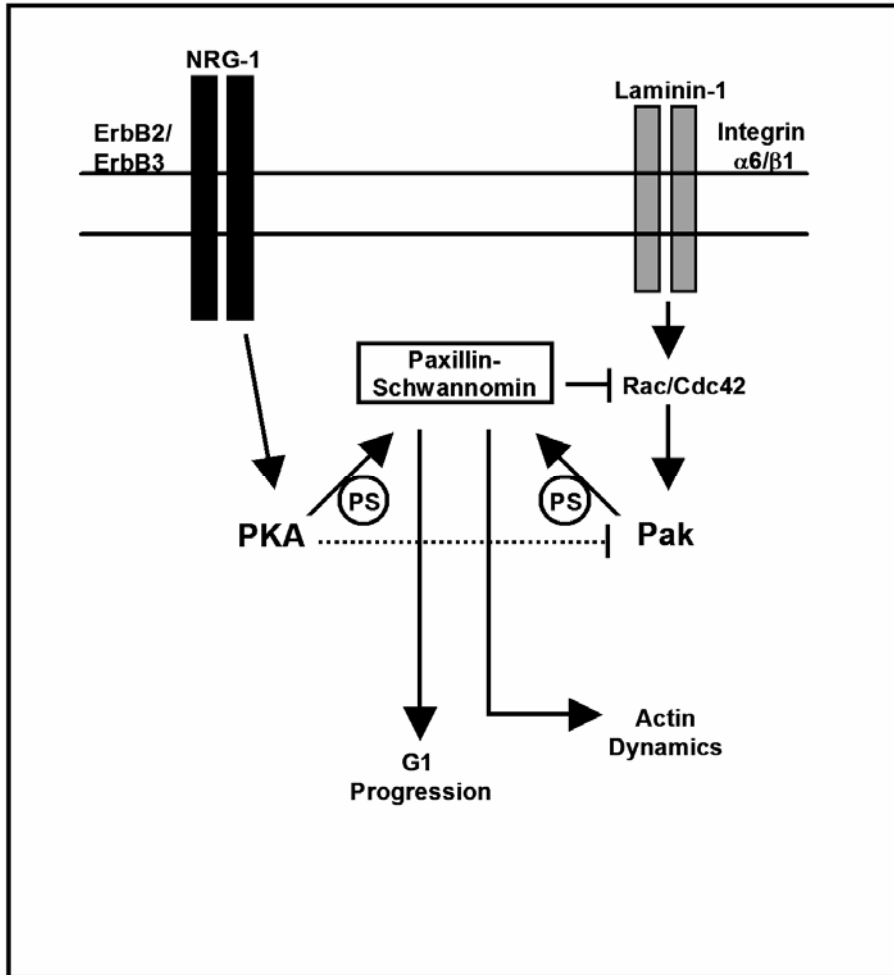


Figure 3.8 Model Of ErbB And β1 Integrin Induced Phosphorylation Of Sch And Inactivation Of Its Tumor Suppressor Function In Subconfluent SCs.

CHAPTER 4

EXPRESSION OF THE NF2 TUMOR SUPPRESSOR IN SCHWANN CELLS PROMOTES PROCESS EXTENSION AND MYELINATION

4.1 Introduction

Schwann cells (SC) are the sole glial cell in the peripheral nervous system responsible for the segregation, ensheathment and myelination of axons in nerves. SC development consists of three main stages: proliferation and migration, defasciculation and radial sorting, and terminal differentiation and myelination. Every stage of SC development progressing towards myelination is accompanied by morphological changes involving the extension of processes along and around axons. Migration requires the simultaneous extension and retraction of bipolar SC processes in contact with axons, and is accompanied by proliferation. Radial sorting requires SCs to extend multiple processes between axon bundles, until each axon is surrounded by SC membrane. Myelination requires SCs to extend bipolar processes in contact with an axon, to define the internode (the length of a SC between consecutive Nodes of Ranvier). This is followed by radial spreading of an expansive membrane sheath inwards around an axon with repeated spiraling to build the multi-lamellar myelin sheath that is compacted through the action of myelin-specific proteins. Although considerable advances have been made in identifying myelin-specific genes and proteins, very little is known about the proteins required, or the mechanisms regulating the changes in morphology necessary for myelination, including the fundamental ability to extend bipolar processes.

Several non-myelin proteins essential for SC ensheathment and myelination have been identified, such as $\beta 1$ integrin, NRG1 type III, actin, and Rac1 (Fernandez-Valle et al., 1994; Fernandez-Valle et al., 1997; Lyons et al., 2005; Tavaggia et al., 2005; Benninger et al., 2007, Nodari et al., 2007). Loss of $\beta 1$ integrin, actin and Rac1 genes in mice results in aberrant radial sorting arising from the inability to extend processes. Disruption of NRG1 type III in mice results in amyelination due to decreased proliferation of SCs. Accordingly, mice with a conditional knockout of ErbB2, the receptor for NRG1 type III, also have peripheral amyelination (Michailov et al., 2004). Together, integrins, Rac1, and ErbB receptors participate in cooperative signaling pathways controlling both cell cycle progression and regulation of actin dynamics in multiple cell types (reviewed in Lee et al., 2004).

Previously, we demonstrated in SCs that Sch exists in a complex with $\beta 1$ integrin and ErbB2 (Fernandez-Valle et al., 2002). More recently, we have shown that stimulation of $\beta 1$ integrin and ErbB2 receptors by laminin-1 and NRG1 β respectively, promotes phosphorylation of the NF2 tumor suppressor Sch at S518. Moreover, we demonstrated that Sch promotes process extension and that the phosphorylation state of S518 specifies cellular morphology (Thaxton et al., 2007a; Thaxton et al., in press). Conditional inactivation of exon 2 in the *nf2* gene in mouse SCs results in dysmyelination, revealing a possible role for Sch during myelination (Giovannini et al., 2000). We reported that exon 2 encodes a direct binding site for paxillin (PBD1) that is necessary for Sch localization to the plasma membrane (Fernandez-Valle et al., 2002). Others have suggested that Sch lacking PBD1 has a decreased half-life and may undergo ubiquitin-mediated degradation (Gautreau et al., 2002). Schwannoma cells lacking functional Sch

expression also lose the ability to extend processes and assume the typical bipolar morphology. Instead, these tumor cells become large and spread with ruffling membrane, indicative of the increased Rac activity (Pelton et al., 1998; Kaempchen et al., 2003). Interestingly, these cells also fail to contact or align on axons *in vitro* (Nakai et al., 2006). The lack of process formation in schwannoma cells suggests that Sch may control process formation and extension in SCs, a basic requirement for its physiological function in the nervous system.

Here, we show that a major effect of Sch expression in SCs is to increase process extension. Exogenous expression of Sch in primary SCs induced an 82% increase in process length, whereas expression of a dominant negative form of Sch, Sch BBA-GFP, reduced process length by 16%. Additionally, overexpression of Sch in myelinating SCs resulted in increased internodal length. These results are consistent with a role for Sch in process extension. However, process extension in myelinating SCs is not regulated by Sch S518 phosphorylation, as both an unphosphorylatable and a phospho-mimicking form of Sch equally increase myelin internodal length. Instead, Sch phosphorylation influenced the frequency of myelination, as myelinating SCs expressing either wild-type Sch or the unphosphorylatable form had increased numbers of myelinating SCs. These results demonstrate that Sch is a key regulator of cytoskeletal dynamics that induces myelination in SCs, and shed's light on its role during SC development and peripheral neuropathies.

4.2 Materials and Methods

4.2.1 Materials

GFP, Sch-GFP, Sch S518A-GFP, Sch S518D-GFP were all previously described (Thaxton et al., 2007). Sch BBA-GFP and CASPR antibodies were a generous gift from Stephen Lambert (University of Central Florida, Orlando, FL, USA). The following materials were used: Natural Mouse Laminin-1 and Lipofectamine 2000 (Invitrogen; Carlsbad, CA, USA). The following antibodies were used: Neurofilament H (Daco), P-ERM (Cell Signaling), PS518-Sch (Abcam), ErbB2 (EMD Biosciences), and Alexa Flour conjugated secondary antibodies (Invitrogen).

4.2.2 Cell Culture

Primary rat SC cultures were prepared from neo-natal pups as described previously (Chen et al., 2000). Primary rat SC cultures were grown on poly-L-lysine (PLL; 200 μ g/ml) and laminin-1 (25 μ g/ml) coated german glass coverslips. The SCs were then transiently transfected with GFP-tagged constructs as described previously (Thaxton et al, 2007). For dissociate rat Schwann cell and dorsal ganglion neuron co-cultures (SC/DRGN), DRGN were harvested from embryonic day 15 rats as described previously (Chen et al., 2000). The equivalent of 1 DRGN is seeded onto each PLL and laminin coated german glass coverslip. One day after harvesting, the media for the DRGN is changed to an anti-mitotic media for purification of the neurons. Once purified, the DRGN are washed over a week with at least three changes of media to remove the anti-mitotic media. Next, the DRGN are seeded with primary rat SC cultures at 2×10^5 SCs per

coverslip. These co-cultures are maintained until the SCs have proliferated and reached a high density, at which point they are either transfected or used in a time course of myelination.

4.2.3 Transfection Of Schwann Cell And Dorsal Root Ganglion Neuron Co-Cultures

SC/DRGN co-cultures described above are transiently transfected with GFP-tagged constructs using Lipofectamine 2000. Briefly, 250ng of GFP-tagged construct is transfected per coverslip according to the manufacturer's protocol. After 4 hours in Lipofectamine 2000, the culture medium was replaced with the standard medium, CB10, containing 10% serum. Twenty hours after transfection, the medium on the SC/DRGN co-cultures was replaced with media containing ascorbic acid to induce myelination. The SC/DRGN co-cultures were then fed every other day with medium containing ascorbic acid for at least 10-12 days, then they were fixed and immunostained to assess myelination.

4.2.4 Immunostaining

Primary rat SC cultures were fixed with 4% paraformaldehyde, washed with phosphate buffer (0.1M phosphate), stained with phalloidin, and mounted. Immunostaining of the SC/DRGN co-cultures was as described previously (Thaxton et al., 2007), with modifications. Briefly, SC/DRGN co-cultures were washed 3 times in Lebovitz 15 (L-15) media, followed by fixation with 4% paraformaldehyde (in 0.1M phosphate) and permeabilization with 4% paraformaldehyde and 0.2% TritonX-100 (in 0.1M phosphate). The co-cultures were blocked in 10% normal goat serum (NGS) in L-15 for 30minutes, incubated for 1 hour with primary antibodies, rinsed 4x in blocking buffer, and incubated with Alexa Flour conjugated secondary antibodies. Finally, the SC/DRGN co-cultures were rinsed 2x in blocking buffer followed by 2 rinses with phosphate

buffer (0.1M) and mounted using BioMedia gel (Biomedica, CA, USA). All cultures were analyzed with a Zeiss scanning laser microscope and LSM510 software. Images shown represent single planes, and all images were processed identically.

4.3 Results

4.3.1 Sch Expression Promotes Process Extension In SCs

Dynamic control of process extension is required at every stage of SC development. This allows SCs to migrate down axons, to proliferate in response to axonal mitogens during radial sorting, and to delineate and establish the location of the internodes and nodes during myelination.

Previously, we showed that Sch regulates cell morphology and process formation in SCs (Thaxton et al., 2007). Additionally, it was shown by others that schwannomas deficient in Sch assumed a rounded shape and failed to contact and align on axons when co-cultured with neurons (Nakai et al, 2006). To examine Sch's role in process elongation, we transiently transfected primary rat SCs with GFP, Sch-GFP, and the dominant negative isoform, Sch BBA-GFP and measured process lengths. SCs expressing GFP extended processes that were most frequently between 51-100 μ m (Figure 4.1 A, B). These SC processes typically remained within a single frame of view, and the mean length was 140 μ m (Figure 4.1 C). SCs expressing Sch-GFP extended processes that were significantly longer than GFP controls. Often the processes extended for 2-4 fields of view (Figure 4.1A). The most frequently occurring lengths of Sch-GFP positive processes ranged between 151-251 μ m, and again at greater than 401 μ m. The average process length of SCs expressing Sch-GFP was 256 μ m, an 82% increase in length compared to SC expressing GFP alone (Figure 4.1 B, C). Processes from SCs expressing Sch

BBA-GFP averaged 118 μ m and the most frequent length was 51-100 μ m (Figure 4.1 A, B, C).

These results demonstrate that Sch modulates process elongation in SCs.

4.3.2 Sch Expression Increases Myelin Internodal Length

To determine if expression of Sch also increased myelin internodal length, we transiently transfected SC/DRGN co-cultures with GFP, Sch-GFP, and Sch BBA-GFP twenty-four hours prior to the addition of ascorbate, that triggers initiation of myelination. After 10 - 12 days in ascorbate containing medium, the SC/DRGN co-cultures were fixed and were immunostained with antibodies against myelin specific proteins. Assessment of internodal length was performed on every GFP positive myelin segment in each culture per condition (Figure 4.2). The most frequent length of a GFP-positive myelin internode fell between 101-125 μ m, with an average internodal length of 125 μ m (Figure 4.2A-C). There was a modest, but consistently observed and significant increase in internodal length in SCs expressing Sch-GFP compared to GFP. The average internodal length was 146 μ m, and the most frequent length fell between 126-150 μ m (Figure 4.2A-C). Quantification of the internodal length could not be assessed for SCs expressing Sch BBA-GFP, as these SC did not myelinate (data not shown). The absence of myelination in SCs expressing Sch BBA-GFP is consistent with the inability of schwannoma cells, lacking Sch expression, to extend processes toward axons and to align on them (Nakai et al., 2006). Moreover, it demonstrates that Sch has a critical role in myelination.

4.3.3 Myelin Formation But Not Internodal Length Is Dependent On Sch-S518

Phosphorylation

We previously demonstrated in isolated SCs that the phosphorylation state of Sch-S518 regulates SC morphology by influencing process formation and cell polarity (Thaxton et al, 2007). SCs expressing Sch-S518A that cannot be phosphorylated at amino acid 518, assume a unipolar morphology, whereas those expressing a phospho-mimicking form, Sch S518D, developed multiple processes. To examine whether Sch-S518 phosphorylation affected the myelin internodal length, we introduced plasmids encoding the S518 Sch-GFP variants in DRGN/SC co-cultures and measured the lengths of GFP-positive myelin segments. Myelinating SCs expressing Sch S518A-GFP were most frequently between 151-175 μ m in length, with an average internodal length of 156 μ m (Figure 4.2 A, B). These SCs were 25% and 7% longer than myelinating SCs expressing GFP and Sch-GFP, respectively. Interestingly, the range of internodal lengths for myelinating SCs expressing Sch S518D-GFP was the same as those expressing Sch S518A-GFP, and the average internodal length was similar at 158 μ m (Figure 4.2 C). These results indicate that Sch's ability to increase process elongation is not regulated by the phosphorylation state of S518, but rather by its increased expression level in the cell that leads to increased concentration of Sch at the plasma membrane.

Although the length of myelin internodes is independent of Sch-S518 phosphorylation, it is known that phosphorylation regulates Sch's ability to suppress growth, with the unphosphorylated form promoting cell cycle arrest (Surace et al., 2004). In order for SCs to begin myelination, they must exit the cell cycle and induce transcription of myelin-specific

genes, such as myelin associated glycoprotein (MAG), myelin basic protein (MBP) and protein zero (P0; reviewed in Jessen and Mirsky, 2005). To further analyze the effects of expression of Sch-S518 phosphorylation variants on myelination, we quantified the ratio of GFP positive myelinating SCs in co-cultures expressing GFP, Sch-GFP, Sch S518A-GFP, and Sch S518D-GFP. These co-cultures were assessed for their overall myelination efficiency and transfection efficiency, and only those experiments (coverslips) exhibiting equivalent transfection and myelination efficiencies were quantified (Figure 4.2 D). Myelinating SCs expressing GFP represented the baseline, and averaged 21 cells per culture. The average number of Sch-GFP positive myelinating SCs per culture increased 1.57-fold, to 35, compared to myelinating SCs expressing GFP alone. Interestingly, Sch S518A-GFP positive myelinating SCs averaged 41 cells per culture, a 1.96-fold increase over those expressing GFP. There was a 20% decrease in myelinating SCs expressing Sch S518D-GFP as compared to those expressing GFP alone, with only 17 cells per culture. These results were observed in three independent experiments, and suggest that dephosphorylation of Sch-S518 regulates either the exit of SCs from the cell cycle, and/or the initiation of differentiation of SC into a myelinating phenotype.

4.3.4 Sch-S518 Phosphorylation Decreases With The Onset Of Myelination

To further investigate the role of Sch phosphorylation during differentiation, we performed a myelination time course in dissociated SC/DRGN co-cultures by examining the levels of phosphorylated Sch and ERM (ezrin/radixin/moesin) at 0 hrs, 24 hrs, 6 days, and 12 days after the addition of ascorbate (Figure 4.3). Twenty-four hours after ascorbate addition, PS518-Sch levels were modestly increased compared to cultures maintained in medium lacking ascorbate

(CB10, 0 hrs), whereas P-ERM levels were reduced compared to CB10. The highest level was observed within the cytosol of SCs aligning on axons (Figure 4.3). PS518-Sch also localized along the processes of these SCs. Six days after the addition of ascorbate, myelin is observed and the levels of PS518-Sch were drastically reduced in myelinating SCs compared to surrounding non-myelinating SCs, and to SCs grown in ascorbate-containing medium for 24 hours. In contrast, P-ERM staining was increased 6 days post ascorbate compared to 24 hrs post ascorbate, and was localized along processes. At 12 days after ascorbate addition, the co-cultures contained large amounts of myelin and Sch-S518 phosphorylation levels were essentially undetectable in myelinating SCs. Focal increases in P-ERM was observed at the distal tips of myelinating SCs representing the nodal microvilli, consistent with the known localization of these proteins in myelinating SCs (Scherer et al., 2001).

4.3.5 GFP-Positive Myelin Segments Express CASPR and P-ERM at the Paranode and Node of Ranvier

We sought to assess the ability of myelinating SCs over-expressing Sch-GFP to properly synthesize and localize paranodal and nodal components. Transiently transfected dissociated SC/DRGN co-cultures expressing GFP, Sch-GFP, Sch S518A-GFP, and Sch S518D-GFP were induced to myelinate by addition of ascorbate, and were immunostained with antibodies against CASPR and P-ERM (Figure 4.4). CASPR, an axonally derived paranodal protein, localized normally in SCs expressing GFP, Sch-GFP, Sch S518A-GFP, and Sch S518D-GFP. Occasionally, a CASPR spiral was observed (Figure 4.4, GFP), indicating that myelination was not complete, as compaction of the myelin layers causes CASPR to compact as well (Einheber et

al., 1997). A few myelinating SCs expressing Sch S518D-GFP had slightly altered CASPR localization, where distinct and separated CASPR staining was observed along one process indicating the formation of two paranodes, or possible dysmyelination (Figure 4.4, Sch S518D-GFP, red). P-ERM, a glial marker for the nodal microvilli, was found localized to the distal most aspects of myelinating SCs expressing GFP, Sch-GFP, Sch S518A-GFP, and Sch S518D-GFP. No abnormalities in the localization and expression of P-ERM were observed in myelinating SCs expressing any of the Sch variants (Figure 4.4, second column). These results indicate that Sch-mediated extension of SC internodal length is not a result of perturbation of paranodal and nodal protein components, in either axons or glia observed at the light level.

4.4 Discussion

Process formation and elongation is a fundamental behavior of SCs required for both proliferation and differentiation in response to axonal contact. Several proteins, including integrins and ErbB receptors, have been linked to SC myelination as they enable process formation and radial sorting of axons in developing nerves. However, the downstream signaling pathways activated by these receptors that dynamically control the cytoskeleton remain unknown. Previous work from this laboratory has shown that Sch, through its interaction with the scaffold protein paxillin, associates with both ErbB2 and β 1 integrin at the plasma membrane of undifferentiated and sub-confluent SCs (Fernandez-Valle et al., 2002). Moreover, activation of each receptor triggers phosphorylation of Sch at S518 and changes in SC morphology and polarity (Thaxton et al., 2007; Thaxton et al., in press). Thus Sch integrates signals from ErbB2 and integrins to coordinate cell cycle and cytoskeletal responses. Here we demonstrate that Sch regulates process elongation and myelin internode length in isolated and myelinating SCs, and it also appears to induce differentiation in a phosphorylation dependent manner. Regulation of Sch-S518 phosphorylation dynamics downstream of ErbB2 and β 1 integrin activation by NRG and laminin may couple cell cycle arrest and initiation of terminal differentiation and myelination in SCs.

4.4.1 Control of Process Formation and Extension By Sch

A key event during SC development is the ability of SCs to regulate the formation of processes in a stage dependent manner. The inability to extend and retract processes leads to aberrant migration, radial sorting, proliferation, and myelination. Our data indicate that Sch, a tumor suppressor that regulates actin dynamics, controls process formation and elongation. We find that Sch expression in both primary and myelinating SCs increased cytoplasmic process and internodal length, respectively. When Sch BBA, a dominant negative form of Sch that interferes with the function of endogenous Sch, is expressed in primary SCs the average process length is reduced by 16%. Interestingly, when Sch BBA is expressed in myelinating SCs, the internodal length cannot be assessed as these SCs fail to myelinate. These results are consistent with the inability of schwannoma cells to extend processes, contact and align on axons, and thus to myelinate in our assays (Pelton et al., 1998; Nakai et al., 2006). Overall, our results indicate that Sch functions to promote process formation and extension during SC development.

4.4.2 SC Myelination is Regulated by Sch-S518 Phosphorylation

The onset of myelination requires three events: (1) the establishment of a 1:1 relationship of a SC with an axon, (2) exit from the cell cycle and (3) induction and expression of myelin specific genes. Previously, we have demonstrated that Sch-S518 phosphorylation regulates SC morphology (Thaxton et al., 2007). Similarly, S518 phosphorylation also controls Sch's tumor suppressor function, with the unphosphorylated form acting as a growth inhibitor (Surace et al.,

2004). Here, we demonstrate that Sch-S518 phosphorylation regulates the frequency of SC myelination. SCs expressing the unphosphorylatable form of Sch, S518A, are two times more likely to myelinate, as indicated by the 96% increase in the number of myelinating SCs compared to control SCs. Conversely, the phospho-mimicking form of Sch, S518D, reduces the number of myelinating SCs by 20%. These results are consistent with accelerated differentiation in SCs expressing the active tumor suppressor form of Sch, S518A. Additionally, when SCs were induced to form basal lamina and myelinate by the addition of ascorbate, Sch-S518 phosphorylation was reduced as the numbers of myelinating SCs increased. These findings indicate that Sch phosphorylation dynamics influences the induction of myelination in SCs.

4.4.3 Implications for the Development of Myelin Abnormalities and Neuropathies

NRG and ErbB2/ErbB3, and laminins (types 2 and 8) and β 1 integrin signaling are critical for every stage of SC development, including maturation, proliferation, migration and myelination (reviewed in Garratt et al., 2000; Court et al., 2006). Conditional mutations in these genes result in aberrant myelination due to reduced proliferation, and failed defasciculation and radial sorting of axon bundles (Feltri et al., 2002; Michailov et al., 2004; Yang et al., 2005; Yu et al., 2005). Recently, it was shown that Rac functions downstream of β 1 integrin to facilitate process extension and radial sorting, but the mechanisms controlling the cytoskeletal changes are unclear (Benninger et al., 2007; Nodari et al., 2007). Interestingly, Sch participates in a negative feedback loop with Rac, and its effector Pak, dependent on its phosphorylation at S518. Unphosphorylated Sch can inhibit Rac activity, whereas activated Rac can phosphorylate and inactivate Sch's ability to restrict proliferation. Accordingly, we previously demonstrated that

Sch is phosphorylated at S518 within radial membrane protrusions similar to those needed for radial sorting, and that Sch regulates SC membrane dynamics and cell morphology in a phosphorylation dependent manner (Thaxton et al., 2007). Additionally, we have shown that Sch is phosphorylated downstream of NRG β 1 and laminin-1, and serves as a convergence point for ErbB2/ErbB3 and β 1 integrin signaling (Thaxton et al., in press). Here we extend our data to show that Sch regulates the ability of SCs to myelinate in a phosphorylation dependent manner. Expression of the unphosphorylated Sch variant was associated with increased numbers of myelin-forming SCs whereas expression of the phosphorylated variant decreased the ability of SCs to differentiate into myelinating cells. Increased Sch expression facilitates process extension and contact with axons. At the time of radial sorting, the SCs would be in close apposition with NRG-expressing axons and basal lamina, allowing the phosphorylation of Sch downstream of ErbB2/B3 and β 1 integrin. The phosphorylation of Sch would initiate process formation and extension in SCs, as the phospho-mimicking form results in multipolarity (Thaxton et al., 2007). This would allow for the defasciculation of axon bundles. As a select group of SC prepare to myelinate, Sch would become dephosphorylated, promoting cell cycle exit and myelination. We predict that SCs that are not associated with large diameter axons requiring myelination would continue to express phosphorylated Sch. In support of this model, it was found that conditional mutation of exon 2 in the *nf2* gene results in dysmyelination (Giovannini et al., 2000). When these cells are co-cultured *in vitro* with neurons, they fail to extend processes and remain large, rounded cells with prominent membrane ruffles (Nakai et al., 2006). Impaired Sch signaling would lead to the deregulation and loss of coordination of

ErB2/ErbB3 and β 1 integrin signaling, resulting in dysmyelination and the formation of schwannomas.

In summary, these results demonstrate that Sch is an integral protein controlling SC process elongation and myelination through its ability to regulate actin dynamics. *In vivo*, as SCs progress through development, the reciprocal phosphorylation and dephosphorylation of Sch would allow for the morphological and physiological changes necessary for migration, radial sorting, proliferation and myelination. By elucidating Sch's cooperative role as an actin regulator and growth inhibitor, we allow for the future development of therapeutic strategies for the treatment of NF2 and other peripheral neuropathies.

Figure 4.1 Expression Of Sch Increases SC Process Length

(A) Primary rat SCs were transiently transfected with either GFP alone, Sch-GFP, or Sch BBA-GFP and were stained with phalloidin to assess process length. The arrows denote the measured lengths. Scale bars indicate 20 μ m. (B) The frequency of process lengths from SCs expressing GFP, Sch-GFP, and Sch BBA-GFP is shown. (C) Quantification of the mean process length for SCs expressing GFP, Sch-GFP, and Sch BBA-GFP is shown. The graphs represent the average distribution and mean length for each condition in three independent experiments. An average of 50-60 processes were assessed for each condition in three independent experiments. Error bars represent the SEM. P-values are indicated as follows: (*) <0.05, (**) <0.01, (***) \leq 0.005.

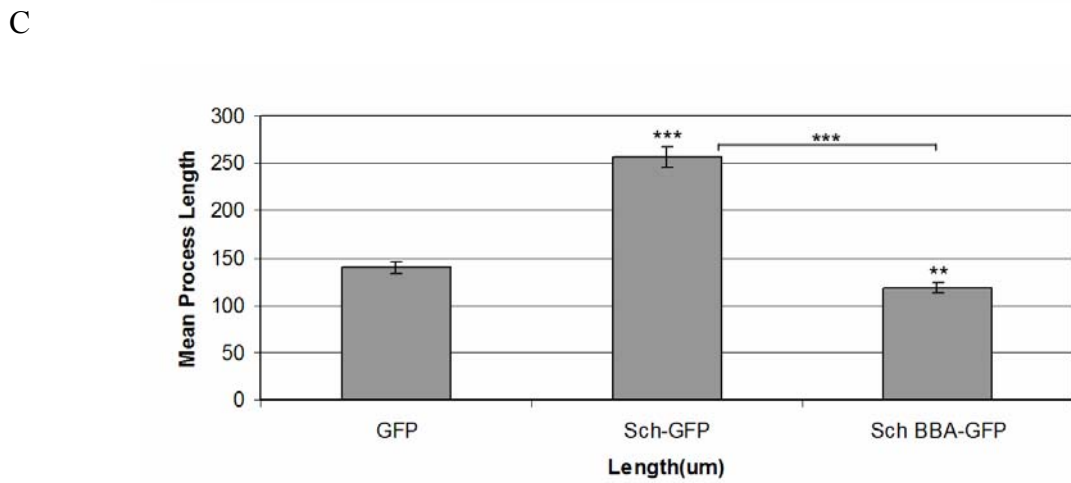
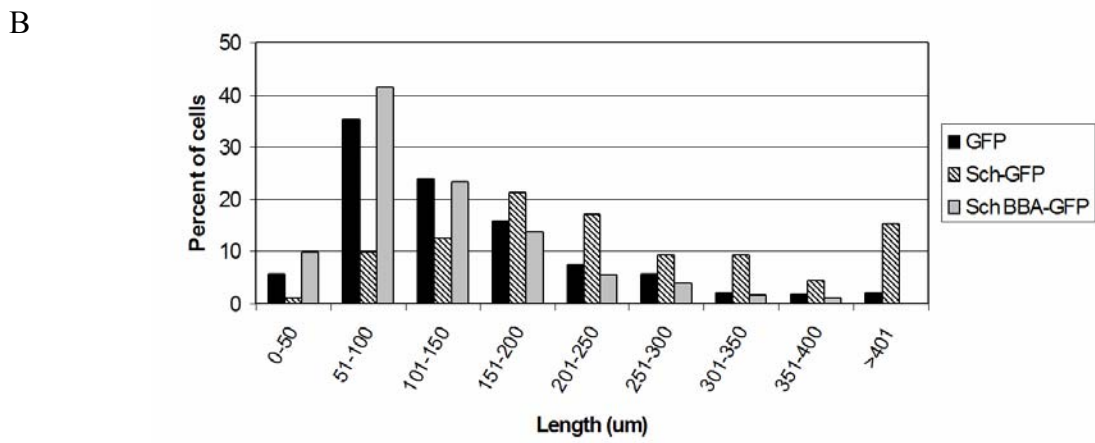
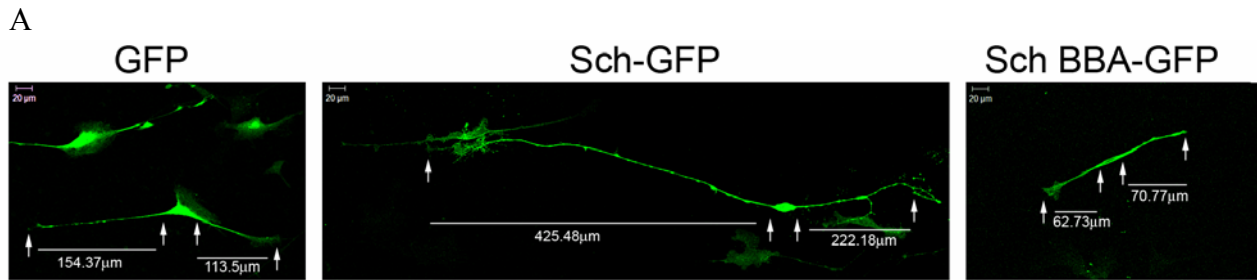


Figure 4.1 Expression Of Sch Increases SC Process Length.

Figure 4.2 Sch Increases The Myelin Internodal Length And The Frequency Of Myelination Is Dependent On S518 Phosphorylation.

(A) Dissociated SC/DRG neuron co-cultures were transiently transfected with either GFP alone, Sch-GFP, or GFP-tagged Sch S518 phospho-variants and were induced to myelinate. The co-cultures were immunostained with antibodies to MAG, P-ERM, and CASPR to assess myelination, and with Neurofilament antibody (blue) to visualize axons. Scale bars indicate 20 μ m. (B) The frequency of internodal lengths from myelinating SCs expressing GFP, Sch-GFP, Sch S518A-GFP, and Sch S518D-GFP is shown. (C) Quantification of the mean internodal length for myelinating SCs expressing GFP, Sch-GFP, Sch S518A-GFP, and Sch S518D-GFP is shown. The graph represents the average myelin internodal length for each condition in 3-4 independent experiments. All GFP+, myelinating SCs were assessed in each culture for all conditions. (D) Quantification of the frequency of appearance of GFP+, myelinating SCs for GFP, Sch-GFP, Sch S518A-GFP, and Sch S518D-GFP is shown. The graph represents the fold change in the number of GFP+, myelinating SCs found in each condition in 3 independent experiments. All GFP+, myelinating SCs were assessed per co-culture for all conditions. Error bars represent the SEM. P-values are indicated as follows: (*) < 0.05, (**) < 0.01, (***) \leq 0.005.

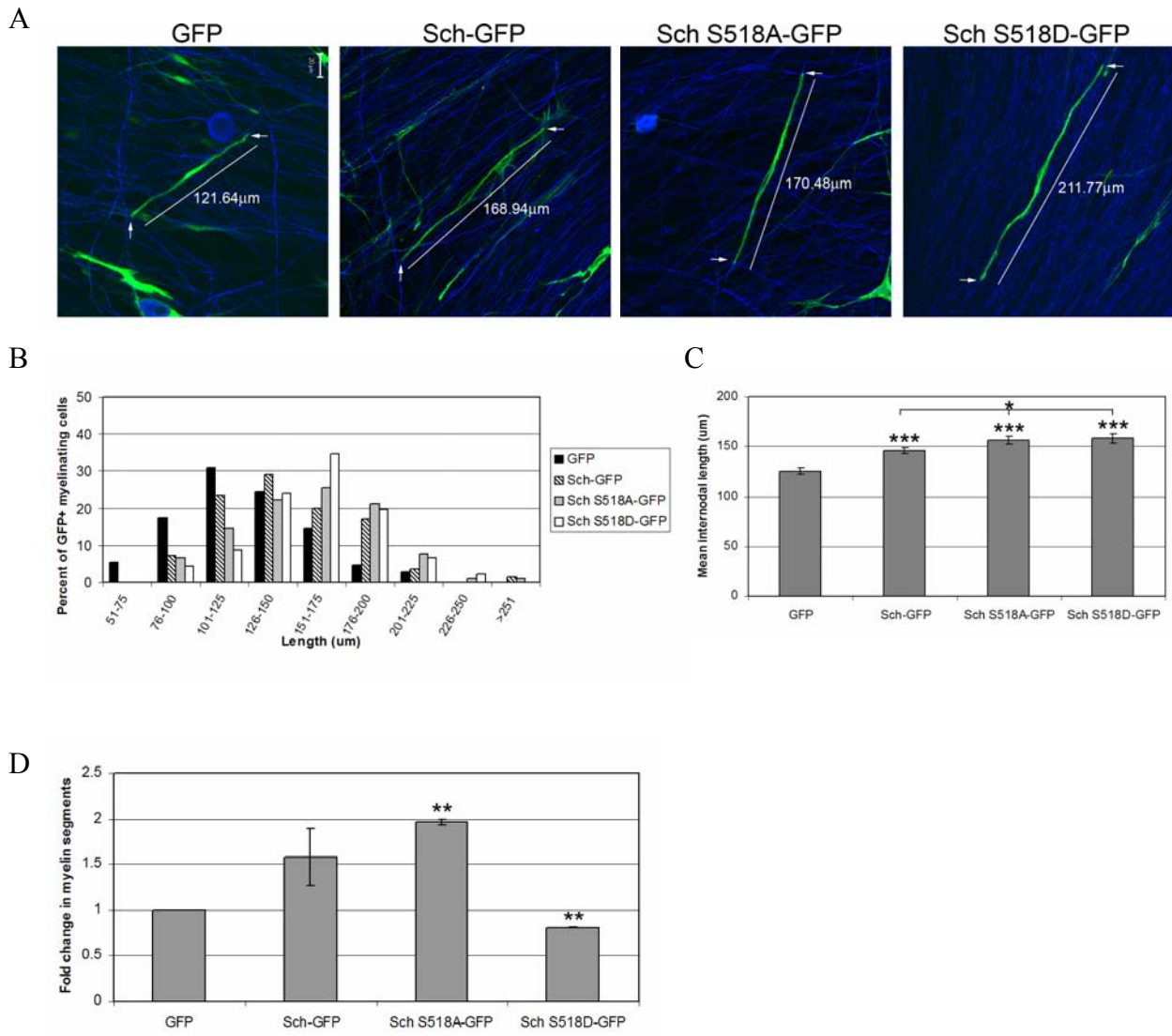


Figure 4.2 Sch Increases The Myelin Internodal Length And The Frequency Of Myelination Is Dependent On S518 Phosphorylation.

Figure 4.3 Sch-S518 Phosphorylation Decreases In SC At The Onset Of Myelination.

Dissociated SC/DRG neuron co-cultures were grown in standard media (CB10) until SC density was very high. The medium was then changed to medium containing ascorbic acid (M-feed) to induce myelination. Co-cultures were immunostained 0 hrs (CB10), 24hrs, 6 days, and 12 days later to assess the localization and expression of ErbB2 (green), PS518-Sch and P-ERM (red) and phalloidin (blue). Low magnification (first column) and high magnification (second column) are shown. Arrows indicate SC of interest. Scale bars indicate 20 μ m.

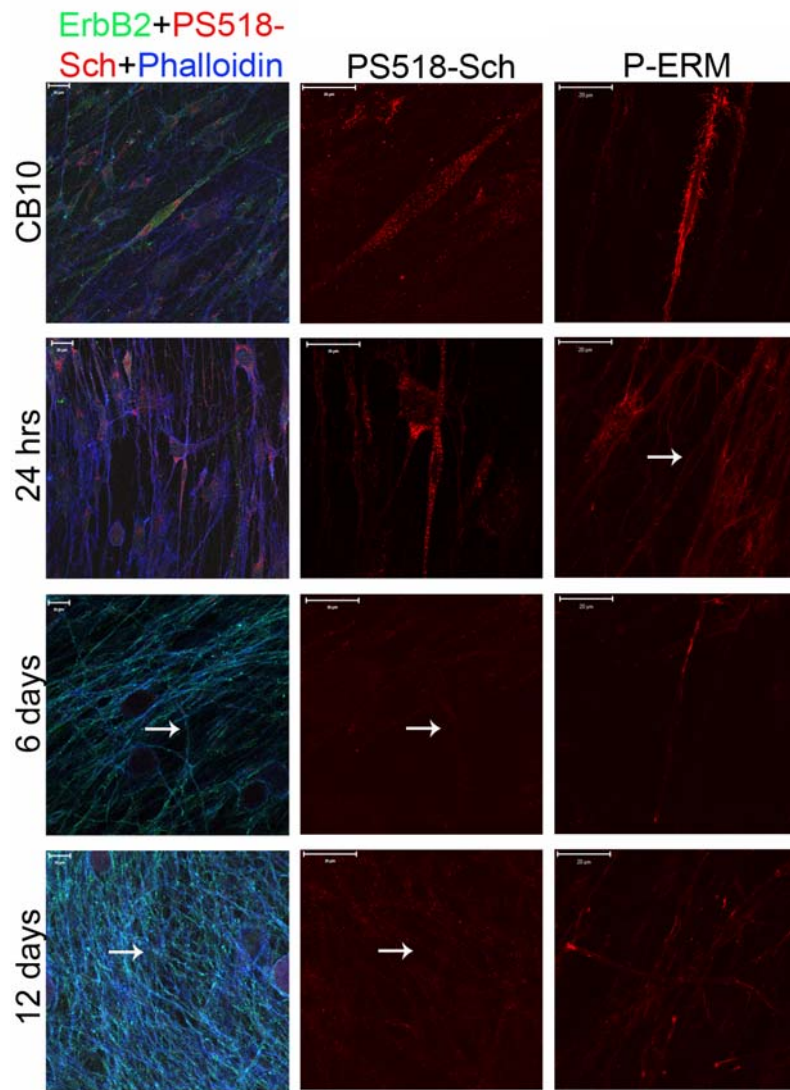


Figure 4.3 Sch-S518 Phosphorylation Decreases In SC At The Onset Of Myelination.

Figure 4.4 Expression Of Sch Phospho-variants Does Not Alter CASPR Or P-ERM

Localization In Myelinating SC/DRGN Co-Cultures. Dissociated SC/DRG neuron co-cultures were transiently transfected with either GFP alone, Sch-GFP, or GFP-tagged Sch S518 phospho-variants and were induced to myelinate. The co-cultures were immunostained with antibodies against CASPR and P-ERM to assess paranodal and nodal structures, respectively, and with Neurofilament antibody (NF) to visualize the axon(s). Scale bars indicate 20 μ m and the insets represent a 2x digital zoom of the paranodal-nodal region.

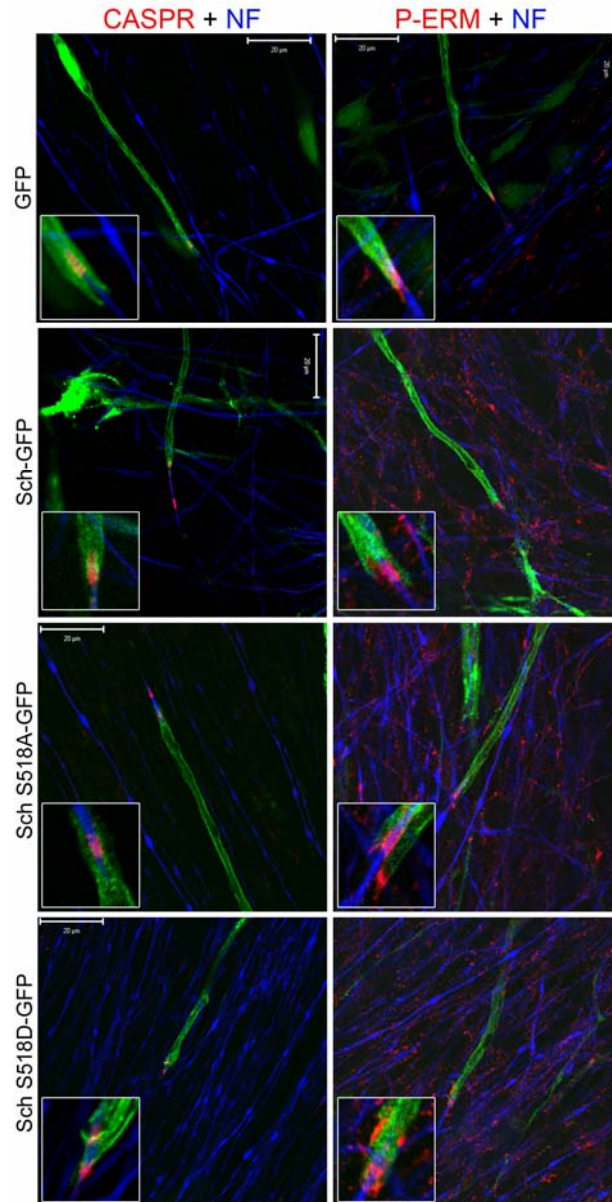


Figure 4.4 Expression Of Sch Phospho-variants Does Not Alter CASPR Or P-ERM Localization In Myelination SC/DRGN Co-Cultures.

CHAPTER 5 GENERAL DISCUSSION

The focus of this dissertation was to study the normal function of the cytoskeleton-associated tumor suppressor, Schwannomin, during Schwann cell (SC) development; specifically on its role in specifying SC morphology and regulating myelination. We have identified paxillin, $\beta 1$ integrin, and ErbB2/ErbB3 as important upstream regulators of Schwannomin function. Control of Schwannomin-S518 phosphorylation by these proteins is likely involved in the cytoskeletal reorganization necessary for proper radial sorting and myelination of SCs. Conversely, Schwannomin serves as to integrate and modify the downstream effector pathways from both $\beta 1$ integrin and ErbB2/ErbB3. Deregulation of Schwannomin signaling would result in morphological defects, abnormal myelination, and tumor predisposition as occurs in NF2. A summation of the results found and their relevance to SC development are discussed below.

5.1 Schwannomin-S518 Phosphorylation Is Dependent On Paxillin Binding and Plasma Membrane Localization

Paxillin binding is essential to Schwannomin's function as a tumor suppressor as mice with a conditional deletion of exon 2, encoding paxillin binding domain 1 (PBD1), in the *nf2* gene develop schwannomas (Giovaninni et al., 2000; Fernandez-Valle et al., 2002). Some of the most severe forms of NF2 arise in patients carrying a mutation in, or deletion of exon 2. Previously it was shown that paxillin binding, through PBD1, was required for Schwannomin's plasma

membrane localization (Fernandez-Valle et al., 2002). Expanding on these initial results, it was shown here that Schwannomin-S518 phosphorylation also requires paxillin binding through PBD1. Accordingly, phosphorylation of Schwannomin-S518 is regulated by its localization to the plasma membrane, as those molecules that fail to target due to deletion of PBD1 remain in the cytosol and are not phosphorylated. Moreover, Cdc42 and Pak mediate Schwannomin-S518 phosphorylation at the plasma membrane. Paxillin promotes this event by binding PKL and Pix, a guanine nucleotide exchange factor for Cdc42, and localizing Cdc42 and Pak to the plasma membrane (reviewed in Turner et al., 2001). Additionally, we demonstrated here that deletion of PBD2, within the C-terminus of Schwannomin, results in unrestricted Schwannomin phosphorylation independent of Pak activity and plasma membrane localization. A possible explanation for this result is that deleting PBD2 perturbed Schwannomin's ability to bind a phosphatase and be dephosphorylated. Together these findings further demonstrate the physiological importance of paxillin binding in regulating Schwannomin phosphorylation at S518 that determines its tumor suppressor function.

5.2 Schwannomin-S518 Phosphorylation Is Stimulated By NRG And Laminin-1 Through Distinct PKA And Pak Mediated Pathways

Mitogenic and extracellular matrix (ECM) signals are fundamental for the proliferation and migration of many types of cells (reviewed in Lee and Juliano, 2004). Specifically in SCs, the axonal mitogen NRG, and the ECM molecule laminin are important for every aspect of SC development (reviewed in Jessen and Mirsky, 2005). Without these ligands or their respective receptors, ErbB2/ErbB3 and β 1 integrin, SCs fail to myelinate due to reduced proliferation

and/or the failure to associate and defasciculate axon bundles. Schwannomin, and paxillin, associate with ErbB2/ErbB3 and β 1 integrin either directly or indirectly (Fernandez-Valle et al., 2002). Because Pak can be activated downstream of ErbB2/ErbB3 and β 1 integrin in other cells, we examined whether Schwannomin-S518 phosphorylation occurred in response to NRG and laminin stimulation of ErbB2/ErbB3 and β 1 integrin in SCs. Stimulation of SCs with NRG and laminin revealed that Schwannomin-S518 was phosphorylated by distinct kinases. NRG stimulation of ErbB2/ErbB3 in SCs triggered PKA dependent phosphorylation of Schwannomin, whereas laminin-1 stimulation of β 1 integrin triggered Pak-mediated phosphorylation of Schwannomin-S518. This is the first study to identify extracellular signals that promote Schwannomin phosphorylation in any cell type. Notably, dual stimulation of SCs with NRG and laminin-1 did not result in a concomitant increase in Schwannomin-S518 phosphorylation, but rather an intermediate level. Co-regulation of receptor dynamics was also observed, as NRG stimulation of SCs led to an increase in β 1 integrin protein levels, while laminin-1 stimulation lead to an increase in ErbB2 protein levels. Overall, these results demonstrate that Schwannomin is a key convergence point for NRG and laminin signaling that integrates and regulates the activation of downstream signaling cascades from ErbB2/ErbB3 and β 1 integrin, allowing for controlled SC proliferation, migration, and possibly myelination.

5.3 Schwannomin Promotes Process Elongation In Primary And Myelinating SCs And Controls Myelination In A Phosphorylation Dependent Manner

Until this point, the focus of this dissertation was to elucidate the mechanisms promoting Schwannomin phosphorylation in SCs. In order to characterize the function of phosphorylated Schwannomin in SCs, the effects of Schwannomin expression and phosphorylation on SC morphology and myelination was examined. Schwannomin expression was found to regulate process formation and elongation in primary SCs. Additionally, Schwannomin-S518 phosphorylation regulated actin dynamics and SC morphology, as unphosphorylated Schwannomin promoted a unipolar phenotype, whereas the phosphorylated form promoted a multipolar phenotype. In myelinating SCs, Schwannomin regulated the length of the internode, consistent with its ability to increase process length in primary SCs, but this effect was independent of S518 phosphorylation. However, S518 phosphorylation was found to be important for the promotion of myelination. SCs expressing an unphosphorylatable form of Schwannomin were more likely to myelinate than SCs expressing a phospho-mimicking or wild-type form of Schwannomin. In accordance, it was shown that Schwannomin phosphorylation levels decreased during the progression of myelination. The increase in internodal length mediated by Schwannomin expression was not attributed to disruption of the paranode or node, as CASPR and P-ERM expression and localization were normal. In summary, these results indicate that Schwannomin phosphorylation is an important event controlling SC morphology, and identifies Schwannomin as a regulator of SC development, specifically during myelination.

5.4 Implications for Schwannomin Phosphorylation During SC Development: Control Of SC Process Formation and Extension, Migration, Proliferation, And Myelination

Migration, for most cells, requires the reciprocal extension and retraction of processes in response to extracellular stimuli. For SCs, the crucial stimulus promoting migration is the axonally derived mitogen, NRG. Because Schwannomin is phosphorylated in response to NRG, and its subsequent phosphorylation results in morphological changes involving process formation and extension, it is likely that Schwannomin phosphorylation mediates SC migration. Initially, NRG would acutely stimulate Schwannomin-S518 phosphorylation downstream of ErbB2, allowing processes to form and extend along an axon. With prolonged exposure to NRG, ErbB2 internalizes and its activity and signaling are reduced (Iacovelli et al., 2007). Therefore with time, Schwannomin-S518 phosphorylation levels will decrease concomitantly with ErbB2 levels, resulting in retraction of processes. It is important to note that at this stage in SC development the basal lamina has not formed, therefore Schwannomin phosphorylation is not induced, nor affected by signaling downstream of laminin and $\beta 1$ integrin. The reciprocal effect of activation and deactivation of Schwannomin and ErbB2 would allow for alternating extension and retraction of SC processes, and movement of SCs down the developing nerve.

Radial sorting of axons immediately follows migration, and is accompanied by proliferation. Sorting allows the SCs to adequately populate and define the axons that will be myelinated, as opposed to those that will be ensheathed. At this stage of development the basal lamina, a specialized form of extracellular cellular matrix (ECM), has begun to form and couples with axonal cues to stimulate SCs to reorganize the actin cytoskeleton. In response to these cues, SCs

will form multiple processes that will intercalate into, and segregate axon bundles until every axon is surrounded by SC membrane. Considering that Schwannomin regulates both the actin cytoskeleton and proliferation, and that this regulation is dependent on its phosphorylation at S518, it is likely that Schwannomin phosphorylation dynamics plays a role during radial sorting of SCs. As proposed during migration, Schwannomin-S518 phosphorylation will initially be stimulated downstream of NRG, through ErbB2/ErbB3 and PKA. In contrast to migration, where Schwannomin-S518 phosphorylation is transient, Schwannomin phosphorylation during radial sorting would be sustained due to the increasing deposition of basal lamina. The presence of laminin would stimulate Schwannomin-S518 phosphorylation through $\beta 1$ integrin and Pak and prolong Schwannomin phosphorylation. Sustained Schwannomin-S518 phosphorylation would promote process formation and elongation required for radial sorting of axons. In support of this model, data presented here demonstrates that Schwannomin is phosphorylated in response to laminin-1 stimulation of SCs, through $\beta 1$ integrin and Pak. Moreover, work by others revealed that Rac functions downstream of $\beta 1$ integrin to promote the formation of radial membrane protrusions required for defasciculation (Benninger et al., 2007; Nodari et al., 2007). In addition, Pak is activated in response to GTP loading of Rac, which leads to Schwannomin-S518 phosphorylation (Shaw et al., 2001; Kissil et al., 2002; Xiao et al., 2002; reviewed in Bokoch, 2003). Although NRG signaling would be transient during radial sorting, it may facilitate laminin signaling, as it was demonstrated here that NRG stimulation of SCs increases $\beta 1$ integrin protein levels. By increasing the levels of $\beta 1$ integrin, or allowing for its stabilization at the plasma membrane, NRG acts to prolong $\beta 1$ integrin dependent phosphorylation of Schwannomin-S518 during radial sorting in response to laminin, and enhance process formation

and extension. Similarly, it was also shown that laminin stimulation increased ErbB2 protein levels, indicating that NRG signaling may be modestly increased in the presence of laminin. The co-regulation of ErbB2/ErbB23 and β 1 integrin receptor signaling is a key event that finely tunes Schwannomin-S518 phosphorylation to regulate process formation and extension, segregation of axons, as well as proliferation.

Proliferation of SCs, and many epithelial and endothelial cell types, requires coordinated signaling between ECM and mitogens, through integrins and receptor tyrosine kinases, like ErbBs (reviewed in Lee and Juliano, 2004). At the time of radial sorting, SCs are exposed to both the basal lamina and to the axon, allowing for full activation of the cell cycle. Of note, Schwannomin's function as a tumor suppressor is regulated by its phosphorylation at S518, as is its ability to regulate actin dynamics (Surace et al., 2004; Rong et al., 2004; Xiao et al., 2005; Thaxton et al., 2007). Therefore as NRG and laminin stimulate Schwannomin phosphorylation, they concomitantly inactivate its growth inhibition to permit proliferation. Repression of Schwannomin's growth regulation would allow for progression through the G1-phase. Work by others has revealed that schwannoma cells lacking Schwannomin expression have increased levels of cyclin D1 resulting in progression through G1 into the S-phase of the cell cycle (Xiao et al., 2005). Re-expression of Schwannomin in these cells resulted in growth inhibition and reduced cyclin D1 levels. Additionally, sustained S518 phosphorylation in response to NRG and laminin might prevent Schwannomin's ability to repress Pak activation, as only the unphosphorylated form of Schwannomin is able to suppress growth. Sustained Pak activity

would couple with ErbB2 induced Raf activation to promote MAPK, MEK, and ERK and progression through the G1-phase of the cell cycle.

Myelination of SCs requires exit from the cell cycle, association of a 1:1 relationship with an axon, and the induction of myelin specific genes. Integration of signals from the axon and basal lamina are necessary for SC differentiation. Axonal NRG determines the ensheathment fate of axons, as well as stimulates the expression of Krox-20, a transcription factor controlling the expression of the myelin specific genes, periaxin and P0 (Murphy et al, 1996; Michailov et al., 2004; Taveggia et al., 2005; Iacovelli et al., 2007). Similarly, basal lamina is required for SCs to myelinate by maintaining the proper expression of transcription factors needed for myelination, like Krox-20, inducing the myelin specific gene P0, and by providing support and stability for SCs during myelination (Eldridge et al., 1989; Fernandez-Valle et al., 1993; Yu et al., 2005). Due to Schwannomin's ability to regulate myelination, and integrate and coordinate proliferative and morphological signaling downstream of NRG and laminin in a phosphorylation dependent manner, it may be possible that Schwannomin contributes to signals inducing SC differentiation into myelinating cells. The work here demonstrates that dephosphorylation of Schwannomin-S518 is critical in promoting myelination. Unphosphorylated Schwannomin would allow for the retraction of multiple processes from radial sorting, and the establishment of a 1:1 ratio with an axon. Moreover, in the unphosphorylated form, Schwannomin would be capable of inhibiting growth, allowing for cell cycle exit and differentiation. At this stage in development, SCs are constantly exposed to NRG and laminin, therefore other factors must contribute to the dephosphorylation of Schwannomin, and one such factor might be cell density. As SCs

progressively sort and proliferate, an increasing number of SCs will be present in the developing nerve. SC: SC contact, possibly mediated through cadherins, would limit Schwannomin's phosphorylation. Accordingly, other labs have shown that cell density and formation of cadherin mediated adherens junctions induce Schwannomin dephosphorylation, resulting in contact dependent inhibition of the cell cycle (Shaw et al., 1998; Lallemand et al., 2003). Another factor that may influence Schwannomin phosphorylation dynamics is the switch in integrins during myelination, in which $\beta 4$ integrin is more highly expressed than $\beta 1$ integrin. This change in expression might contribute to an altered response in Schwannomin phosphorylation, as $\beta 1$ integrin-dependent phosphorylation may no longer occur or may be significantly reduced. Therefore, only a transient and modest level of Schwannomin phosphorylation may present and localized to discrete areas such as the inner mesaxon (the inner membrane responsible for initiating wrapping of the SC membrane around the axon). Additional support is provided by our observation that continued deposition of the basal lamina leads to a reduction of Schwannomin phosphorylation and its re-localization to the cytosol. Eventually, Schwannomin expression would be reduced or restricted, as is evident by the finding that in myelinated SCs, Schwannomin is found only in the paranodal region (Scherer and Gutmann, 1996). In contrast to myelination, those select SCs destined to an ensheathing fate would have increased levels of Schwannomin-S518 phosphorylation. By maintaining Schwannomin phosphorylation in discrete membrane domains, these SCs will maintain multiple processes that contact and wrap the axon just once.

5.5 Implications for the Development of Schwannomas and Neurofibromatosis Type 2

Altered expression and signaling of the tumor suppressor Schwannomin is the cause of Neurofibromatosis type 2 (NF2), and leads to the development of schwannomas and other peripheral nervous system tumors (Rouleau et al., 1993; Trofatter et al., 1993). The ability of Schwannomin to control the signaling and response of SCs to potent stimuli, like NRG and laminin, as shown here, conveys the importance of its expression in maintaining homeostasis of SCs during development. This work reveals that if Schwannomin function is perturbed, deregulation of signaling would ensue downstream of NRG and laminin, through ErbB2/ErbB3 and $\beta 1$ integrin respectively. These cascades are major avenues for controlling proliferation and actin reorganization. As a result, SCs would no longer be able to integrate signaling from the axon or basal lamina to allow process formation and extension necessary for migration, proliferation, radial sorting and myelination. This would lead to increased proliferation in SCs, altered migration and radial sorting, and the inability of SCs to maintain a myelinating phenotype. Coincidentally, schwannoma cells expressing mutant Schwannomin or those lacking Schwannomin expression are known to have increased activation of ErbB2/ErbB3 and $\beta 1$ integrin (Utermark et al., 2003; Hansen and Linthicum, 2004). These schwannomas also fail to contact and align on axons (Nakai et al., 2006). Additionally, contact inhibition of growth is disrupted, resulting in tumor formation (Rosenbaum et al., 1998). Moreover, SCs containing a conditional deletion of Schwannomin that is induced at the beginning stages of myelination, have disrupted and unorganized myelin, and are prone to hyperplasia (Giovannini et al., 2000). Although it is not currently known whether schwannomas formed in NF2 originate from unmyelinated, ensheathed or myelinated SCs, this work, as well as work by others suggests that

schwannomas may in fact arise from myelinating SCs that have dedifferentiated (Hung et al., 2002). Because NF2 is a disease that presents during puberty, it is possible that the tumors may arise from SCs that were once myelinating but have subsequently reentered the cell cycle, due to disrupted regulation of integrin and ErbB signaling.

Overall, the findings presented here reveal Schwannomin as a critical regulator of SC morphology and myelination. The perturbation of Schwannomin function may not only lead to the development of NF2, but also to the development of demyelinating diseases such as Schwannomatosis, congenital hypomyelinating neuropathy, and congenital muscular dystrophy. By examining the regulation of Schwannomin function by paxillin, ErbB2/ErbB3, β 1 integrin, PKA, and Pak, we have exemplified these proteins as potential therapeutic targets for the treatment of NF2 and other peripheral neuropathies.

**APPENDIX:
EXPERIMENTAL PROCEDURES**

A.1 Molecular Cloning Procedures

A.1.1 Bacterial Transformation of Plasmid DNA

1. Pre-chill sterile electroporation cuvette(s) (0.1 cm gap), one for each sample, and a sterile 1.5 ml eppendorf tube(s) for each sample on ice.
2. Prepare a 200 μ l aliquot of SOC media in a 2ml tube and place on ice.
3. Place a 40 μ l aliquot of electro-competent bacterial cells on ice.
4. Set the electroporator to 1.7 kV, 25 μ F, 200 Ω .
5. At the electroporator, add 1 μ l of ligated DNA (or the equivalent of 50ng DNA) to the electro-competent cells with gentle mixing.
6. Transfer the cell-DNA mixture to a chilled electroporation cuvette, tapping the cuvette until the mixture settles evenly to the bottom.
7. Pulse the sample once and remove from the electroporator.
8. Add 42 μ l of SOC media to the cuvette.
9. Remove the 84 μ l of sample and transfer to the tube containing the SOC media.
10. Incubate at 37°C for 1 hr at 225 rpm.
 - a. Prepare LB Agar plates with the appropriate antibiotics for the plasmids that were electroporated into the bacterial cells.
11. Plate 50 μ l of bacterial cells on 1 LB Agar plate, and 100 μ l of bacterial cells on another LB Agar plate.

- a. Make sure to flame the bacterial spreader before and after each sample. Let the spreader cool or it will kill the bacterial cells.
12. Incubate plates at 37°C overnight (less than 24 hrs).
 13. Remove the plates from the incubator, you should have nice individual colonies
 14. At this point you can pick individual colonies to grow up and purify, or you can wrap the plates with parafilm and save at 4°C until ready to use (for at least a week).

For culturing Individual Colonies:

15. Prepare 5ml of LB broth plus the appropriate antibiotic for each colony to be isolated.
 - a. Label tubes carefully to distinguish each individual colony.
16. Using a sterile toothpick or a sterile pipet tip, scrape the individual colony of the plate, making sure not to scrape any surrounding colonies.
17. Place the toothpick/ pipet tip into the appropriately labeled culture tube containing the 5ml of LB broth.
18. Incubate the colonies at 37°C while shaking at 225 rpm overnight (less than 24 hours).
19. The next day the broth should be cloudy, indicating growth.
20. Prepare a glycerol stock of the cultures by mixing 1ml of culture to 500µl of sterile filtered 50% glycerol and label tube appropriately and place at -80 °C.
21. Aliquot the remaining culture(s) into 1.5ml microcentrifuge tubes and spin down at 14,000 rpm.
22. Remove the supernatant (and discard), leaving the bacterial pellet.
23. Perform a mini prep.

A.1.2 Mini Prep of Plasmid DNA (Qiagen QIAprep Miniprep Protocol/Method)

1. Resuspend pelleted bacterial cells in 250µl of Buffer P1.
 - a. If you have more than one tube of the same culture then resuspend sequentially.
2. Add 250µl of Buffer P2 and mix by inverting the tubes 4-6 times.
3. Add 350µl of Buffer N3 and mix thoroughly by inverting the tube 4-6 times.
 - a. A white precipitate should have formed.
4. Centrifuge sample(s) at 10,000 rpm for 10 mins.
5. Apply the supernatants from step 4 to the QIAprep spin column, making sure to avoid the precipitate.
6. Centrifuge sample(s) for 30-60s. Discard flow through.
7. Wash the column by adding 750µl of Buffer PE and centrifuge for 30-60s at 10,000 rpm.
8. Discard the flow through and centrifuge for an additional 30-60s at 10,000 rpm.
 - a. This removes the excess wash buffer from the column.
9. Place the QIAprep column in a clean 1.5ml centrifuge tube and elute the DNA by adding 30ul of DNase-, RNase-, Protease-free water to the center of the column.
10. Let the water stand for 2 mins and centrifuge for 1 min at 10,000 rpm to elute the DNA.
11. Calculate the DNA concentration by using the spectrophotometer.
 - a. Compare OD₂₆₀ between a 1:50 and a 1:100 dilution of the DNA, and average the concentration. Make sure the OD₂₆₀/280 ratio is between 1.6-1.8 for good DNA preps.

A.2 Biochemical Procedures

A.2.1 Transfection of Primary Rat Schwann Cells (Lipofectamine 2000)

Solution A: 20ul (OptiMEM+ DNA)/ coverslip

Solution B: 0.5ul Lipofectamine 2000/ 20ul OptiMEM for coverslips or 5ul Lipofectamine 2000/250ul Opti-MEM

Note: Schwann cells are grown on German glass round coverslips. The coverslips are coated with 200ug/ml poly-L-lysine or 200ug/ml poly-L-lysine and 25ug/ml Laminin. Once the Schwann cells have been seeded on coverslips, they are fed with D10M media until ready for transfection.

1. Calculate the amount of DNA you want to transfect into cells.
 - a. Ex. I use 250ng of GFP tagged construct / coverslip or 1ug of Xpress-tagged construct/well.
2. Prepare Sol'n B: Add the Lipofectamine 2000 to OptiMEM (in the ratio stated above). Let it incubate for 5 mins. At RT.
 - a. While Sol'n B is incubating prepare Sol'n A
3. Prepare Sol'n A: by adding DNA to the appropriate amount of OptiMEM (in the ratio above).
 - a. Ex. If you are transfecting 2 coverslips with the same DNA, you should add the DNA (500ng) to OptiMEM so the final volume is 40ul.
4. Mix solutions A and B at a 1:1 ratio.
 - a. Ex. 20ul of Solution B/ 20ul Solution A for the coverslips.
5. Let the mixture incubate at room temperature for 20 mins, but no longer than an hour.
6. Prepare final solution: Once solution mixture (Solution B+A) is finished incubating add OptiMEM to the mixture to a final ratio of 100ul of solution per coverslip, or 2ml of solution per well.

- a. Ex. If you are transfecting 2 coverslips with the same DNA, you should add 120ul of OptiMEM to the Solution B +Solution A mixture (from step 4).
7. Remove medium from coverslips
8. Add 100ul of final solution (OptiMEM + Solution mixture (from step 6)) per coverslip, or 2ml for wells.
9. Let cells incubate for 4 hours in 5% CO₂ at 37°C.
10. Remove transfection media from cells and add fresh media (D10M).
11. Mount or extract cells ~36 hours post transfection.

A.2.2 Transfection of Dissociated Schwann Cell/ Dorsal Root Ganglion Neuron Co-cultures (Lipofectamine 2000)

Solution A: 20ul (OptiMEM+ DNA)/ coverslip

* the amount of DNA and OptiMEM should total 20ul/coverslip

Solution B: 0.5ul Lipofectamine 2000/ 20ul OptiMEM

* prepare this in advance for the total number of coverslips you will be transfecting; it needs to incubate for at least 5 mins but no longer than 30 min. It will then be aliquoted out at step 3.

1. Calculate the amount of DNA you want to transfect into cells.
 - a. I transfect 250ng of DNA/cs.
2. Prepare Solution B as stated above. Let incubate at room temp. for 5 mins.
3. Solution A: Add DNA to the appropriate amount of OptiMEM
 - a. Ex. I am transfecting 8 coverslips with the same DNA, so I added the DNA (2ug) to OptiMEM so the final volume is 160ul.
4. Mix Solution A and Solution B in a 1:1 ratio for each coverslip to be transfected.
 - a. Ex. If transfecting 8 coverslips with the same DNA, add 160ul of Solution B to 160ul of Solution A.
5. Let the mixture incubate at room temperature for 20 min.
6. Once solution mixture (Solution A+B) is finished incubating add, CB10 media to equal 100ul of final solution/coverslip. Mix well.
 - a. Ex. If am transfecting 8 coverslips with the same DNA, add 480ul of CB10 to the Solution B +Solution A mixture (from step 3), this should equal 800ul of final solution, for a ration of 100ul/ coverslip.
7. Remove media from coverslips.
8. Add 100ul of final solution from step 6/ coverslip.
9. Let cells incubate for 4 hours in 5%-5.5% CO₂ at 37°C.
10. Remove transfection mixture from cells and add CB10 media.

11. Change media from CB10 to M-feed (myelinating feed) 20hrs post transfection.
12. Continue to feed the co-cultures M-feed every other day for 10-12 days until myelination is visible.
13. Immunostain co-cultures according to protocol and assess coverslips for GFP expressing, myelinating Schwann cells

Condition/ Methods for Myelination of Dissociated Co-cultures

Conditions	
Media before transfection	CB10
Media during transfection	CB10
Media immediately after transfection	CB10
Media 20 hrs after transfection	M Feed

A.2.3 Extraction of Primary Rat Schwann Cells (transfected and non-transfected)

Materials:

Ice

Cell Scraper(s) – one per condition

Cold PBS

Extraction Buffer (see recipe below)

Blue Microcentrifuge Pestle Tubes - 1 per condition

Pestle(s) – 1 per condition

Cells (type of cell, size of dish, and number of dishes to be determined by the experiment)

Procedure:

1. Prepare extraction buffer, chill before use.

TAN Extraction Buffer:

	Stock Concentration	Final Concentration
Tris-Acetate (pH 8.0)	200mM	10mM
IGEPAL	100%	2%
NaCl	5M	100mM
ddH ₂ O	Depends on final vol.	Depends on final vol.
Aprotinin	1mg/mL	20µg/mL
Leupeptin	1mg/mL	10µg/mL
SPP	100mM	1mM
NaF	1M	50mM

PMSF	100mM	2mM
SOV	100mM	1mM

Note: PMSF has a half life of only 30 minutes, so do not add it until immediately before use***

Cell Extraction

1. Rinse the dish to be extracted 2x with 4 mL chilled PBS.
2. Remove the PBS.
3. Add 80-500 μ l of TAN (depending on the size of the well to be extracted).
4. Scrape dish/well with cell scraper(s).
5. Pipette extract into blue pestle microcentrifuge tubes.
6. Pellet cells by centrifugation at 14000 rpm for 10 min(s) at 4°C
7. Crush cell pellet by grinding with pestle for 20 strokes.
 - a. Make sure that the extract does not overflow out of tube during pestle grinding.
8. Rotate pestle tubes at 4°C for 15 minutes.
9. Pellet cells by centrifugation at 14000 rpm for 10 minutes at 4°C.
10. Remove supernatant and place in a new, pre-chilled 1.5 ml microcentrifuge tube.
11. Perform Bio-Rad DC Protein Assay (Lowry).

A.2.4 Lowry Method For The Determination Of Cell Lysate Protein Concentration

Note: Based on the Bio-Rad DC Protein Assay Protocol.

1. Calculate Reagent A, use 25 μ l of Reagent A per well.
2. Calculate Reagent S, use 20 μ l of Reagent S per 1000 μ l of Reagent A.
3. Combine Reagent A and Reagent S, this is the Working Reagent (WR).
4. Prepare the protein Standards using BSA (2mg/ml)

Standard	BSA Conc. I	BSA vol.	Extract. Buffer Vol.	Final Vol.	BSA Conc. F
#5	2.0 mg/ml	70 μ l	30 μ l	100 μ l	1.4 mg/ml
#4	1.4 mg/ml	60 μ l	24 μ l	84 μ l	1.0 mg/ml
#3	1.4 mg/ml	20 μ l	20 μ l	40 μ l	0.7 mg/ml
#2	1.0 mg/ml	30 μ l	30 μ l	60 μ l	0.5 mg/ml
#1	0.5 mg/ml	30 μ l	30 μ l	60 μ l	0.25 mg/ml

5. Add 5 μ l of Blank (extraction buffer used), in duplicate, in a 96-well plate.
6. Add 5 μ l of Standards (1-5) to the subsequent wells following the blank, in duplicate.
7. Add 5 μ l of each Sample to the wells subsequent to the standards, in duplicate.
8. Add 25 μ l of WR to each well.
9. Add 200 μ l of Reagent B to each well and incubate for 15 min(s) at room temp.
10. Read plate using the Lowry assay protocol in the KC Junior program.

A.2.5 Immunoprecipitation using Total Schwann Cell Extract

A) Calculate the volume of total cell lysate required = usually 300-500ug of total lysate for ErbB2 and integrin immunoprecipitation and 100ug for Schwann cells transfected with Xpress-tagged constructs

B) Calculate volume of normal IgG required = 1ug IgG / 200ug cell lysate

C) Calculate volume of Primary Antibody required = 1ug Ab / 100ug cell lysate

1. Aliquot the appropriate amount of Total cell lysate needed (amount calculated in A)
 - a. Label tube Pre-clear Control (PC)
2. Add appropriate amount of IgG (from B) into Pre-clear tube
3. Rotate at 4°C for 2 hours
4. Add 50ul of appropriate beads (Protein G or Protein A)
 - a. Beads are located in the 4°C fridge
5. Rotate at 4°C for 4 hours or overnight
6. Centrifuge samples at 510g at 4°C for 5 min
7. Transfer supernatant into a new tube labeled Immunoprecipitation (IP)
 - a. The supernatant should know be clear of all non specific binding proteins
8. Save the Pre-cleared beads, until ready to wash, at 4°C
9. Add required amount of Primary antibody (part C) to the supernatant in the IP labeled tube (from step 7)
10. Rotate at 4°C for 2-4 hours
11. Add 50ul of appropriate beads (Protein G or Protein A), the same used for the pre-clearing.
12. Rotate at 4°C for 4 hours to overnight
13. Centrifuge IP sample at 510g at 4°C for 5 min
14. Transfer supernatant to a new tube labeled post IP store at 4°C until ready to run on gel
15. Re-suspend the remaining IP beads in 1ml of TAN extraction buffer
16. Centrifuge sample(s) at 510g at 4°C for 5 min

17. Remove supernatant from the sample carefully, DO NOT REMOVE BEADS, and discard
18. Wash IP sample and Pre-clear sample (separately)
19. Add 1 ml of Wash B to each and rock for 1 min (RT)
20. Centrifuge samples at 510g at 4°C for 5 min.
21. Remove and discard supernatant, STAYING AWAY FROM BEADS
22. Add 1ml of Wash C to each and rock for 1 min
23. Centrifuge samples at 510g at 4°C for 5 min
24. Remove and discard supernatant, STAYING AWAY FROM BEADS
25. Add 1ml of Wash A to each and rock for 1 min
26. Centrifuge samples at 510g at 4°C for 5 min
27. Remove and discard supernatant, STAYING AWAY FROM BEADS
28. Resuspend samples (beads) in 25-50ul of 2x SDS sample buffer.
29. Boil for 5-10 mins at 95°C.
30. Save samples at -20°C, or run of an SDS-PAGE gel.

Wash A: 10mM Tris pH 7.0, 1mM EDTA, 0.5% TritonX-100

Wash B: 10mM Tris pH 7.0, 1mM EDTA, 1M NaCl, 0.5% TritonX-100

Wash C: 10mM Tris pH 7.0, 1mM EDTA, 0.2M NaCl, 0.5% TritonX-100, 0.1% SDS

A.2.6 Magnetic Bead Immunoprecipitation of β 1 integrin

Note: protocol based on the Dynal protocol for IP of M280 Tosylactivated Dynabeads.

Lifting Schwann Cells

1. Rinse dish of cells 2x with 3-4ml of HBSS (Hank's balanced salt solution, Ca^{2+} and Mg^{2+} free)
2. Using 3-4ml of HBSS with 2mM EDTA, lift cells.
 - a. Note: if the cells do not lift within 10 min(s), add 0.05% Trypsin.
3. Once lifted, transfer lifted cells into a centrifuge tube containing 5ml of L-15.
 - a. If using trypsin, inactivate by adding serum.
4. Centrifuge cell suspension at 1500 rpm at 4°C for 5 min.
5. Remove the supernatant, and discard, being careful not to disturb the cell pellet.
6. Resuspend cells in 1-2 ml of L-15 + 0.1% BSA.
7. Triturate cells to create a single cell suspension.

Determination of the amount of Ab coated beads required for IP.

1. Determine the number of cells using the hemacytometer.
2. Determine the number of Ab coated beads required.
 - a. You want a ratio of 6 Ab-coated beads per cell.
- 3.

A.2.7 Preparation Of SDS-PAGE Gel And Electrophoretic Separation Of Proteins

For a 10% resolving gel:

Components	For 10ml final Vol.
H ₂ O	4 ml
30% Acrylamide Mix	3.3 ml
1.5 M Tris (pH 8.8)	2.5 ml
10% SDS	100 µl
10% Ammonium Persulfate (APS)	100 µl
TEMED	4 µl

For a 5% Stacking Gel:

Components	For 4ml final Vol.
H ₂ O	2.7 ml
30% Acrylamide Mix	670 µl
1.5 M Tris (pH 8.8)	500 µl
10% SDS	40 µl
10% Ammonium Persulfate (APS)	40 µl
TEMED	4 µl

1. Assemble glass plates and gel apparatus according to the Bio-Rad manufacturer protocol.
2. Add approximately 5ml of 10% resolving solution in between the glass plates per gel.

3. Pipette ddH₂O gently over top of the resolving solution.
4. Let the gel(s) polymerize for at least 25 min(s).
 - a. Note: IF the gel doesn't polymerize after an hour, then something went wrong.
5. After the resolving gel is polymerized, remove the ddH₂O from the gel ad using filter paper, remove any excess ddH₂O.
6. Pipette approximately 2ml of 5% stacking gel over the resolving.
7. Place the well comb into the unpolymerized stacking gel.
8. Incubate for at least 15-20 min(s) to allow the gel to polymerize.
9. Remove comb, and assemble plates into running apparatus.
10. Add SDS-Running buffer to the inside well and the out.
11. Load samples into the gel wells
12. Run gel at 200V for 45-60min(s).

A2.8 Electrophoretic Transfer Of SDS-PAGE To A PVDF Membrane.

Note: Before assembling the apparatus, label a PVDF membrane with your initials and gel number in the top right hand corner, then pre-soak the membrane in 100% methanol for at least 2-5 min(s).

13. Prepare a gel set-up sheet
14. Assemble the transfer apparatus.
15. Place holder into a dish filled with pre-chilled SDS Transfer Buffer.
16. Lay the Black side of apparatus down, with the white side open and facing out.
17. Place a filter pad down on the black side followed by a filter paper.
18. Remove the gel(s) from the glass plates and place on top of the filter paper.
 - a. When separating the glass plates, try and have the gel lay on the short glass plate.
 - b. When placing the gel on the filter paper, turn the short plate with the gel, gel side down onto the filter paper.
19. Place the pre-soaked PVDF membrane on top of the gel
 - a. Place the membrane label side down on top of the gel, this way when it transfers, your membrane will read as the gel set-up sheet does.
20. Place a filter paper followed by another filter pad on top of the membrane.
21. Carefully close the white side of the apparatus down on top of the gel sandwich and close.
 - a. Try not to move the pads, papers, membrane, or gel.
22. Place the gel sandwich into the running chamber with the black sides facing, and the white and red side facing the same way.
23. Fill the chamber with the pre-chilled SDS Transfer Buffer
24. Transfer the gel overnight at 10V.
 - a. If the transfer buffer is not pre-chilled you can use an ice block to cool the apparatus.

A.2.9 Immunoblotting

* TBST=Tris-buffered Saline with Tween-20

1. Remove membrane(s) from transfer cassette(s).
2. Ink membranes with India ink (70ul/15ml TBST).
3. Rinse membrane(s) 2x for 10 mins in TBST.
4. Block membrane(s) for 30 mins at room temp while rocking.
 - a. Blocking solutions are as follows: 5% Bovine Serum Albumin (BAS) for phosphorylated proteins, or 5% non-fat milk for non-phosphorylated proteins.
5. Incubate membrane(s) with primary antibody(s) for either 1 hr (non-phosphorylated proteins) @ room temp with rocking, or overnight (phosphorylated proteins) @ 4°C while rocking.
 - a. Prepare primary antibody at a final volume of 100ul in TBST
6. Remove membrane(s) from surf blotter and rinse 3x for 10 mins each at room temp.
7. Incubate membrane(s) with secondary antibodies for 30 mins at room temp.
 - a. Prepare secondary antibody at a final volume of 15ml in TBST.
8. Rinse membrane(s) 3x for 10 mins each in TBST.
9. Prepare the chemiluminescence detection reagents at a 1:1 ratio
 - a. Total volume of 6 ml needed for each membrane.
10. Lift membrane(s) and blot of excess TBST
11. Place membrane(s) on saran wrap, with the protein side facing up.
12. Incubate membrane(s) with detection reagents for 5 mins at room temp.
13. Lift membrane(s) and blot off excess detection reagent
14. Transfer membrane(s) to a new piece of saran wrap, and wrap the membrane making sure to remove all bubbles from the protein side.
15. Expose membrane(s) to film in the dark room, and process the film.

A.2.10 Immunostaining of Primary Rat Schwann Cells

* Use 100ul for all amounts when using coverslips

1. Remove culture medium
2. Rinse coverslips 2x with 0.1M PO₄.
3. Fix: Incubate cells on coverslips with 4% paraformaldehyde for 10mins at room temp.
4. Rinse cells 3x with 0.1M PO₄.
5. Permeablize: Incubate cells on coverslips with 4% paraformaldehyde + 0.2% TX-100 for 10mins at room temp.
6. Rinse coverslips 2x with 0.1M PO₄ + 0.2% TX-100.
7. Block: Incubate cells on coverslips with appropriate serum at 10% (v/v) (usually 10% Normal Goat Serum) for 30mins at room temp.
 - a. Type of serum used depends on the secondary antibody and what animal the secondary Ab was made in.
 - b. While blocking prepare primary Ab in 10% serum.
8. Remove serum and incubate with primary Ab for 1hr at room temp.
 - a. While incubating prepare the secondary Ab, remembering to spin down to collect particulates and to only take from the top.
9. Rinse cells 4x with 10% serum.
10. Incubate with secondary Ab for 30mins at room temp...in the dark (put in a drawer or cover with foil).
11. Rinse 4x with 0.1M PO₄.
12. Post-Fix: Incubate cells on coverslips with 4% paraformaldehyde for 5 mins at room temp.
13. Rinse 2-3x with 0.1M PO₄.
14. Mount coverslips on slides using Gel mount.

*Make all solutions up in 0.1M PO₄, by diluting from a 0.2M PO₄.

A.2.11 Immunostaining of Dissociated Schwann Cell/ Dorsal Root Ganglion Neuron Co-cultures

* Use 100ul for all amounts when using coverslips

* Using L-15 to wash with Co-cultures so that the matrix doesn't pull up.

1. Remove culture medium
2. Rinse coverslips 2x with 0.1M PO₄.
3. Fix cells with 4% paraformaldehyde (in 0.1M PO₄) for 10mins at room temp.
 - a. Cannot use L-15 as it changes the pH of the paraformaldehyde.
4. Rinse cells 3x with L-15
5. Permeabilize cells with 4% paraformaldehyde + 0.2% TX-100 (in 0.1M PO₄) for 10mins at room temp.
6. Rinse coverslips 2x with L-15 + 0.2% TX-100.
7. Block cells with appropriate serum at 10% (v/v) in L-15 for 30mins at room temp.
 - a. Type of serum used depends on the secondary antibody and what animal the secondary Ab was made in, usually Normal Goat Serum.
 - b. While blocking prepare primary Ab in 10% serum (in L-15).
8. Remove serum and incubate with primary Ab for 1hr at room temp.
 - a. While incubating prepare the secondary Ab (in 10% serum in L-15), remembering to spin down to collect particulates and to only take from the top.
9. Rinse cells 4x with 10% serum (in L-15).
10. Incubate with secondary Ab for 30mins at room temp. in the dark (put in a drawer or cover with foil).
11. Rinse 2x with 10% Serum (in L-15).
12. Rinse 2x with 0.1M PO₄.
13. Post-Fix cells with 4% paraformaldehyde (in 0.1M PO₄) for 5 mins at room temp.
14. Rinse 2-3x with 0.1M PO₄.
15. Mount coverslips on slides.

16. *Make all solutions up in 0.1M PO₄, by diluting from a 0.2M PO₄.

A.3 Cell Culture Procedures

A.3.1 Rat Sciatic Nerve Dissection

Materials:

- Dissection kit: 1 pair large curved scissors, 1 pair small curved scissors, 1 pair spring scissors, 1 pair curved forceps
- Dissecting Platform (Blue Goo – Carolina Biologicals vinyl dissection pad)
- 2 Pairs of Large Forceps (autoclaved)
- 4 Large Glass Petri Dishes (autoclaved)
- 2 Large Glass Petri Dishes with Filter Paper in the bottom (autoclaved)
- 4 each of Fine Forceps, and Extra Fine Forceps
- 2 250mL Beakers with blue goo pad
- 1 60mm Dish (sterile)
- 1 35mm Dish (sterile)
- 2mL 1mg/mL Collagenase (Worthington Biochemical L50041714)
- 2mL 0.25% Trypsin/EDTA (Gibco 15015-065)
- 1 Aliquot D10
- L15 (Gibco 11415-064)
- 70% Isopropanol
- 4 Long Needles (22G1½)
- 8 Short Needles (25G5/8)
- PBS (sterile) (Gibco 20012-027)
- 3 Sterile Crystallizing Dishes
- Ice
- Glass Pasteur Pipets, regular and small bore (autoclaved)
- 1 15mL Centrifuge Tube
- 2 Small Red Biohazard Bags

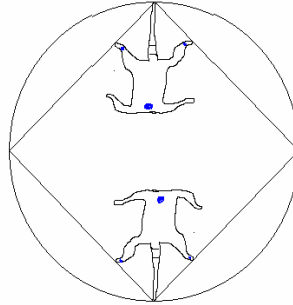
Preparation:

1. Wipe down hood and microscope with 70% isopropanol.
2. Make sure the light source is in place and the cord is taped to the walls of the hood and out of the way.
3. Place unautoclaved instruments (fine and ultra fine forceps), and dissecting platforms into large petri dishes and cover with 70% isopropanol. Add 70% isopropanol to 250mL beakers with blue goo pads in them. Allow to soak for 30 minutes. (After 30 minutes remove alcohol from dishes and beakers containing blue goo and allow to air dry under the hood)
4. Add 2-3mL L-15 media to the 35mm dish, and to a 60mm dishes.
5. Fill 2 of the sterile crystallizing dishes with L-15, and put one on ice.
6. Fill the third crystallizing dish with 70% isopropanol.
7. When the blue goo pads in the 250mL beakers are dry, add some PBS to each. Keep one on each side of the microscope. These will be for keeping instruments clean during dissection.

Dissection:

1. Place 4-6 pups (an even number) into a large, filter –paper lined petri dish. Place pups evenly in dish, not touching one another. Place the dish into the –20°C freezer for about 20 minutes, or until the pups are sedated.
2. Once sedated, use the large curved scissors from the dissection kit to decapitate the pups in the dish.
3. Place the bodies of the pups on ice in L15. Discard the heads and filter paper into a small, red biohazard bag, labeled with the date and number of pups.
4. Remove one pup at a time and rinse with clean L15, followed by a rinse in 70% isopropanol.
5. Pin the pup dorsal side up onto the blue goo, a secure in place with needles. Place one needle through the spinal cord where decapitated, and one through each hind

limb. When placing needles through the hind limbs, pull the limbs out perpendicularly and secure on the dissection pad. Re-secure the top needle if needed making sure that the limbs are taut, as shown below::



6. Use the spring scissors and the curved forceps to remove the skin from the legs of each animal.
7. Using one pair of fine forceps, insert closed forceps into the right fossa behind the femur, and open the forceps. Locate the sciatic nerve through the opening. With a second pair of fine forceps, hold the incision open and use the first pair to clear away connective tissue. Use both sets of fine forceps to hold the nerve at 2 ends, one close to the knee, and the other close to the spine. Pinch the forceps to sever the nerve at both ends while pulling up to remove the nerve segment. Place nerve segment into the 60mm dish of L15.
8. Once all of the nerve segments have been collected, clean the segments with extra fine forceps to remove epinurium, muscle, fat, and blood vessels that are attached.
9. Place cleaned nerves into the 35mm dish of L15.

Dissociation:

**Remember, always rinse Pasteur pipets with media containing serum before picking up nerve segments, this will keep the nerve segments from sticking to the glass.

1. Remove L15 from 35mm dish without removing the nerve segments.
2. Add 2 mL of collagenase (1mg/mL) and incubate for 30 min at 37°C.
3. Remove collagenase without removing the nerve segments.

4. Add 2mL Trypsin (0.25%) and incubate for 30 min at 37°C.
5. Pre-rinse glass Pasteur pipet (regular bore) with D10, then transfer the nerve segments, in the trypsin, to a 15mL centrifuge tube containing 5mL of D10. Triturate several times to remove nerve segments remaining in the pipet.
6. Rinse the 35mm dish with fresh D10, and then transfer it to the 15ml centrifuge tube.
7. Bring the volume in the centrifuge tube up to 10mL with D10.
8. Centrifuge for 10 min at 1500 rpm.
9. Remove supernatant, staying away from the pellet, and discard.
10. Add 2mL of D10 to the tube and triturate to break up the nerve segments at least 20 times with a regular bore Pasteur pipet, followed by trituration with a small bore Pasteur pipet.
11. Bring the volume in the tube up to 10mL.
12. Centrifuge for 10 min at 1500rpm.
13. Resuspend into 3mL of D10, and plate on to a non-coated 60mm dish. This will be day 0, P0 of the culture.

Culture:

Day 1: Feed with 3mL D10 + AraC (add 15µL AraC for every 3mL D10).

Day 3: Feed with 3mL D10 + AraC.

Day 7: Perform Thy 1.1 Treatment. Schwann cells will be considered P1 when finished.

Day 8: Wash 2X with HBSS, then add D10M.

Day 11: Feed with D10M.

Day 14: Passage to 6 dishes. Feed with D10M. (=P2).

Day 15: Wash 2X with HBSS and feed with D10M.

Day 19: Feed with D10M

Day 21: Freeze cells.

A.3.2 THY 1.1 Treatment

Materials:

- 2 PLL coated 100mm dishes
- 1 Aliquot of D10
- 1 Aliquot of D10M
- Hank's Free (Gibco 14170-112)
- 2mL 0.05% Trypsin/EDTA (Gibco 25300-062)
- 2mL Thy 1.1 (must be filter sterilized)
- 1mL Guinea Pig Complement (Rockland Inc. C300-0010)
- 1 15mL Centrifuge tube
- Ice

Method:

1. Rinse the 60mm dish containing the culture 2X with Hank's Free.
2. Add 2mL 0.05% Trypsin, and observe until cells come up from the plate.
3. Transfer cells to Centrifuge tube, and bring to 10mL with D10.
4. Centrifuge for 10 min at 4°C, 1500rpm.
5. Remove supernatant and discard.
6. Resuspend the cells in 2mL of Thy1.1 and incubate on ice for 30 min.
7. Bring to 10mL with D10.
8. Centrifuge for 10 min at 4°C, 1500rpm.
9. Remove supernatant and discard.
10. Resuspend in 1mL Guinea Pig Complement and incubate at 37°C for 20-30 min.

11. Bring to 10mL with D10.
12. Centrifuge for 10 min at 4°C, 1500rpm.
13. Resuspend cells in 2mL D10 and triturate 10 times. Bring the volume in the tube up to 10mL with D10.
14. Centrifuge for 10 min at 4°C, 1500rpm.
15. Resuspend into 2mL D10M, and plate onto 2 PLL coated dishes with 6mL of D10M.

A.3.3 Rat Dorsal Root Ganglion Dissection

Note: Laminin coating must be performed on coverslips at least 48 hours in advance

Materials:

- 1 pregnant Sprague Dawley Rat at E16 at time of dissection (Charles River)
- Rat C-Section Kit (1 pair large sharp scissors, 1 pair large blunt scissors, 1 pair large curved scissors, 3 pairs rat tooth forceps, 2 hemostats), autoclaved
- Embryo Dissection Kit (3 pairs small curved scissors, 3 pairs curved forceps), autoclaved
- 4 Pairs Fine Forceps, sterilized in 70% isopropanol
- 4 Pairs Extra Fine Forceps, sterilized in 70% isopropanol
- 1 250mL Beaker with Blue Goo Insert
- 70% isopropanol
- PBS (Gibco 20012-027)
- L15 Media (Gibco 11415-064)
- 1 Crystallizing Dish
- Tub with Tergazyme Detergent
- 1-100mm Sterile Petri Dishes
- 1-60mm Sterile Petri Dish
- 1-35mm Sterile Petri Dish
- Plastic Box With Lid
- Halothane or Isoflurane
- 50mL Conical Tube
- Gauze
- Small Red Biohazard Bags
- Dissection Board, with 4 nails for tying back limbs
- Electric Shaver

- 2 Large Glass Petri Dishes
- Ice
- Large Petri Dish with Filter Paper Insert, autoclaved
- Pasteur Pipets (Sterile)
- 2mL 0.25% Trypsin/EDTA (Gibco25200-056)
- CB10 Media
- 15mL Centrifuge Tube
- CH5 Media
- 150mm Sterile Petri Dishes (1 for every 10 coverslips)
- Sterile Water

Preparation:

1. Wipe down hood and microscope with 70% isopropanol.
2. Wipe down light source with 70% isopropanol and put into place under the hood, taping the loose cord to the walls of the hood so it is out of the way.
3. Place forceps into large glass petri dishes and cover with 70% isopropanol. Place under hood, and allow them to rinse in isopropanol for 30 minutes before using.
4. Place blue goo insert into sterile 250mL glass beaker and cover with 70% isopropanol. Allow to rinse in isopropanol for 30 minutes. After 30 minutes remove isopropanol and allow pad to air dry under the hood. Once dry, add 200-250mL of sterile PBS. This will be for keeping instruments clean during dissection.
5. Add about 10mL of L15 media to the 100mm dish.
6. Add about 3mL of L15 to the 60mm dish.
7. Add 1-2mL L15 to 35mm dish.
8. Fill a sterile crystallizing dish with L15 media and place on ice.

Dissection:

1. Work under the fume hood: Stuff some gauze into the 50mL conical tube and saturate gauze with 2mL of Isoflurane, and place into the glass dessicator and secure the lid.

2. Transfer the pregnant rat into the glass dessicator with isofluorane and sedate (do not kill) the rat.
3. Once sedated, transfer the rat to the dissection board, dorsal side down. Secure the limbs with twine, so that the rat is taut.
4. Shave the rat's stomach, and sterilize with 70% isopropanol.
5. Use the rat tooth forceps and lift the skin near the genital area of the rat.
6. Use the large, sharp scissors, cut an opening in the skin. Remove the connective tissue holding the skin to the muscle of the abdomen, and place skin to the outer sides.
7. Using the blunt scissors and a new pair of rat tooth forceps, cut a small incision into the abdominal muscles, then using the hemostats, clamp each side of the cut, and lay the hemostats to the outside of the rat (the hemostats will hold back the muscle). Proceed cutting an incision with the blunt scissors from the lower abdomen up to the chest.
8. Locate the uterus and lift it out with a new rat tooth forceps. Use the sharp, curved scissors and cut the uterus at the cervix, while lifting the intact uterine horn out of the abdomen.
9. Place the uterine horn into a filter lined, sterile, petri dish, and carry into the tissue culture room.
 - a. Using the sharp curved scissors, reach into the cavity of the adult rat, and cut the aorta. Place the rat into a biohazard bag.
10. At this point change gloves.
11. Use a sterile set of small curved scissors, and forceps to remove cut away the outer layer of the uterine horn; this should expose each individual placenta.
12. Using a new, sterile set of small curved scissors and curved forceps, cut the embryo (still within its amniotic sac) away from the placenta, and place into a pre-chilled crystallizing dish of L-15.
13. Transfer about 5 pups at a time into a 100mm dish of L15.
14. Use a new sterile set of curved scissors and forceps to remove the amniotic sac from around each embryo. Check for the developmental stage under the microscope (The

digits on its front paws can be webbed or separated, while the digits on its hind paws should still be webbed)

15. Align the scissor blades from under the chin of the pup across its ear, and to the air sac dent in the back of its head (see figure). Hold the pup firmly in place with forceps and decapitate with scissors.



16. Using fine forceps turn the embryo onto its back, grip the umbilical cord and use a second pair of forceps to stabilize its shoulders.
17. Once the shoulders are stabilized firmly, release the umbilical cord, and use forceps to dislocate hip joints, allowing the embryo to lay flat. Eviscerate the embryo using the same forceps.
18. Remove all internal organs, i.e. esophagus, from neck and abdomen of pup, being careful not to pierce the spinal cord.
19. Reposition the pup, if necessary, and re-stabilize the shoulders using fine forceps.
20. Insert one side of another pair of extra fine forceps into the vertebral column, being careful not to gouge or cut the spinal cord.
21. Squeeze the forceps to break the vertebrae, and continue down the vertebral column until all vertebrae are broken. If the vertebrae will not break by squeezing with the forceps place one set of forceps as indicated above and then use a second set of forceps to break the bones by dragging the pointed end across the vertebrae.
22. Separate vertebrae so that the spinal cord is exposed.
23. Use forceps to tease some of the connective tissue away from the spinal cord around the neck/shoulder area.

24. Using one pair of fine forceps, grasp the top of the spinal cord and hold firmly in place.
Avoid squeezing forceps too tightly, as to not cut the spinal cord. If the spinal cord is too fragile, and breaks apart during this step, it may be an indication that the embryonic stage of this animal is too early.
25. Use a second pair of fine forceps and grasp the neck/shoulder of the embryo.
26. Hold the spinal cord in place, and pull the body of the embryo out from under the spinal cord.
27. Transfer the spinal cord, with its attached DRGs to the 60mm dish of L-15. If the DRGs do not come out attached to the spinal cord, it may be an indication that the developmental stage of the embryo is too late or early.
28. Using extra fine forceps remove only the cervical DRGs from spinal cord and transfer to the 35mm dish of L-15. Cervical DRGs can be distinguished because of their large, rounded size (while thoracic DRGs tend to be smaller and more elongated).
29. Repeat until the desired amount of cervical DRGs are collected.

Enzyme Treatment:

**Remember to always wash Pasteur pipets with media containing serum before transferring DRGs to keep the DRGs from sticking to the glass.

1. Once all ganglia are collected, remove L-15, without removing the ganglia, from the 35mm dish.
2. Add 2mL of Trypsin (0.25%)/EDTA to the 35mm dish and incubate at 37°C for 30 minutes.
3. Using a Pre-rinsed Pasteur Pipet, add CB10 directly to the dish, and then transfer ganglia to a 15mL centrifuge tube.
4. Bring the volume of the centrifuge tube up to 10mL with CB10, and spin at 1500rpm for 10 minutes.
5. Remove supernatant, staying away from the bottom pellet, and discard. Add 10 mL fresh CB10 and triturate well, then spin at 1500 rpm for 10 minutes.

6. Remove supernatant, staying away from the bottom pellet, and discard.
7. Resuspend neurons into 5mL of the seeding media (CH5 or neurobasal media) and triturate well. Spin at 1500rpm for 10 minutes.
 - a. While spinning, rinse laminin coated coverslips 2x with sterilized dH2O, then once with L-15. Add 100 μ L of CH5 to each coverslips and place in incubator until ready to seed neurons.
8. Remove and discard supernatant.
9. Resuspend neurons into enough CH5 to allow for 50 μ L/coverslip at 1 ganglion/coverslip.
10. Seed neurons onto coverslips containing CH5.
11. Place each 100mm dish of coverslips into the incubator at 37°C, on the bottom shelf.

Care and Feeding:

1. The day after the dissection, change the media to E2F (this is an anti-mitotic). They should remain in E2F for three days.
2. After anti-mitotic treatment, feed the cultures with CB5 (100 - 120 μ L) every other day. Check the cultures every day to make sure they are not drying, and maintain the water in the outer 150mm dish.
3. After 3 changes of CB5, the neurons are ready to be seeded with Schwann cells (2x10⁵ Schwann cells/coverslip) in CB10 media.
4. Feed the co-cultures with CB10 every other day until the Schwann cells have proliferated enough for the induction of myelination.
5. When the Schwann cells are plentiful enough for myelination, change the media to M-feed (this contains 15% serum and ascorbic acid).
6. Continue to change M-feed media every other day until myelin is evident.

A.3.4 Laminin Coating

Materials:

- Teflon Discs
- 2 Pairs of Fine Forceps
- Alconox Soap (1% solution)
- 3% Acetic Acid
- 70% Isopropanol
- 12mm German Glass Coverslips (Carolina Biologicals)
- Sterile Water (Gibco 15230-162)
- Poly-L-Lysine (PLL; Sigma P2636)
- Borate Buffer
- Laminin (Gibco 23017-015) – thawed on ice
- Carbonate Buffer
- 100mm Sterile Petri Dishes (1 for every 10 coverslips to be coated)
- Crystallizing dishes (autoclaved)
- Side Arm Bottle
- Mesh Sheet
- Rubber Band
- Tubing
- Large Glass Petri Dish
- Large Glass Petri Dish With Filter Paper Insert (Sterile)
- Ice
- 15mL conical tube, prechilled
- Dessicator(s) Assembly(ies)
- Silicon Vacuum Grease

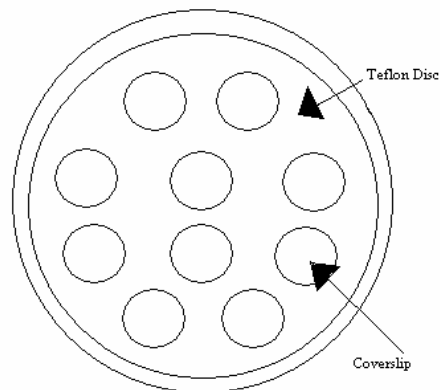
Preparing coverslips:

1. Wash each coverslip with a kimwipe andalconox soap, and place into a crystallizing dish with water.
2. Rinse with water several times until all soap is removed. Pour excess water out of crystallizing dish being careful to avoid dropping coverslips into the sink.
3. Cover the coverslips with 3% Acetic Acid and agitate for several minutes.
4. Attach the tubing to the de-ionized water faucet and to the side arm bottle and fill the bottle with water.
5. Pour as much of the acetic acid off of the coverslips as possible, being careful not to drop any coverslips into the sink.
6. Use the forceps to transfer the coverslips into the side arm bottle. Tilt the bottle onto its side to allow the coverslips to slide down to the bottom rather than dropping.
7. Use the mesh sheet and the rubber band to cover the top of the bottle and rest the bottle on its side in the sink (prop the neck of the bottle with another crystallizing dish).
8. Turn on the water and allow the coverslips to rinse for 20 minutes. The water should be on just enough to agitate the coverslips – do not let the water pressure get too high or it will break the coverslips.
9. Turn off the water and tilt the bottle down so that the coverslips start to flow to the neck of the bottle and onto the mesh. (Turn the water on and off gently until all coverslips wash toward the mesh)
10. While the bottle is upside down, remove the mesh with all the coverslips on it and transfer the coverslips to a sterile crystallizing dish and cover them with 70% isopropanol.
11. Allow them to sit in 70% isopropanol for at least 30 minutes before using.
12. Place the forceps into the large glass petri dish and cover them with 70% isopropanol. Allow to sit in 70% isopropanol for 30 minutes before using.
13. Use template to cut Teflon discs that will fit into 100mm petri dish (one disc for every 10 coverslips to be coated).
14. Wash each Teflon disc with kimwipes andalconox soap.
15. Rinse thoroughly with tap water, de-ionized water, and distilled de-ionized water.

16. Place discs into 100mm petri dish and cover with 70% isopropanol. Allow them to sit in 70% isopropanol for 30 minutes before using.

Coating:

1. Use forceps to remove Teflon discs from 70% isopropanol and blot dry on filter paper insert of large glass petri dish that has been autoclaved to sterilize.
2. Once dry, transfer Teflon disc to 100mm petri dish (dishes for agar plates can be used rather than dishes treated for tissue culture, but they must be sterile), and repeat until all dishes have Teflon discs.
3. Use forceps to transfer some coverslips to the filter paper.
4. Carefully separate each coverslip and set aside to dry. Allow only one side of the coverslip to touch the filter paper. This will become the bottom, so it will not matter if it has picked up lint from the filter paper.
5. Place 10 coverslips into each 100mm petri dish with a Teflon disc in the bottom.



6. Use Borate buffer to dilute PLL down to 200ug/mL and put 100uL onto each coverslip. Go around the edges, including the outer edges, of each coverslip with the pipet tip to make sure that PLL completely coats the coverslip.
7. Allow to sit under the hood for 1 hour.
8. Wash coverslips 2 times with sterile water.
9. Dilute Laminin to 50ug/mL with cold carbonate buffer, cool pipet tip in chilled carbonate buffer before transferring laminin. Keep laminin solution on ice.

10. Put 100uL of the 50ug/mL laminin onto each coverslip. Use pipet tip to go around edges, including outer edges, and ensure that laminin completely coats coverslip. A complete laminin coating will help to prevent the cultures from detaching.
11. Place dishes of laminin coated coverslips inside the incubator at 37°C for at least 48 hours prior to dissection.

LIST OF REFERENCES

Adam L., Vadlamudi R., Kondapaka S.B., Chernoff J., Mendelsohn J., Kumar R. (1998).

Heregulin regulates cytoskeletal reorganization and cell migration through the p21-activated kinase-1 via phosphatidylinositol-3 kinase. *J. Biol. Chem.* 273, 28238-46.

Akiyama S.K. (1996). Integrins in cell adhesion and signaling. *Hum. Cell.* 9: 181-6.

Alfthan K., Heiska L., Gronholm M., Renkema G.H., Carpen O. (2004). Cyclic AMP-dependent protein kinase phosphorylates merlin at serine 518 independently of p21-activated kinase and promotes merlin-ezrin heterodimerization. *J. Biol. Chem.* 279, 18559-66.

Baser ME, Kuramoto L, Woods R, Joe H, Freidman JM, Wallace AJ et al. (2005). The location of the constitutional neurofibromatosis 2 (NF2) splice site mutations is associated with the severity of NF2. *J Med Genet.* 42: 540-6.

Bashour AM, Meng JJ, Ip W, MacCollin M, Ratner N. (2002). The neurofibromatosis type 2 gene product, merlin, reverses the F-actin cytoskeletal defects in primary human Schwannoma cells. *Mol. Cell Biol.* 22, 1150-7.

Benninger Y, Thurnherr T, Pereira JA, Krause S, Wu X, Chrostek-Grashoff A et al. (2007).

Essential and distinct roles for cdc42 and rac1 in the regulation of Schwann cell biology during

peripheral nervous system development. *J Cell Biol.* 177: 14051-61.

Billings-Gagliardi S, Webster H.F., O'Connell M.F. (1974). In vivo and electron microscopic observations on Schwann cells in developing tadpole nerves. *Am. J. Anat.* 141, 375-91.

Bokoch GM. (2003). Biology of the p21-activated kinases. *Annu Rev Biochem.* 72: 743-81.

Brault E, Gautreau A, Lamarine M, Callebaut I, Thomas G, Goutebroze L. (2001). Normal membrane localization and actin association of the NF2 tumor suppressor protein are dependent on its N-terminal domain. *J Cell Sci.* 114: 1901-12.

Bretscher A., Reczek D., Berryman M. (1997). Ezrin: a protein requiring conformational activation to link microfilaments to the plasma membrane in the assembly of cell surface structures. *J. Cell. Sci.* 110, 3011-8.

Bretscher A., Chambers D., Nguyen R., Reczek D. (2000). ERM-Merlin and EBP50 protein families in plasma membrane organization and function. *Ann. Rev. Cell. Dev. Biol.* 16, 113-43.

Brockes J.P., Fields K.L., Raff M.C. (1979). Studies on cultured rat Schwann cells. I. Establishment of purified populations from cultures of peripheral nerve. *Brain Res.* 165, 105-18.

Brown MC, Perrotta JA, Turner CE. (1996). Identification of LIM3 as the principal determinant of paxillin focal adhesion localization and characterization of a novel motif on paxillin directing vinculin and focal adhesion kinase binding. *J Cell Biol.* 135: 1109-23.

Brown MC, West KA, Turner CE. (2002). Paxillin-dependent paxillin kinase linker and p21-activaed kinase localization to focal adhesions involves a multistep activation pathway. *Mol Biol Cell* 13: 1550-65.

Chen L.M., Bailey D., Fernandez-Valle C. (2000). Association of beta 1 integrin with focal adhesion kinase and paxillin in differentiating Schwann cells. *J. Neurosci.* 20, 3776-84.

Chen ZL, Strickland S. (2003). Laminin gamma 1 is critical for Schwann cell differentiation, axon myelination, and regeneration in the peripheral nerve. *J Cell Biol.* 163: 889-99.

Chernousov MA, Carey DJ. (2000). Schwann cell extracellular matrix molecules and their receptors. *Histol Histopathol.* 15: 593-601.

Citri A, Skaria KB, Yarden Y. (2003). The deaf and the dumb: the biology of ErbB-2 and ErbB-3. *Exp Cell Res.* 284: 54-65.

Claudio JO, Veneziale RW, Manko AS, Rouleau GA. (1997). Expression of Schwannomin in the lens and Schwann cells. *Neuroreport* 8: 2025-30.

Coles LC, Shaw PE. (2002). PAK1 primes MEK1 for phosphorylation by Raf-1 kinase during cross-cascade activation of the ERK pathway. *Oncogene*. 21:2236-44.

Colognato H, Yurchenco PD. (200). Form and function: the laminin family of heterotrimers. *Dev Dyn*. 218: 21-34.

Court FA, Wrabetz L, Feltri ML. (2006). Basal lamina: Schwann cells wrap to the rhythm of space-time. *Curr Opin Neurobiol*. 16: 501-7.

Curto M, Cole BK, Lallemand D, Liu CH, McClatchey AI. (2007). Contact-dependent inhibition of EGFR signaling by Nf2/Merlin. *J Cell Biol*. 177: 893-903.

Decker L, Desmarquet-Trin-Dinh C, Taillebourg E, Ghislain J, Vallat JM, Charnay P. (2006). Peripheral myelin maintenance is a dynamic process requiring constant Krox20 expression. *J Neurosci*. 26: 9771-9.

del Pozo M.A., Price L.S., Alderson N.B., Ren X.D., Schwartz M.A. (2000). Adhesion to the extracellular matrix regulates the coupling of the small GTPase Rac to its effector PAK. *EMBO J.* 19, 2008-14.

del Pozo MA, Alderson NB, Kiosses WB, Chiang HH, Anderson RG, Schwartz MA. (2004). Integrins regulate Rac Targeting by internalization of membrane domains. *Science* 303: 839-42.

den Bakker MA, Vissers KJ, Molijn AC, Kros JM, Zwarthoff EC, van der Kwast TH. (1999). Expression of the neurofibromatosis type 2 gene in humans. *J Histochem Cytochem.* 47: 1471-80.

Dupovy P, Svizenska I, Jancalek R, Klusakova I, Houstava L, Haninec P, et al. (1999). Immunohistochemical localization of laminin-1 in the acellular nerve grafts is associated with migrating Schwann cells which display corresponding integrin receptors. *Gen Physiol Biophys.* 18 63-5.

Einheber S, Zanazzi G, Chiang W, Scherer S, Milner TA, Peles E et al. (1997). The axonal membrane protein Caspr, a homologue of neurexin IV, is a component of the septate-like paranodal junctions that assemble during myelination. *J Cell Biol.* 139: 1495-506.

Eldridge CF, Bunge MB, Bunge RP. (1989). Differentiation of axon-related Schwann cells in vitro: II. Control of myelin formation by basal lamina. *J Neurosci.* 9: 625-38.

Evans DG, Huson SM, Donnai D, Neary W, Blair V, Newton V et al. (1992). A genetic study of type 2 neurofibromatosis in the United Kingdom. II. Guidelines for genetic counseling. *J Med Genet.* 29: 847-52.

Evans DG, Watson C, King A, Wallace AJ, Baser ME. (2005). Multiple meningiomas: differential involvement of the NF2 gene in children and adults. *J Med Genet.* 42: 45-8.

Falls DL. (2003). Neuregulins: functions, forms, and signaling strategies. *Exp Cell Res.* 284: 14-30.

Feldner J.C., Brandt B.H. (2002). Cancer cell motility—on the road from c-erbB2 receptor steered signaling to actin organization. *Exp. Cell Res.* 272, 93-108.

Feltri M.L., Graus Porta D., Previtali S.C., Nodari A., Migliavacca B., Cassetti A., et al. (2002). Conditional disruption of beta 1 integrin in Schwann cells impedes interactions with axons. *J. Cell Biol.* 156, 199-209.

Feltri ML, Wrabetz L (2005). Laminins and their receptors in Schwann cells and hereditary neuropathies. *J Peripher Nerv Syst.* 10: 128-43.

Fernandez-Valle C, Fregien N, Wood PM, Bunge MB. (1993). Expression of the protein zero myelin gene in axon-related Schwann cells is linked to basal lamina formation. *Develop.* 119: 867-80.

Fernandez-Valle C., Gwynn L., Wood P.M., Carbonetto S., Bunge M.B. (1994). Anti-beta 1 integrin antibody inhibits Schwann cell myelination. *J Neurobiol.* 25, 1207-26.

Fernandez-Valle C., Gorman D., Gomez A.M., Bunge M.B. (1997). Actin plays a role in both changes in cell shape and gene-expression associated with Schwann cell myelination. *J. Neurosci.* 17, 241-50.

Fernandez-Valle C., Tang Y., Ricard J., Rodenas-Ruano A., Taylor A., Hackler E., et al. (2002). Paxillin binds schwannomin and regulates its density-dependent localization and effect on cell morphology. *Nat. Genet.* 31, 354-62.

Ferner RE. (2007). Neurofibromatosis 1 and neurofibromatosis 2: a twenty first century perspective. *Lancet Neurol.* 6: 340-51.

Gao Y., Dickerson J.B., Guo F., Zheng J., Zheng Y. (2004). Rational design and characterization of a Rac GTPase specific small molecule inhibitor. *Proc Natl Acad Sci U.S.A.* 101, 7618-23.

Garratt A.N., Britsch S., Birchmeier C. (2000). Neuregulin, a factor with many functions in the life of a Schwann cell. *Bioessays* 22, 987-96.

Garratt AN, Voiculescu O, Topilko P, Charnay P, Birchmeier C. (200b). A dual role for erbB2 in myelination and expansion of the Schwann cell precursor pool. *J Cell Biol.* 148: 1035-46.

Gary R., Bretscher A. (1995). Ezrin self-association involves binding of an N-terminal domain to a normally masked C-terminal domain that includes the F-actin binding site. *Mol. Biol. Cell.* 6, 1061-75.

Gatto C.L., Walker B.J., Lambert S. (2003). Local ERM activation and dynamic growth cones at Schwann cell tips implicated in efficient formation of nodes of Ranvier. *J. Cell Biol.* 162, 489-98.

Gautreau A, Manent J, Fievet B, Louvard D, Giovannini M, Arpin M. (2002). Mutant products of the NF2 tumor suppressor gene are degraded by the ubiquitin-proteasome pathway. *J Biol Chem.* 277: 31279-82.

Giovannini M, Robanus-Maandag E, van der Valk M, Niwa-Kawakita M, Abramowski V, Goutebroze L, et al. (2000). Conditional biallelic Nf2 mutation in the mouse promotes manifestations of human neurofibromatosis type 2. *Genes Dev.* 14: 1617-30.

Gonzalez-Agosti C., Wiederhold T., Herndon M.E., Gusella J., Ramesh V. (1999). Interdomain interaction of merlin isoforms and its influence on intermolecular binding to NHE-RF. *J. Biol. Chem.* 274, 34438-42.

Gronholm M, Muranen T, Toby GG, Utermark T, Hanemann CO, Golemis EA et al., (2006). A functional association between merlin and HEI10, a cell cycle regulator. *Oncogene* 25: 4389-98.

Gutmann DH, Giordano MJ, Fishback AS, Guha A. (1997). Loss of Merlin expression in sporadic meningiomas, ependymomas and schwannomas. *Neurology* 49: 267-70.

Gutmann D.H., Sherman L., Seftor L., Haipek C., Hoang L.K., Hendrix M. (1999a). Increased expression of the NF2 tumor suppressor gene product, merlin, impairs cell motility, adhesion and spreading. *Hum. Mol. Genet.* 8, 267-75.

Gutmann D.H., Haipek C.A., Hoang L.K. (1999b). Neurofibromatosis 2 tumor suppressor protein, merlin, forms two functionally important intramolecular associations. *J. Neurosci. Res.* 58, 706-16.

Guy PM, Platko JV, Cantley LC, Cerione RA, Carraway KL 3rd. (1994). Insect cell –expressed p180erbB3 possess an impaired tyrosine kinase activity. *Proc Natl Acad Sci U S A*. 16: 8132-6.

Hall A. (2005). Rho GTPases and the control of cell behavior. *Biochem Soc Trans*. 33: 891-5.

Hamada K, Shimizu T, Matsui T, Tsukita S, Hakoshima T. (2000). Structural basis of the membrane-targeting and unmasking mechanisms of the radixin FERM domain. *EMBO J*. 19: 4449-62.

Hanemann CO, Evans DG. (2006). News on the genetics, epidemiology, medical care and translational research of schwannomas. *J Neurol*. 253: 1533-41.

Hann J, Liu S, Rose DM, Schlaepfer DD, McDonald H, Ginsberg MH. (2001). Phosphorylation of the integrin alpha 4 cytoplasmic domain regulates paxillin binding. *J Biol. Chem*. 276: 40903-9.

Hansen MR, Linthicum FH. (2004). Expression of neuregulin and activation of erbB receptors in vestibular schwannomas: possible autocrine loop stimulation. *Otol Neurotol* 25: 155-9.

Hildebrand J.D., Schaller M.D., Parsons J.T. (1995). Paxillin, a tyrosine phosphorylated focal adhesion-associated protein binds to the carboxyl terminal domain of focal adhesion kinase. *Mol. Biol. Cell* 6, 637-47.

Hirao M, Sato N, Kondo T, Yonemura S, Monden M, Sasaki T et al. (1996). Regulation mechanism of ERM (ezrin/radixin/moesin) protein/plasma membrane association: possible involvement of the phosphatidylinositol turnover and Rho-dependent signaling pathway. *J cell Biol.* 135: 37-51.

Hirokawa Y., Tikoo A., Huynh J., Utermark T., Hanemann C.O., Giovannini M., et al. (2004). A clue to the therapy of neurofibromatosis type 2: NF2/merlin is a PAK1 inhibitor. *Cancer J.* 10, 20-6.

Houshmandi SS, Gutmann DH. (2007). All in the family: Using inherited cancer syndromes to understand de-regulated cell signaling in brain tumors. *J Cell Biochem.* 102: 811-19.

Howe AK, Juliano RL. (2000). Regulation of anchorage-dependent signal transduction by protein kinase A and p21-activated kinase. *Nat Cell Biol* 2: 593-600.

Hseih AC, Moasser MM. (2007). Targeting HER proteins in cancer therapy and the role of the non-target HER3. *Br J Cancer* 97: 453-7.

Huang L., Ichimaru E., Pestonjamas K., Cui X., Nakamura H., Lo G.Y., et al. (1998). Merlin differs from moesin in binding to F-actin and in its intra- and intermolecular interactions. *Biochem. Biophys. Res. Commun.* 248, 548-53.

Hung G, Colton J, Fisher L, Oppenheimer M, Faudoa R, Slattery W, et al. (2002). Immunohistochemistry study of human vestibular nerve schwannoma differentiation. *Glia* 38: 363-70.

Hynes RO. (2002). Integrins: bidirectional, allosteric signaling machines. *Cell* 110: 673-87.

Iacovelli J, Lopera J, Bott M, Khaled A, Uddin N, et al. (2007). Serum and forskolin cooperate to promote G1 progression in Schwann cells by differentially regulating cyclin D1, cyclin E1, and p27(Kip) expression. *Glia* 55: 1638-47.

James M.F., Manchanda N., Gonzalez-Agosti C., Hartwig J.H., Ramesh V. (2001). The neurofibromatosis 2 protein product merlin selectively binds F-actin but not G-actin, and stabilizes the filaments through a lateral association. *Biochem J.* 356, 377-86.

Jessen KR, Mirksy R. (2005). The origin and development of glial cells in the peripheral nerves. *Nat Rev Neurosci.* 6: 671-82.

Juliano R.L., Reddig P., Alahari S., Edin M., Howe A., Aplin A. (2004). Integrin regulation of cell signaling and motility. *Biochem. Soc. Trans.* 32, 443-6.

Kaempchen K, Mielke K, Utermark T, Langmesser S, Hanemann CO. (2003). Upregulation of the Rac1/JNK signaling pathway in primary human schwannoma cells. *Hum Mol Genet.* 12: 1211-21.

Kim HA, DeClue JE, Ratner N. (1997). cAMP-dependent protein kinase A is required for Schwann cell growth: interactions between the cAMP and Neuregulin/tyrosine kinase pathways. *J Neurosci Res.* 49: 236-47.

Kissil J.L., Johnson K.C., Eckman M.S., Jacks T. (2002). Merlin phosphorylation by p21-activated kinase 2 and effects of phosphorylation on merlin localization. *J. Biol. Chem.* 277, 10394-9.

Kissil J.L., Wilker E.W., Johnson K.C., Eckman M.S., Yaffe M.B., Jacks T. (2003). Merlin, the product of the Nf2 tumor suppressor gene, is an inhibitor of the p21-activated kinase, Pak1. *Mol.*

Cell 12, 841-9.

Kjoller L., Hall A. (1999). Signaling to Rho GTPases. *Exp. Cell Res.* 253, 166-79.

Klapper LN, Glathe S, Vaismen N, Hynes NE, Andrews GC, Sela M et al. (1999). The ErbB-2/HER2 oncoprotein of human carcinomas may function solely as a shared coreceptor for multiple stroma-derived growth factors. *Proc Natl Acad Sci U S A.* 96: 4995-5000.

Lai C. (2005). Peripheral glia: Schwann cells in motion. *Curr Biol.* 15: R332-4.

Lallemand D, Curto M, Saotome I, Giovannini M, McClatchey AI. (2003). NF2 deficiency promotes tumorigenesis and metastasis by destabilizing adherens junctions. *Genes Dev.* 17: 1090-100.

Lee JW, Juliano RL. (2004). Mitogenic signal transduction by integrin- and growth factor receptor-mediated pathways. *Mol Cells* 30: 188-202.

Lotti LV, Di Lazzaro, Zompetta C, Frati L, Torrisi MR. (1992). Surface distribution and internalization of erbB-2 proteins. *Exp Cell Res* 202: 274-80.

Lustig LR, Yeagle J, Driscoll CL, Blevins N, Francis H, Nirparko JK. (2006). Cochlear implantation in patients with neurofibromatosis type 2 and bilateral vestibular schwannoma. *Otol Neurotol.* 27: 512-18.

Lyons D.A., Pogoda H.M., Voas M.G., Woods I.G., Diamond B., Nix R., et al (2005). ErbB3 and erbB2 are essential for Schwann cell migration and myelination in zebrafish. *Curr. Biol.* 15, 513-24.

MacCollin M, Mautner VF. (1998). The diagnosis and management of neurofibromatosis 2 in childhood. *Semin Pediatr Neurol.* 5: 243-52.

Maitra S, Kulikaukas RM, Gavilan H, Fehon RG. (2006). The tumor suppressors Merlin and Expanded function cooperatively to modulate receptor endocytosis and signaling. *Curr Biol.* 16: 702-9.

Manser E., Loo T.H., Koh C.G., Zhao Z.S., Chen X.Q., Tan L., et al. (1998). PAK kinases are directly coupled to the PIX family of nucleotide exchange factors. *Mol. Cell* 1, 183-92.

Matsui T, Maeda M, Doi Y, Yonemura S, Amano M, Kaibuchi K et al. (1998). Rho-kinase phosphorylates COOH-terminal threonines of ezrin/radixin/moesin (ERM) proteins and regulates

their head-to-tail association. *J cell Biol.* 140: 647-57.

McClatchey AI, Giovannini M. (2005). Membrane organization and tumorigenesis – the NF2 tumor suppressor, merlin. *Genes Dev* 19: 2265-77.

Michailov GV, Sereda MW, Brinkmann BG, Fischer TM, Haug B, Birchmeier C., et al. (2004). Axonal neuregulin-1 regulates myelin sheath thickness. *Science* 304, 700-3.

Milner R, Wilby M, Nishimura S, Boylen K, Edwards G, Fawcett J, et al. (1997). Division of labor of Schwann cell integrins during migration on peripheral nerve extracellular matrix ligands. *Dev Biol.* 185: 215-28.

Monje PV, Bunge M, Wood PM. (2006). Cyclic AMP synergistically enhances Neuregulin-dependent ERK and Akt activation and cell cycle progression in Schwann cells. *Glia* 3: 649-59.

Morrison H., Sherman LS., Legg J., Banini F., Isacke C., Haipek CA., et al. (2001). The NF2 tumor suppressor gene product, merlin, mediates contact inhibition of growth through interactions with CD44. *Genes Dev.* 15, 968-80.

Muranen T, Gronholm M, Lampin A, Lallemand D, Zhao F, Giovannini M et al. (2007), The tumor suppressor merlin interacts with microtubules and modulates Schwann cell microtubule cytoskeleton. *Hum Mol Genet.* 16: 1742-51.

Murphy P, Topilko P, Schneider-Maunoury S, Seitandou T, Baron-Vann Evercooren A, Charnay P. (1996). The regulation of Krox-20 expression reveals important steps in the control of peripheral glial cell development. *Development* 122: 2847-57.

Nakai Y., Zheng Y., MacCollin M., Ratner N. (2006). Temporal control of Rac in Schwann cell-axon interaction is disrupted in NF2-mutant schwannoma cells. *J. Neurosci.* 26, 3390-5.

Nave KA, Salzer JL. (2006). Axonal regulation of myelination by neuregulin 1. *Curr Opin Neurobiol.* 16: 492-500.

Nikitin A Yu, Ballering LA, Lyons J, Rajewsky MF. (1991). Early mutation of the neu (erbB-2) gene during ethylnitrosourea-induced oncogenesis in the rat Schwann cell lineage. *Proc Natl Acad Sci U S A.* 88: 9939-43.

Nodari A, Zambroni D, Quattrini A, Court FA, D'Ursa A, Racchia A et al. (2007). Beta1 integrin activates Rac1 in Schwann cells to generate radial lamellae during axonal sorting and myelination. *J Cell Biol.* 177: 1063-75.

Obremski VJ, Hall AM, Fernandez-Valle C. (1998). Merlin, the neurofibromatosis type 2 gene product, and $\beta 1$ integrin associate in isolated and differentiating Schwann cells. *J Neurobiol.* 37: 487-501.

Okada T., Lopex-Lago M., Giancotti FG. (2005). Merlin/NF-2 mediates contact inhibition of growth by suppressing recruitment of Rac to the plasma membrane. *J. Cell Biol.* 171, 361-71.

Osherov N, Gazit A, Gilon C, Levitzki A. (1993). Selective inhibition of the epidermal growth factor and HER2/neu receptors by tyrophostins. *J Biol Chem.* 268: 11134-42.

Otey CA., Burridge K. (1990). Patterning of the membrane cytoskeleton by the extracellular matrix. *Semin. Cell Biol.* 1, 391-9.

Patronas NJ, Courcoutsakis N, Bromley CM, Katzman GL, MacCollin M, Parry DM. (2001). Intramedullary and spinal canal tumors in patients with neurofibromatosis 2: MR imaging findings and correlation with genotype. *Radiology* 218: 434-42.

Patton BL. (2000). Laminins of the neuromuscular system. *Microsc Res Tech.* 51: 247-61.

Pearson MA, Reczek D, Bretscher A, Karplus PA. (2000). Structure of the ERM protein moesin reveals the FERM domain fold masked by an extended actin binding tail domain. *Cell* 101: 259-

70.

Pelton P.D., Sherman L.S., Rizvi T.A., Marchionni M.A., Wood P., Freidman R.A., et al. (1998). Ruffling membrane, stress fiber, cell spreading and proliferation abnormalities in human Schwannoma cells. *Oncogene* 17, 2125-209.

Ramesh V. (2004). Merlin and the ERM proteins in Schwann cells, neurons, and growth cones. *Nat Rev Neurosci.* 5: 462-70.

Rangwala R, Banine F, Borg JP, Sherman LS. (2005). Erbin regulates mitogen-activated protein (MAP) kinase activation and MAP kinase-dependent interactions between Merlin and adherens junction protein complexes in Schwann cells. *J Biol Chem.* 280: 11790-7.

Rong R., Surace E.I., Haipek C.A., Gutmann D.H., Ye K. (2004). Serine 518 phosphorylation modulates merlin intramolecular association and binding to critical effectors important for NF2 growth suppression. *Oncogene* 23, 8447-54.

Rosenbaum C, Karyala S, Marchionni MA, Kim HA, Krasnoselsky AL, Happel B, et al. (1997). Schwann cells express NDF and SMDF/n-ARIA mRNAs, secrete neuregulin, and show constitutive activation of erbB3 receptors: evidence for a neuregulin autocrine loop. *Exp Neurol.* 148: 604-15.

Rosenbaum C, Kluwe L, Mautner VF, Friedrich RE, Muller HW, Hanemann CO. (1998).

Isolation and characterization of cells from neurofibromatosis type 2 patients. *Neurobiol. Dis.* 5: 55-64.

Rouleau G.A., Merel P., Lutchman M., Sanson M., Zucman J., Marineau C., et al. (1993).

Alteration in a new gene encoding a putative membrane-organizing protein causes neurofibromatosis type 2. *Nature* 363, 515-21.

Rowe JG, Radatz M, Walton L, Kemeny AA. (2002). Stereotatic radiosurgery for the type 2

neurofibromatosis acoustic neuromas: patient selection and tumour size. *Stereotact Funct Neurosurg.* 79: 107-16.

Sainio M., Zhao F., Heiska L., Turunen O., den Bakker M., Zwarthoff E., et al. (1997).

Neurofibromatosis 2 tumor suppressor protein colocalizes with ezrin and CD44 and associates with actin-containing cytoskeleton. *J. Cell Sci.* 110, 2249-60.

Schaller M.D., Otey C.A., Hildebrand J.D., Parsons J.T. (1995). Focal adhesion kinase and paxillin bind to peptides mimicking beta integrin cytoplasmic domains. *J. Cell Biol.* 130, 1181-7.

Scherer SS, Gutmann DH. (1996). Expression of the neurofibromatosis 2 tumor suppressor gene product, merlin, in Schwann cells. *J Neurosci Res.* 46: 595-605.

Scherer SS, Xu T, Crino P, Arroyo EJ, Gutmann DH. (2001). Ezrin, radixin and moesin are components of Schwann cell microvilli. *J Neurosci Res.* 65: 150-64.

Schulze K.M., Hanemann C.O., Muller H.W., Hanenberg H. (2002). Transduction of wild-type merlin into human schwannoma cells decreases schwannoma cell growth and induces apoptosis. *Hum. Mol. Genet.* 11, 69-76.

Scoles D.R., Huynh D.P., Morcos P.A., Coulsell E.R., Robinson N.G., Tamanoi F., et al. (1998). Neurofibromatosis 2 tumour suppressor schwannomin interacts with betaII-spectrin. *Nat. Genet.* 18, 354-9

Scoles DR, Qin Y, Nguyen V, Gutmann DH, Pulst SM. (2005). HRS inhibits EGF receptor signaling in the RT4 rat schwannoma cell line. *Biochem Biophys Res Commun.* 335: 385-92.

Shaw R.J., McClatchey A.I., Jacks T. (1998). Regulation of the neurofibromatosis type 2 tumor suppressor protein, merlin, by adhesion and growth arrest stimuli. *J. Biol. Chem.* 273, 7757-64.

Shaw R.J., Paez J.G., Curto M., Yaktine A., Pruitt W.M., Saotome I., et al. (2001). The Nf2 tumor suppressor, merlin, functions in Rac-dependent signaling. *Dev. Cell* 1, 63-72.

Sherman L., Xu H.M., Geist R.T., Sporito-Irwin S., Howells N., Ponta H., et al. (1997). Interdomain binding mediated tumor growth suppression by the NF2 gene product. *Oncogene*

15, 2505-9.

Sherman L.S., Gutmann D.H. (2001). Merlin: hanging tumor suppression on the Rac. *Trends Cell. Biol.* 11, 442-4.

Stokowski RP, Cox DR. (2000). Functional Analysis of the neurofibromatosis type 2 protein by means of disease-causing point mutations. *Am J Hum Genet.* 66: 873-91.

Surace E.I., Haipek C.A., Gutmann D.H. (2004). Effect of merlin phosphorylation on neurofibromatosis 2 (NF2) gene function. *Oncogene* 23, 580-7.

Tachibana K., Sato T., D'Avirro N., Morimoto C. (1995). Direct association of pp125FAK with paxillin, the focal adhesion-targeting mechanism of pp125FAK. *J. Exp. Med.* 182,1089-99.

Takeuchi K., Kawashima A., Nagafuchi A., Tsukita S. (1994). Structural diversity of band 4.1 superfamily members. *J. Cell Sci.* 107, 1921-8.

Tanaka T, Yamaguchi R, Sabe H, Sekiguchi K, Healy JM. (1996). Paxillin association in vitro with integrin cytoplasmic domain peptides. *FEBS Lett.* 399: 53-8.

Tang X, Jang SW, Wang X, Liu Z, Bahr SM, Sun SY et al. (2007). Akt phosphorylation regulates the tumour-suppressor merlin through ubiquitination and degradation. *Nat Cell Biol.* 9:

1199-207.

Taveggia C., Zanazzi G., Petrylak A., Yano H., Rosenbluth J., Einheber S., et al. (2005).

Neuregulin-1 type III determines the ensheathment fate of axons. *Neuron* 47, 681-94.

Taylor A.R., Geden S.E., Fernandez-Valle C. (2003). Formation of a beta 1 integrin signaling complex in Schwann cells is independent of rho. *Glia* 41, 94-104.

Thaxton C, Lopera J, Bott M, Baldwin ME, Kalidas P, Fernandez-Valle C. (2007).

Phosphorylation of the NF2 tumor suppressor in Schwann cells is mediated by Cdc42-Pak and requires paxillin binding. *Mol Cell Neurosci* 34: 231-42.

Thaxton C, Lopera J, Bott M, Fernandez-Valle C. (in press). Neuregulin and laminin stimulate phosphorylation of the NF2 tumor suppressor in Schwann cells by distinct protein kinase A and p21-activated kinase-dependent pathways. *Oncogene*.

Thompson G., Owen D., Chalk P.A., Lowe P.N. (1998). Delineation of a Cdc42/Rac-binding domain of p21-activated kinase. *Biochemistry* 37, 7885-91.

Trofatter J.A., MacCollin M.M., Rutter J.L., Murrell J.R., Duyao M.P., Parry D.M., et al. (1993).

A novel moesin-, ezrin-, radixin-like gene is a candidate for the neurofibromatosis 2 tumor

suppressor. *Cell* 72, 791-800.

Tsukita S, Yonemura S. (1999). Cortical actin organization: lessons from ERM (ezrin/radixin/moesin) proteins. *J Biol Chem.* 274: 34507-10.

Turner C.E., Brown M.C., Perrotta J.A., Riedy M.C., Nikolopoulos S.N., McDonald A.R., et al. (1999). Paxillin LD4 motif binds PAK and PIX through a novel 95-kD ankyrin repeat, ARF-GAP protein: A role in cytoskeletal remodeling. *J. Cell Biol.* 145, 851-63.

Turner C.E. (2000). Paxillin interactions. *J. Cell Sci.* 113, 4139-40.

Turner CE, West KA, Brown MC. (2001). Paxillin-ARF GAP signaling and the cytoskeleton. *Curr Opin Cell Biol.* 13: 593-9.

Utermark T, Kaempchen K, Hanemann CO. (2003). Pathological adhesion of primary human schwannoma cells is dependent on altered expression of integrins. *Brain Pathol* 13: 352-63.

Vartanian T, Goodearl A, Viehover A, Fischbach G. (1997). Axonal neuregulin signals cells of the oligodendrocyte lineage through the activation of Er4 and Schwann cells through HER2 and HER3. *J Cell Biol.* 137: 211-20.

West K.A., Zhang H., Brown M.C., Nikolopoulos S.N., Riedy M.C., Horwitz A.F., Turner C.E. (2001). The LD4 motif of paxillin regulates cell spreading and motility through an interaction with paxillin kinase linker (PKL). *J. Cell Biol.* 154, 161-76.

Xiao GH, Beeser A, Chernoff J, Testa JR. (2002). p21-activated kinase links Rac/Cdc42 signaling to merlin. *J. Biol. Chem.* 277, 883-6.

Xiao GH, Gallagher R, Shetler J, Skele K, Altomare DA, Pestell RG, et al. (2005). The NF2 tumor suppressor gene product, merlin, inhibits cell proliferation and cell cycle progression by repressing cyclin D1 expression. *Mol Cell Biol.* 25: 2384-94.

Xu HM, Gutmann DH (1998). Merlin differentially associates with the microtubule and actin cytoskeleton. *Hum Mol Genet.* 7: 335-45.

Yang D, Beirman J, Tarumi YS, Zhong YP, Rangwala R, Proctor TM et al. (2005). Coordinate control of axon defasciculation and myelination by laminin-2 and laminin-8. *J Cell Biol* 168:655-66.

Yoshihara T, Yamamoto M, Doyu M, Mis KI, Hattori N, Hasegawa Y et al. (2000). Mutations in the peripheral myelin protein zero and connexin32 genes detected by non-isotopic RNase cleavage assay and their phenotypes in Japanese patients with Charcot-Marie-Tooth disease.

Hum Mutat. 16: 177-8.

Yu WM, Feltri ML, Wrabetz L, Strickland S, Chen ZL. (2005). Schwann cell-specific ablation of laminin gamma1 causes apoptosis and prevents proliferation. J Neurosci. 25: 4463-72.

Zenke, F.T., King, C.C., Bohl, B.P., Bokoch, G.M. (1999). Identification of a central phosphorylation site in p21-activated kinase regulating autoinhibition and kinase activity. J. Biol. Chem. 274, 32565-73.